

INTERACTIONS OF FIBRINOGEN WITH
BOVINE LUNG SURFACTANT EXTRACT IN
BULK BILAYER PHASES AND FILMS

CENTRE FOR NEWFOUNDLAND STUDIES

**TOTAL OF 10 PAGES ONLY
MAY BE XEROXED**

(Without Author's Permission)

RAVI DEVRAJ



Interactions of Fibrinogen with Bovine Lung Surfactant Extract in Bulk Bilayer Phases and Films

*Thesis submitted in partial fulfillment of the requirements for the degree of
Master of Science (Biochemistry), Memorial University of Newfoundland*

By

RAVI DEVRAJ (M. Pharm - Pharmaceuticals)

Department of Biochemistry, Memorial University of Newfoundland

St. John's, NL, A1B 3X9

December, 2005



Library and
Archives Canada

Bibliothèque et
Archives Canada

Published Heritage
Branch

Direction du
Patrimoine de l'édition

395 Wellington Street
Ottawa ON K1A 0N4
Canada

395, rue Wellington
Ottawa ON K1A 0N4
Canada

Your file *Votre référence*
ISBN: 978-0-494-19356-3
Our file *Notre référence*
ISBN: 978-0-494-19356-3

NOTICE:

The author has granted a non-exclusive license allowing Library and Archives Canada to reproduce, publish, archive, preserve, conserve, communicate to the public by telecommunication or on the Internet, loan, distribute and sell theses worldwide, for commercial or non-commercial purposes, in microform, paper, electronic and/or any other formats.

The author retains copyright ownership and moral rights in this thesis. Neither the thesis nor substantial extracts from it may be printed or otherwise reproduced without the author's permission.

AVIS:

L'auteur a accordé une licence non exclusive permettant à la Bibliothèque et Archives Canada de reproduire, publier, archiver, sauvegarder, conserver, transmettre au public par télécommunication ou par l'Internet, prêter, distribuer et vendre des thèses partout dans le monde, à des fins commerciales ou autres, sur support microforme, papier, électronique et/ou autres formats.

L'auteur conserve la propriété du droit d'auteur et des droits moraux qui protègent cette thèse. Ni la thèse ni des extraits substantiels de celle-ci ne doivent être imprimés ou autrement reproduits sans son autorisation.

In compliance with the Canadian Privacy Act some supporting forms may have been removed from this thesis.

Conformément à la loi canadienne sur la protection de la vie privée, quelques formulaires secondaires ont été enlevés de cette thèse.

While these forms may be included in the document page count, their removal does not represent any loss of content from the thesis.

Bien que ces formulaires aient inclus dans la pagination, il n'y aura aucun contenu manquant.


Canada

Dedicated to my

Wife (Sriphani Vidya, *Bangaaram*) and

Daughter (Vaishnaviraman, *Buji Bangaaram*)

ABSTRACT

Lung surfactant (LS), a secretory product of the alveolar type-II cells stabilizes the alveoli during normal respiration. LS reduces surface tension of the alveolar air-water interface during expiration preventing alveolar collapse. During acute respiratory distress syndrome (ARDS) and in other lung diseases, serum proteins leak into the alveolar space and inhibit LS surface activity. Interaction of bovine lipid extract surfactant (BLES) (a clinical replacement LS) with soluble fibrinogen (Fbg) was studied employing various biophysical techniques in bulk bilayer and monolayer films. BLES contains all lipids and proteins of LS except cholesterol and surfactant protein-A and D. From our monolayer studies (surface balance and adsorption studies) fibrinogen decreased the surface activity of BLES. Langmuir-Blodgett films of adsorbed BLES and BLES with fibrinogen were studied using Langmuir-Wilhelmy surface balance and were imaged employing atomic force microscopy (AFM). AFM images show that fibrinogen is mainly associated with the fluid phase of BLES films and aggregated the gel lipid domains. Fibrinogen was found to induce two sets of domains in BLES, one associated with the gel (condensed) lipids, while the protein aggregate was mainly present in the fluid phase. BLES bilayer dispersions showed a diffuse gel to liquid-crystalline phase transition between 10-35°C as measured by differential scanning calorimetry (DSC). Fibrinogen was found to denature at 50°C using DSC. DSC of BLES: Fbg (1:0, 1:0.5, 1:1, 1:1.4; wt/wt) dispersions, suggested that with increasing protein, the peak of maximal heat flow (T_{max}) was shifted from 27°C to 31°C. Raman and Fourier Transform Infrared Spectroscopy (FTIR) of the BLES: Fbg bilayers dispersions suggested that fibrinogen altered the CH_2 , CH_3 , and PO_4^-

vibrational modes of the BLES phospholipids. The vibrational shifts of frequencies were consistent with slight increase in hydration of the headgroups (PO_4^-) as well as slightly increased ordering (condensation) of the hydrocarbon chains (CH_2 and CH_3) of BLES. This result was in direct contrast to the disordering effects of BLES observed with another serum protein, albumin. Raman spectroscopy of BLES with Fbg performed below and above the T_{max} , correlated well with changes of chain conformation obtained using DSC. The monolayer and bilayer studies suggested that Fbg induces two separate sets of lipid domains in the surfactant. Such serum protein induced alterations of surfactant lipid packing may alter the materials surface activity as in ARDS and other lung diseases.

ACKNOWLEDGEMENTS

I express my deep sense of gratitude and indebtedness to my supervisor Dr. Kaushik Nag for his inspiring guidance, constructive criticism, valuable suggestions, constant encouragement, and advice in carrying out this work. Also his great scientific spirit has prompted me to take up this project with a great deal of enthusiasm.

I express my whole-hearted thanks to my supervisory committee members Dr. Dave Thompson and Dr. Nathan Rich for providing me guidance in my experiments to get going smoothly. I am thankful to both of my committee members for providing me useful ideas especially in the Infrared spectroscopic studies.

Next I would like to thank Dr. Chet Jablonski (Dean of Graduate studies), Dr. Phil Davis and my supervisor (Department of Biochemistry) and Dr. Linda Hensman, and Dr. Daneshtalab (School of Pharmacy) for being highly solicitous in my securing of a M. Sc admission in the Department of Biochemistry and ultimately building my career. I would also like to thank Dr. Kevin Keough for keeping abreast with my progress.

A special thank you goes to my colleague Mauricia Fritzen Garcia for helping me out in carrying out the atomic force microscopic (AFM) studies.

I would like to thank Lisa Lee for her assistance in electron microscopy, Linda Windsor and Kai Zhang for their assistance in handling FTIR, and June Stewart, Marie Codner, and Donna Jackman of the Keough's lab for all their help in handling DSC.

I am highly thankful to my former and current lab members: Sangeeta, Mauricia, Erin, Helene, Stephanie, Ashley, Tara, Kyle, Kylie, Julia, Shannon, Danielle, Jackie, and Adam for their support, assistance, and most of all friendship during my program.

Furthermore, I'd like to thank, The School of Graduate Studies for providing me the financial support, The Department of Biochemistry for allowing me to carry out this project, and the Memorial University of Newfoundland for providing me the requisite education to succeed in my life.

The grant for the purchase of a Raman and Atomic Force Microscopy was from CFI new opportunity research grants to Dr. K. Nag. We (K. Nag and I) would also especially like to thank Dr. David Bjarneson of BLES Biochemicals Inc. for his generous gifts of BLES used in the study.

I will be failing in my duty if I don't acknowledge the never tiring support I always receive from my wife (Vidhu), brother (Kavi), and father/mother (D. Rambhau / D. Ratnamala). Also, not to mention, I will not forget the affection delivered by my family members - sister (P. Madhavi), brother-in-law (P. Sunil kumar), nephew (Abhi), and niece (Alekhya); brother, Kavi and his wife Gayatri; father-in-law and mother-in-law (Shri Rangachary and Smt. Swarnalatha). I would like to specially thank Divu and Sree for creating a wonderful environment around me.

I am highly indebted to my close friends (*Jaan-Jigrees*) back home: Sunil, Ram, Shyam, and Vinay for always being caring about me in all my aspects of life. I would also like to thank Ranjit and other Torontonians friends for giving me excellent company while writing this thesis.

Last but not the least, my happiness, my well-being, and ultimately positive attitude towards life is all because of my loving daughter, Vaishnaviraman (*my little gold*) and wife, Vidya to whom this thesis has been dedicated.

TABLE OF CONTENTS

Abstract	iii
Acknowledgements	v
Table of Contents	vii
List of Figures	ix
List of Abbreviations	xi

Chapter 1: INTRODUCTION 1

1.1. Lung Surfactant (LS)	1
1.2. Composition of LS	1
1.3. Structural and Morphological forms of LS	2
1.4. Acute Respiratory Distress Syndrome (ARDS)	3
1.5. Lung Surfactant and ARDS	8
1.6. Surfactant therapy	9
1.7. Bovine Lipid Extract Surfactant (BLES™)	9
1.8. Lung Surfactant Inhibition upon Interaction with Serum Proteins	10
1.9. Suggested mechanisms of LS inhibition by serum proteins	13
1.10. Fibrinogen	16
1.11. Current project	18

Chapter 2: MATERIALS AND METHODS 21

2.1. Material	21
2.2. Preparation of DPPC multilamellar Vesicles	22
2.3. Methods	22
2.3.1. Surface balance (monolayer) studies	23
2.3.2. Adsorption Experiments	24
2.3.3. Atomic Force Microscopy	25
2.3.4. Differential Scanning Calorimetry	27
2.3.5. Raman Spectroscopy	29
2.3.6. Fourier Transform Infrared Spectroscopy	30
2.3.7. Transmission Electron Microscopy	32

Chapter 3: RESULTS	34
3.1. Adsorption Isotherms	34
3.2. Monolayer (surface balance) experiments	37
3.3. Atomic Force Microscopic studies	42
3.4. Differential Scanning Calorimetric studies	54
3.5. Transmission Electron Microscopy	64
3.6. Fourier Transform Infrared Spectroscopic studies	64
3.7. Raman Spectroscopy of BLES with Fibrinogen	80
Chapter 4: DISCUSSION	98
4.1. Film Adsorption and Isotherm studies	100
4.2. Atomic Force Microscopic studies	104
4.3. Differential Scanning Calorimetric studies	106
4.4. Transmission Electron Microscopy	108
4.5. Fourier Transform Infrared spectroscopic studies	109
4.6. Raman spectroscopic studies	112
SUMMARY AND CONCLUSIONS	114
FUTURE DIRECTIONS	116
REFERENCES	117

LIST OF FIGURES

Figure 1: (a) TEM of the lamellar body unfolding into tubular myelin (TM). (b) TEM of normal LS rat lavage (LB and TM)	5
Figure 2: Trinodular structure of fibrinogen showing D and E globular domains, α – chain protuberances, and fibrinopeptides A (F _P A) and B (F _P B)	19
Figure 3: Adsorption isotherms (surface tension vs. time) of BLES dispersion in buffer (6.75 mg/ml) and with varying amounts of Fbg in the dispersions at $23 \pm ^\circ\text{C}$	35
Figure 4: Surface tension vs. Pool area isotherms for compression-expansion cycles of BLES in buffer (a) and BLES : Fbg (1 : 1, w/w) (b) adsorbed onto a buffer subphase.	38
Figure 5: (a) Percent change in film area at increasing weight of fibrinogen in BLES. (b) Surface tension Vs. Pool area isotherm for compression-expansion cycles of pure fibrinogen adsorbed onto a buffer subphase.	40
Figure 6: Atomic force microscopic images of deposits of films on mica taken at a γ of 52 mN/m for BLES: Fbg dispersions (wt/wt) – (a) 1: 0 (b) 1: 0.5 (c) 1: 1 (d) 1: 10 (e) 0: 1 (Fbg).	43
Figure 7: AFM height difference section analysis and three dimensional view of Fbg film deposited on mica taken at a γ of 52 mN/m.	45
Figure 8: AFM height difference section analysis and three dimensional view of deposited films on mica taken at a γ of 52 mN/m - (a) BLES and (b) BLES: Fbg (1: 1, w/w)	48
Figure 9: AFM height difference section analysis and three dimensional view of deposited films on mica taken at a γ of 42 mN/m - (a) BLES and (b) BLES: Fbg (1: 1, w/w)	51
Figure 10: DSC thermograms of DPPC dispersion (a) and with fibrinogen at (1: 10, w/w) dispersion (b).	56
Figure 11: DSC thermograms (first cycles) of BLES dispersion and human fibrinogen	58
Figure 12: DSC melting profiles of BLES: Fbg (wt/wt) dispersions – (a) 1: 0, (b) 1: 0.1 (c) 1: 0.5, (d) 1: 1, and (e) 1: 1.4	60

Figure 13: DSC melting profiles of BLES: Fbg (wt/wt) dispersions – cycle1 (a) cycle2 (b), and cycle3 (c) for 1:0 (wt/wt) and cycle1 (a ¹), cycle2 (b ¹), and cycle3 (c ¹) for 1:1 (wt/wt)	62
Figure 14: TEM of (a) BLES dispersion and (b) with fibrinogen (1: 1, w/w).	65
Figure 15: A typical Phospholipid molecule showing the various group vibrations in the acyl chains and in the headgroup region.	67
Figure 16: Complete spectra of 27mg/ml BLES dispersion (a) FTIR (b) Raman.	69
Figure 17: FTIR spectra of the C-H stretching spectral region (2800 – 3000cm ⁻¹) showing the Symmetric (Vs) and Asymmetric (Vas) methylene/methyl stretches in (a) dispersions of BLES : Fbg (wt/wt) – (i) 1:0 (ii) 1: 0.25 (iii) 1: 0.5 (iv) 1: 1 and (v) 1: 1.4 and (b) dispersions of BLES : BSA (wt/wt) – (i) 1:0 (ii) 1: 0.5 (iii) 1: 1 and (iv) 1: 10	73
Figure 18: FTIR spectra of the polar (PO ₂ ⁻ stretching) region (1000 – 1500cm ⁻¹) showing the Symmetric (Vs) and Asymmetric (Vas) phosphate stretches in (a) dispersions of BLES : Fbg (wt/wt) – (i) 1:0 (ii) 1: 0.25 (iii) 1: 0.5 (iv) 1: 1 and (v) 1: 1.4 and (b) dispersions of BLES : BSA (wt/wt) – (i) 1:0 (ii) 1: 0.5 (iii) 1: 1 and (iv) 1: 10	77
Figure 19: Raman spectra of the 2800 – 3100 cm ⁻¹ region of (a) BLES at (i)13.7°C, (ii) 15°C, (iii) 20°C, (iv) 25°C, (v) 30°C, (vi) 40°C, (vii) 45°C and (b) BLES : Fbg (1: 1, wt/wt) at the same temperatures.	83
Figure 20: A comparison between thermotropic behaviors of Vibrational shift of Raman frequency for (a) BLES from 10°C to 50°C shown in open circles and (b) BLES with Fbg (1: 1, w/w) shown in triangles, in the same temperature range.	88
Figure 21: Raman spectra of the 1000-1200 cm ⁻¹ region of (a) BLES at (i)10°C, (ii) 15°C, (iii) 25°C, (iv) 40°C, (v) 45°C and (b) BLES : Fbg (1: 1, wt/wt) at the same temperatures; (c) Changes with temperature in the ratio of Raman peak intensities (I ₁₀₉₁ /I ₁₀₆₂). BLES (O) and BLES: Fbg (1: 1, w/w) (Triangles).	90
Figure 22: Raman spectra of the 2800-3100 cm ⁻¹ region of BLES : Fbg (wt/wt) dispersions, (a) 1 : 0 ; (b) 1:1 and (c) 1 : 10 shown at 25°C (panel A); 40°C (panel B); 15°C (panel C).	94
Figure 23: Changes with temperature in the ratio of Raman peak intensities (I ₂₉₃₇ /I ₂₈₈₆). (a) BLES (Open circles) and (b) BLES: Fbg (1: 1, w/w) (Triangles).	96

LIST OF ABBREVIATIONS

AFM	Atomic force microscopy
ALI	Acute lung injury
ARDS	Acute respiratory distress syndrome
ATR	Attenuated total reflection
BLES	Bovine lipid extract surfactant
BSA	Bovine serum albumin
CLL	Calf lung lipids
CLSE	Calf lipid surfactant extract
CRP	C-reactive protein
DPPC	Dipalmitoylphosphatidylcholine
DPPG	Dipalmitoylphosphatidylglycerol
DSC	Differential scanning calorimetry
Fbg	Fibrinogen
FTIR	Fourier transform infrared spectroscopy
γ	Surface tension
γ -A	Surface tension- pool area
IR	Infrared spectroscopy
LA	Large aggregate
LB	Lamellar bodies
LPC	Lysophosphatidylcholine
LS	Lung surfactant
π	Surface pressure
mN/m	Millinewtons/meter
MLV	Multilamellar vesicles
PC	Phosphatidylcholine
PE	Phosphatidylethanolamine
PG	Phosphatidylglycerol
PI	Phosphatidylinositol
POPC	Palmitoyl-oleoylphosphatidylcholine
POPG	1-palmitoyl-2-oleoyl-phosphatidylglycerol
PS	Phosphatidylserine
RDS	Respiratory distress syndrome
SM	Sphingomyelin
SP-A	Surfactant protein A
SP-B	Surfactant protein B
SP-C	Surfactant protein C
SP-D	Surfactant protein D
TEM	Transmission electron microscopy
TM	Tubular myelin
wt/wt	Weight by weight
MUN	Memorial University of Newfoundland

Chapter – 1

INTRODUCTION

1.1. Lung Surfactant

Lung Surfactant (LS) is a complex lipid-protein mixture secreted by type II cells of the pulmonary wall in the terminal air-way called the 'alveolus'. The secreted material at the air-water interface undergoes transformations and self assembles into various supra-molecular membranous structures which eventually lead to formation of stable mono-molecular films at that interface (reviewed by Goerke, 1998 and 1974). By forming highly surface active films at the air-alveolar interface, surfactant reduces the work of breathing (Clements, 1957; Goerke 1998; Notter et.al., 1997; Perez-Gil et.al., 1998; Possmayer 1997; Schurch *et al.*, 1992; Veldhuizen *et al.*, 2000; Veldhuizen *et al.*, 1998). Because films can lower surface tension (γ) to near 0 mN/m during lateral compression, they prevent alveolar collapse at end-expiration. LS also prevent alveolar edema, and some components of it at least have an important role in lung defense. Also it was proposed that LS is required to keep the bronchiolar thin airways open, thereby securing an unrestricted flow of air to and from the alveoli (Mingyao *et. al*, 1991).

1.2. Composition of LS

LS is composed mainly of phospholipids (85%), and small amounts of surfactant-associated proteins SP-A, SP-B, SP-C, and SP-D (Possmayer, 1997; Veldhuizen *et.al.*, 1998). The major mammalian surfactant phospholipids are dipalmitoyl-phosphatidylcholine (DPPC around 35-50%), unsaturated phosphatidylcholine (25-35%)

and the acidic phospholipids, phosphatidylglycerol (PG) around 8-15% (Veldhuizen *et al.*, 1998). The LS also contains other lipids such as sphingomyelin (SM), phosphatidylserine (PS) and cholesterol in smaller amounts (Veldhuizen *et al.*, 1998). Significant amounts of di-saturated phospholipids DPPC and PG make the LS somewhat unique in composition, since these phospholipids are absent or lacking in any significant amounts in most mammalian cellular membrane systems (Goerke, 1974; Griese, 1999; Johansson *et al.*, 1997). The surfactant associated proteins SP-A and SP-D are water soluble, large molecular weight glycoproteins (>650kDa) and are functionally important in preventing disease processes in the lung. The hydrophobic SP-B (8.7kDa) and SP-C (4.1kDa) help in the high surface activity of LS lipids. The functional importance of the formation of stable film in the lung by LS preventing alveolar collapse (Batenberg *et al.*, 1998; Possmayer, 1997; and Veldhuizen *et al.*, 1998) is due to the combined interaction of the lipids and hydrophobic proteins.

1.3. Structural and Morphological forms of LS

LS components are synthesized in the endoplasmic reticulum, transported to the golgi apparatus, and packaged into lamellar bodies (LB) of the alveolar type II cells (recently reviewed by Veldhuizen and Haagsman, 2000). These lamellar bodies are secreted into the hypophase via exocytosis across the type II cell plasma membrane where they swell and unravel to form a cross-hatched structure called tubular myelin (TM). The Transmission electron micrograph (TEM) image in Figure 1 (a) shows lamellar bodies, which have TM forming inside the structure by lamellar expansion.

Surfactant components are released from TM to form a 'surface active layer' at the air-liquid interface (reviewed by Goere, 1998; Lumb, 1989). When the alveoli are compressed during expiration, various unsaturated phospholipids and neutral lipids are squeezed out from the surface active film leaving the disaturated phospholipids, particularly DPPC. The DPPC-enriched film is capable of reducing the surface tension to near 0 mN/m (Haagsmann *et.al*, 1991). Figure 1 (b) shows a TEM of the process of forming TM from LB's in rat surfactant lavage.

1.4. Acute Respiratory Distress Syndrome (ARDS)

Acute respiratory distress syndrome (ARDS) is a sudden life threatening lung failure affecting adults and was first discovered by Ashbaugh *et al* (1967). They monitored 12 patients who were not responding to the usual modes of therapy, and were exhibiting symptoms similar to infant respiratory distress syndrome (previously known as hyaline membrane disease) which was found to be due to lack of ample secretion of LS (Avery and Mead, 1959). In ARDS the patients exhibited severe dyspnoea, tachypnoea, cyanosis that is refractory to oxygen therapy, loss of lung compliance, and diffuse alveolar infiltration (Ashbaugh *et al.*, 1967; reviewed by Greise 1999 and Lewis and Jobe, 1993). In all patients, ventilation was assisted or controlled by a respirator and measurements were made when the patient was in a relaxed or steady state. The minimum γ observed in patients was 24 mN/m whereas in normal situations it was less than 10 mN/m, when LS from such lungs were studied *in vitro* (Ashbaugh *et al*, 1967). The acute phase of ARDS is characterized by the influx of protein rich edema fluid into

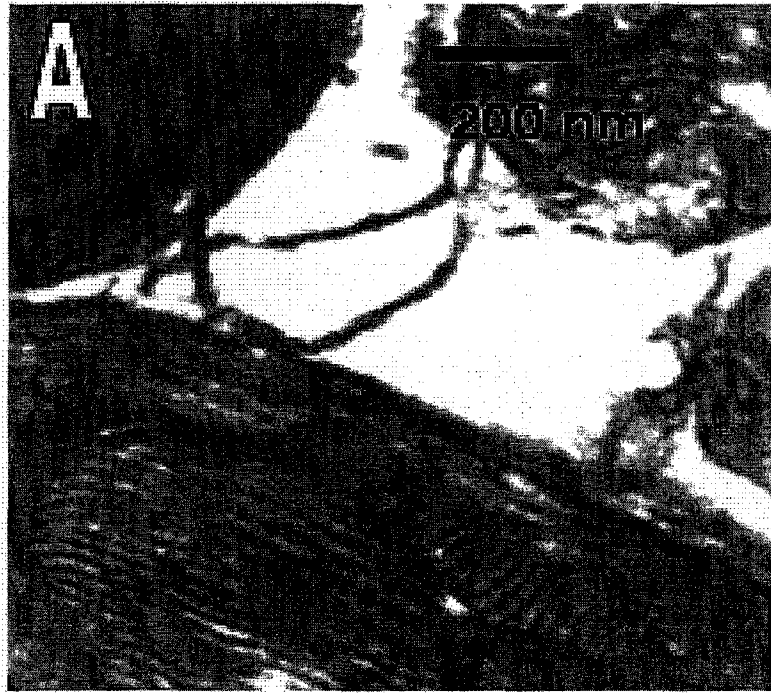
air spaces as a consequence of increased permeability of the alveolar-capillary barrier or leakage of blood vessels (Pugin *et al.*, 1999). There are two types of cells present in the alveolar epithelium of adult lungs. Flat type I cells, which make up 90% of the surface area, are easily injured. However, the cubical type II cells make up the remaining 10% and are more resistant to injury. The functions of the type II cells include surfactant production, ion transport, and uptake of LS lipids (reviewed by Ware and Matthay, 2000). Increased permeability of the epithelium can contribute to alveolar flooding. As well, the loss of epithelial integrity and injury to type II cells disrupts normal epithelial fluid transport, impairing the removal of edema fluid from the alveolar space (Sznajder, 1999). Also, injury to type II cells reduces the production and turnover of LS, contributing to surfactant abnormalities. In addition, loss of the epithelial barrier can lead to septic shock in patients with bacterial pneumonia (reviewed by Ware and Matthay, 1999).

In ARDS, inflammation gives rise to phospholipases, proteases, and other mediators within lung tissue. Damage to the alveolar capillary membrane allows these compounds, along with cellular degradation products and blood derived lipids and proteins, access to the alveoli where they can impair the surface-active function of LS (Holm *et al.*, 1999).

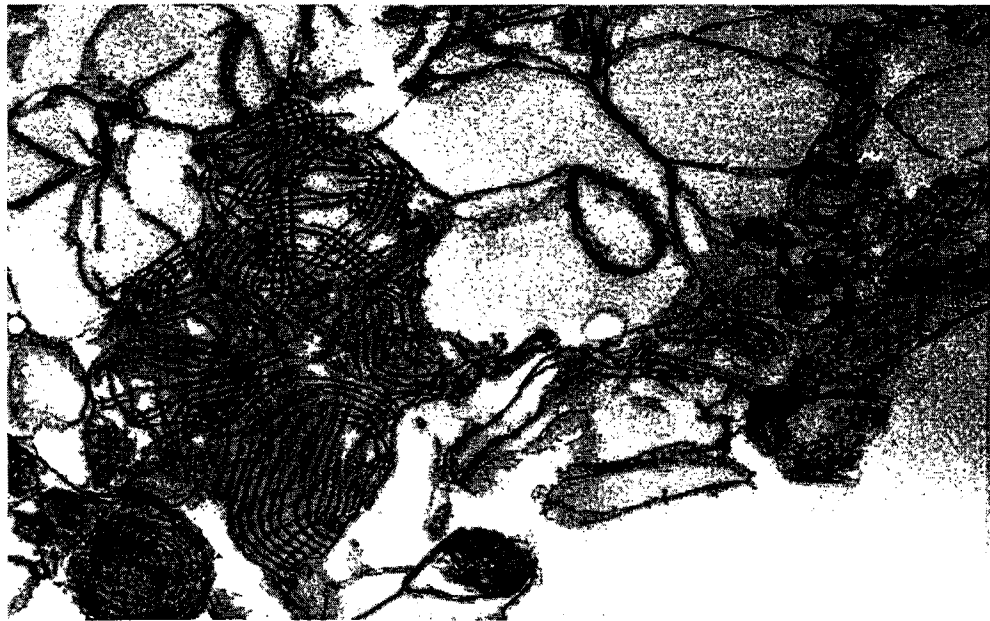
Another mechanism of injury is evident when neutrophils predominate in pulmonary edema fluid obtained from affected patients, suggesting neutrophil dependent lung injury (Pittet *et al.*, 1997). Other mechanisms included injury by cytokines, ventilator-induced lung injury due to high volumes and pressures of mechanical

Figure 1: (a) TEM of the lamellar body unfolding into tubular myelin (TM). This figure was a generous gift by Dr. Kaushik Nag. **(b)** TEM of Normal LS rat lavage (LB and TM) (Panda *et al.*, 2004 – adapted from the M. Sc thesis of Vidyasankar, 2004).

(a)



(b)



ventilation, and abnormalities in the production, composition, and function of LS (Greise, 1999; Ware and Matthay, 2000). To resolve the cause of this disease, many suggestions have been made. Alveolar edema can be resolved by the transport of sodium and chloride from the distal air spaces into the lung interstitium (Matalon *et al.*, 1996). As well, in clinical studies, clearance of alveolar fluid can cause improved oxygenation, a shorter duration of mechanical ventilation, and an increased likelihood of survival. Also the removal of insoluble protein is important since hyaline membranes provide a framework for the growth of fibrous tissue (reviewed by Griese, 1999; and Ware and Matthay, 2000).

Several approaches to treatment have been discussed. These include prophylaxis, supplementation with oxygen and positive end-expiratory pressure, mechanical ventilation, pharmacologic therapy through the use of corticosteroids, and nonsteroidal anti-inflammatory drugs, fluid and hemodynamic management, synthetic and natural surfactant therapy, and inhaled nitric oxide and other vasodilators (Bernard and Brigham, 1986; Spragg and Lewis 2003; reviewed by Ware and Matthay, 2000). Although these may help, there is still an onset of the disease, with a 40-60% mortality rate, so more studies have to be carried out to understand the mechanisms of dysfunction for more effective modes of therapy. This study is directed towards modeling the mechanisms of interaction of a serum protein (Fbg) with bovine lipid extract surfactant (BLES) *in vitro*. Fbg is known to be one of the most potent inhibitors of surfactant function. As previous studies in our laboratory (Vidysankar *et al*, 2004) had shown that another serum protein albumin inhibits surfactant activity by disrupting the packing of monolayers and bilayers,

we used Fbg to compare these two proteins. The study is unique in the sense that no other previous study have looked at the bilayer as well as the monolayer packing perturbations caused by these proteins on surfactant complementarily, using structure as well as functional techniques.

1.5. Lung Surfactant and ARDS

Increased alveolar protein load due to increased endothelial and epithelial permeability represents one of the key events in ARDS (Petty *et al.*, 1979; Pison *et al.*, 1989; Rinaldo *et al.*, 1982; Seeger *et al.*, 1986). Large amounts of serum proteins and red blood cell components were found in the alveoli during permeability edema and hemorrhage (Clark *et al.*, 1971; Fuchimukai *et al.*, 1987; Hallman *et al.*, 1982; Holm *et al.*, 1985a, Vol 38; Holm *et al.*, 1985b, Vol 59; Holm and Notter, 1987; Ikegami *et al.*, 1984) resulting in the inhibition of surfactant function as seen from the pathophysiological changes.

Jacobson *et al* (1993) found the presence of fibrinogen (Fbg) in the tracheal aspirates of only 5 of 30 in normal compared to 20 out of 21 patients with ARDS. There are several studies, which show the importance of LS in lung activity, and the inactivation causing ARDS (reviewed by Griese, 1999). Studies have shown that phospholipid composition was altered (decreased PC and PG with increased PI and PE), surfactant associated proteins were decreased (SP-A), and alveolar LS aggregate forms were altered (reviewed by Lewis and Jobe, 1993).

1.6. Surfactant therapy

Since its introduction to clinical medicine in 1980 by Fujiwara and coworkers, surfactant therapy of respiratory distress syndrome (hyaline membrane disease) has revolutionized the care of newborn infants in neonatal intensive care units (Fujiwara *et al.*, 1980). Replacement therapy with natural surfactant extracts has been proven to be beneficial in both experimental and clinical studies (Avery *et al.*, 1986; Robertson and Lachmann, 1988; Van Golde *et al.*, 1988). With the discovery of hydrophobic surfactant proteins, SP-B and SP-C, and their role in adsorption facilities and dynamic surface tension lowering properties, a reasonable method for a suitable and logistical surfactant therapy has been achieved (Curstedt *et al.*, 1987; Notter *et al.*, 1987; Revak *et al.*, 1988; Shiffer *et al.*, 1988; Whitsett *et al.*, 1986; Yu *et al.*, 1988; Yu *et al.*, 1986). Rapid adsorption facilities and surface tension lowering properties to near zero values under dynamic conditions are generally accepted criteria that have to be fulfilled by any artificial surfactant preparation. In addition, sensitivity or resistance to the inhibitory capacity of serum-derived proteins must be assumed to represent an additional important functional aspect (Enhorning, 1989).

1.7. Bovine Lipid Extract Surfactant (BLES™)

Bovine lipid extract surfactant (BLES™) is a clinically used surfactant preparation obtained from bovine lung lavage (washings) and has been used in this project. BLES is currently being used for the treatment of neonatal respiratory distress syndrome in human premature infants and is the only LS developed in Canada. BLES contains all the

phospholipids and proteins commonly present in a lung surfactant except that the hydrophilic SP-A, SP-D, and the neutral lipids (cholesterol) are removed during extraction. The neutral lipids are removed for better surface activity (Yu and Possmayer, 1988 & 1983). Thus the phospholipids and hydrophobic SP-B and SP-C proteins normally present in most mammalian LS is similar in composition to BLES. BLES is used as a standard model of natural LS due to its consistent composition and surface activity, its availability in large amounts and its cost effectiveness as a Canadian product. Previous studies using various extracted surfactant preparations (as noted in section 1.8.) have suggested somewhat contradictory views of LS inhibition due to various extraction processes, contaminants, and multiple compositional LS being used. Also, BLES has been extensively studied by us (Nag *et al* 2004c, 2002a, and 2002b; reviewed by Veldhuizen *et al*, 1998; Vidyasankar, 2004) and previously by the group which developed this product (Yu and Possmayer, 1983).

1.8. Lung Surfactant Inhibition upon Interaction with Serum Proteins

Seeger *et al* (1985) found that fibrinogen which was more potent at increasing the minimum surface tension of LS films than albumin. Albumin was more potent than immunoglobulin-M and immunoglobulin-G. Among different proteins tested, they found that the fibrin monomers are especially effective and more potent in inhibiting LS. This result, i.e. the greater effectiveness of fibrinogen compared with the other proteins (albumin and globulins) in raising the minimum surface tensions has also been noted previously by others (Abrams, 1966; Taylor and Abrams, 1966). They found that albumin

was a stronger inhibitor than the immunoglobulins, which was in contrast to findings by Keough *et al* (1987 and 1988) who observed that albumin was less potent than either of the globulin fractions (reviewed by Holm, 1998).

Using a pulsating bubble surfactometer, Fuchimukai *et.al.* (1987) have assessed the ability of various agents (fibrinogen, human serum, albumin, and a 55,000-Dalton serum protein) to inhibit the surface activity of a surfactant preparation, TA. The pulsating bubble surfactometer provides a model of an alveolus wherein a small bubble undergoes cyclic compression and expansion in a fashion that might imitate the action in the lung while the pressure needed to keep the bubble open is monitored continuously (Enhorning, 1977). Surfactant TA is semi-synthetic and was first described by Fujiwara *et .al.* 1980. A LS lipid: soluble protein (wt/wt) ratio ranging from 1:0.02 to as high as 1:3.2 was employed to evaluate the inhibitory effect of these proteins. The strongest inhibiting action was exerted by fibrinogen, followed by human serum and the 55,000 Da serum protein while the weakest inhibitor was albumin.

Seeger *et al.* (1993) have shown the differential sensitivity of various surfactant preparations towards inhibition by serum proteins. Serum proteins which have been used include fibrinogen, albumin, and hemoglobin. Calf lung surfactant extracts (CLSE), Alveofact, Curosurf, and Survanta (all used as clinical replacement surfactants) were the surfactant preparations used in their study. They concluded that this differential sensitivity is due to differences in phospholipid profiles, hydrophobic apoprotein contents (e.g., low SP-B quantities in Curosurf and Survanta, high quantities in CLSE and Alveofact), and the presence of contaminating materials. Curosurf and Survanta were

severely inhibited by low fibrinogen concentrations, and for the CLSE and Alveofact, a high fibrinogen-phospholipid ratio of 2:1 was needed for significant inhibition. These authors attributed this to the SP-B levels in the surfactant preparations employed. CLSE and Alveofact contained higher amounts (> 1.5%, of phospholipids), whereas Curosurf and Survanta contained low percentages (< 0.25%) of SP-B. This result supported their previous studies wherein they have shown that fibrinogen inhibition of a recombinant SP-C based phospholipid mixture was markedly counteracted by supplementation with small amounts of SP-B (Seeger *et al.*, 1991). Also, their result was in agreement with those by Hagwood *et al.* (1987), wherein fibrinogen sensitivity of a natural surfactant (CLSE) was found to be substantially increased by functional inhibition of SP-B by anti-SP-B.

Keough *et al.* (1987) have examined ways in which the serum proteins, fibrinogen, globulin, and albumin influence the properties of LS in monolayers. They found that all three major protein fractions from human serum interfered with the ability of LS to lower surface tension to near 0 mN/m values when films were compressed at the air-water interface. At low protein: surfactant ratios of 0.023, 0.07, and 0.139 (given as mg protein/ μ g surfactant), the order of potency for the 'inhibitory' effect of the proteins on minimum surface tension (maximum surface pressure) was fibrinogen > globulins > albumin. They also found that there was little difference between the effects of α -globulins and the β -plus γ -globulins. These results extend previous findings on the interaction of proteins with other surfactant preparations (Rüfer and Stolz, 1969; Seeger *et al.*, 1985; Taylor and Abrams, 1966).

Holm *et al.* (1985a) have shown that albumin in concentrations >20 mg/ml increased the minimum dynamic surface tension of natural lung surfactant (LS) from 1 mN/m to 21 mN/m at 37°C. Albumin in low concentrations (2mg/ml) had a similar detrimental effect on the dynamic surface activity of extracted calf lung lipids (CLL). Also albumin inhibited the adsorption of bovine LS and Calf lung lipids (CLL); instead of adsorbing rapidly to their equilibrium spreading pressure of 45 mN/m, both surfactant mixtures (at 0.063 and 0.125mg phospholipids/ml) adsorbed more slowly or reached lower final surface pressures in the presence of albumin. An important observation was that albumin inhibition of surface activity was moderated or abolished by increasing the lipid concentrations. Similarly, LS and CLL adsorption was protected from albumin inhibition at sufficiently high phospholipid concentrations. They also found that this was true even when the molar ratio of protein to phospholipids is increased as much as five fold. Also the effects of serum proteins on monolayers of DPPC, the major component of LS have been studied (Colacicco and Basu, 1978; Holm *et al.*, 1985a; Ikegami *et al.*, 1984; Mutafchieva *et al.*, 1984; Phang and Keough, 1986; Rüfer and Stolz, 1969; Seeger *et al.*, 1985; Tabak and Notter, 1977; Taylor and Abrams, 1966).

1.9. Suggested mechanisms of LS Inhibition by Serum Proteins

Holm *et al.* (1988) have suggested that the inhibitory effects of serum proteins may arise from their competing with the surfactant phospholipids at a clean air-aqueous interface during the adsorption process. However, they have not ruled out the possibility of some type of protein-surfactant molecular interactions occurring in the bulk phase.

They have proposed the above mechanism which was based on their results of centrifugation studies, wherein they suggested that physical interactions of serum proteins with the surfactant phospholipids may not be the only mechanism. The adsorption isotherms for surfactant-protein mixtures with inhibited surface activity were similar to the adsorption isotherm of the pure protein (Holm *et al.*, 1985a).

According to these authors, if a strong interaction between the inhibitory proteins and the surfactant mixture had occurred, the protein-surfactant complex should have pelleted together after minimum centrifugation at 12,500 x g ('g' the acceleration due to gravity) and this pelleted LS-serum protein material would have lacked surface activity upon re-suspension at the same concentration in normal saline. They found that, this however, was not the case for any of the specific CLSE mixtures they studied. Instead of showing an inhibition, all of the re-suspended pellets had absolutely normal adsorption and surface tension lowering abilities. These results were similar to the early findings of Shelley *et al* (1977) and Balis *et al* (1971) who used ultracentrifugation, with and without a sodium bromide gradient, to purify surfactant from lung washings contaminated with blood components. The centrifugation studies by these authors also agree with the previous work by Ikegami *et al* (1982 and 1984) showing that the abnormal surface activity of lung washings from premature lambs with respiratory failure (containing large amounts of protein) could be reversed by isolating the surfactant material by ultra centrifugation (27,000 x g).

Holm *et al.* (1988) have shown that the soluble protein molecules at the hypophase can prevent the LS phospholipid molecules from rapidly forming a surface

film. This arises in preformed films of albumin, hemoglobin, or fibrinogen because the CLSE adsorption to the air-liquid interface at high phospholipid concentration was inhibited. Similarly reverse experiments have shown that the injection of high concentrations of serum proteins beneath a preformed film of CLSE phospholipids had no effect on the surface pressure indicating that the proteins which should come into random contact with the surface film do not appear to interact with the phospholipids and displace them from the air-liquid interface. The data presented by Holm *et al* (1988) do not completely agree with the conclusions of Seeger *et al* (1985). However, the biophysical experiments performed by Seeger *et al* (1985) were carried out only at one low surfactant phospholipid concentration (unlike Holm *et al.*, 1988) and as well used only fibrin monomer.

Fuchimukai *et al* (1987), using pulsating bubble surfactometer studies, have shown that serum proteins with the ability to act as inhibitors probably become integrated with LS bilayers and liposomes. This may increase the stability of LS-serum protein complex formed in the hypophase, hence reducing the likelihood that the complex when in contact with an air-liquid interface, will easily break up and become part of the surface film. Molecules squeezed out of the film as the film approaches the minimum area becomes united and incorporated into protein-stabilized bilayers or liposomes, and thus the chance of their returning to the previous site in the film is reduced. This sequence of events could explain why, with high concentration of surfactant and inhibiting protein, it was noted that surface tension gradually increased at maximal and decreased at minimal film area during the 10 minutes recorded in their study.

Holm *et al.* (1999), using a pulsating bubble apparatus, custom designed hypophase exchange studies, and custom designed Wilhelmy balance, demonstrated that albumin acted primarily through competitive adsorption and blocking of the air-water interface. In studies with albumin, the results were consistent with their previous findings indicating that albumin and other blood proteins such as fibrinogen and hemoglobin inhibit the surface activity of lung surfactant primarily through competitive adsorption (Holm *et al.*, 1988). According to Holm *et al.* (1999), since serum proteins cannot readily penetrate an existing interfacial film of LS, their inhibitory effects are most substantial if they reach the surface when it is not fully occupied by surfactant molecules. This is the case when serum proteins adsorb simultaneously with lung surfactant into a clean surface when the hypophase surfactant concentration is low. Under such conditions, albumin substantially inhibited LS adsorption to an extent that exceeded the detrimental effects of lysophosphatidylcholine (LPC). It was noted previously that as the concentration of surfactant in the subphase increases, albumin (like other serum proteins) was less effective in competing for the interface, mitigating the magnitude of its inhibitory effect (Cockshutt *et al.*, 1990; Fuchimukai *et al.*, 1987; Holm *et al.*, 1988; Holm *et al.*, 1985a; Holm and Notter, 1987; Keough *et al.*, 1989; Seeger *et al.*, 1985).

1.10. Fibrinogen (Fbg)

Fibrinogen (also called serum Fbg, plasma Fbg, and Factor I), is the main protein of the blood coagulation system produced by the parenchymal cells of liver. Fbg helps stop bleeding by helping the formation of blood clots. During normal blood clotting, Fbg

is polymerized by an enzyme called thrombin into long fibrous materials (fibrin) which forms the clot. Thrombin also activates a substance called Factor XIII. Factor XIII helps weave the fibrin into a complex lattice, closing off injured blood-vessel walls. Blood platelets attach to fibrin, clumping together to form a blood clot and stop bleeding. The normal Fbg concentration in serum is about 200-400 mg/dl and has a molecular mass of ~ 340 kDa.

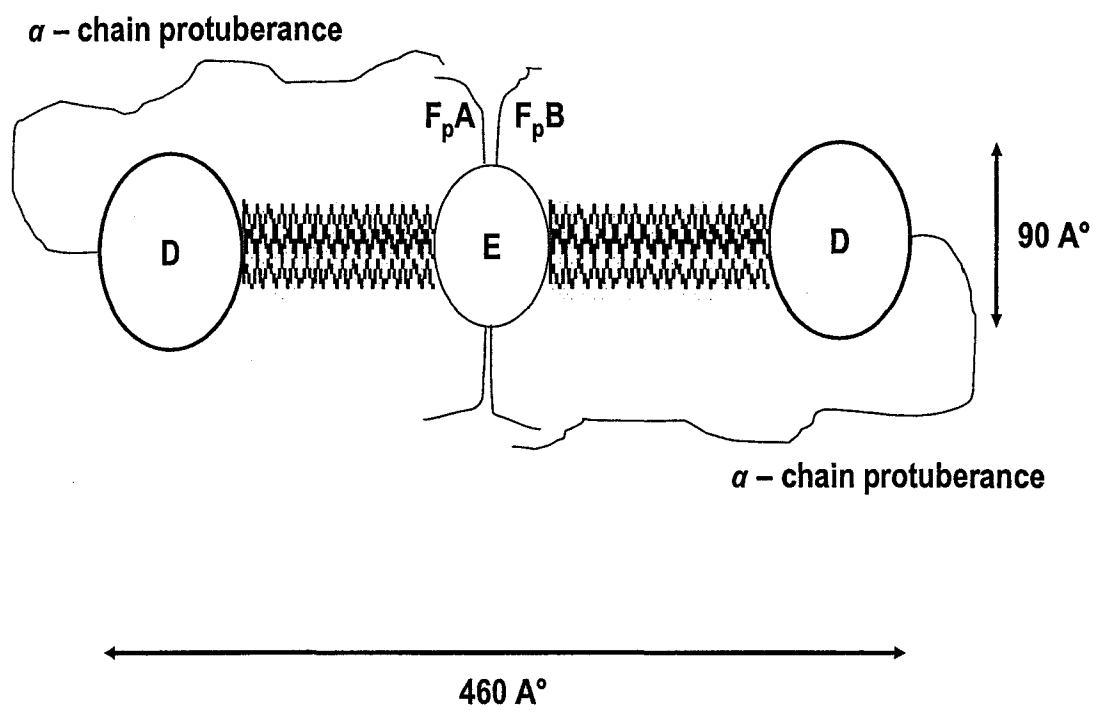
Fbg clotting underlies pathogenesis of myocardial infarction, thromboembolism and thromboses of arteries and veins, since fibrin is the main substrate for thrombus formation. Fbg activation is also involved in the pathogenesis of inflammation, tumor growth and many other diseases. Increase in blood Fbg concentration has been shown to be a strong predictor of coronary heart disease (Lowe *et al.*, 2000 and Danesh *et al.*, 1998). All these facts make Fbg an important parameter in the diagnosis of cardiovascular diseases. Fbg is a dimeric protein, each half of which is composed of disulfide-bonded polypeptide chains designated $A\alpha$, $B\beta$, and γ . "A" and "B" refer to the fibrinopeptides A (FpA) and B (FpB) that constitute the amino terminal 16 and 14 residues, respectively, of the $A\alpha$ - and $B\beta$ -chains. Figure 2 shows the model of a human fibrinogen with its subunits. Early electron micrographs (Hall and Slayter, 1959) showed Fbg to be an elongated protein which had a trinodular structure composed of two larger terminal globular domains and a smaller central globular domain, all connected by intervening linear segments. The length of the molecule is ~ 460 Å along its major axis and 60 - 90 Å along its minor axis (Figure 2). In this model, the outermost globules are referred to as D-domains, and the central globule is referred to as the E-domain.

Biochemical and physico-chemical studies have revealed much about the detailed structure of Fbg. The halves of the protein are linked in antiparallel fashion within the central E-domain (Hoperich and Doolittle, 1983). That domain consists of the N-terminal portions of the six constituent chains and is stabilized by eleven inter-chain disulfide bonds. The linear segments that join an E-domain to its flanking D-domains are suprahelical arrangements of the $A\alpha$ -, $B\beta$ - and γ -chains, and are often referred to as “coiled-coil” regions. Whereas the carboxyl halves of the $B\beta$ - and γ -chains fold extensively and terminate as the bulk of the globular D-domains (Weisel et.al., 1985), the $A\alpha$ -chains extend from the D-domains, fold back across the molecule, and appear to terminate juxtaposed to the E-domain, perhaps in close proximity to the FpA’s (Lorand, 1983). That segment of an $A\alpha$ -chain that projects beyond a D-domain is referred to as an $A\alpha$ -chain extension or protuberance.

1.11. Current project

Interaction of fibrinogen with LS extract in bulk bilayer phases and films was studied in this project. Biophysical studies of monolayer films of BLES with and without fibrinogen were carried out employing techniques such as, Langmuir-Wilhelmy surface balance and AFM. Also, DSC, FTIR, Raman, and TEM were employed to probe the interaction in bulk bilayer phases of the surfactant.

Figure 2: Trinodular cartoon structure of Fibrinogen showing D and E globular domains, α – chain protuberances and fibrinopeptides A (F_pA) and B (F_pB). This figure is adapted from the reference by Hall and Slayter (1959).



Chapter – 2

MATERIALS AND METHODS

2.1 Materials

Bovine Lipid Extract Surfactant (BLESTTM) was obtained as 5 ml vials of 27 mg/ml suspension in saline from BLESTTM Biochemicals Inc. (London, Ontario, Canada). DPPC (1, 2-dipalmitoyl-*sn*-glycero-3-phosphatidylcholine), fibrinogen (Fraction-1; Type 1 from human serum; Lot. No. 072k7606) containing 90% clottable protein in dry form., delipidated bovine serum albumin (BSA) (protease free, fraction V, 99%, catalogue number- A3059-50G) in powdered form, and Trizma. HCl were obtained from Sigma Chemical Co (St. Louis, MO). Chloroform and methanol, HPLC grade solvents (99%) and sodium chloride were obtained from Fisher Scientific (Ottawa, ON, Canada).

All experiments were carried out in NaCl-Trizma.HCl buffer, pH 7, unless otherwise stated. Glassware used in the monolayer experiments was all chromo-sulfuric acid washed and rinsed thoroughly in distilled water, and dried at 180°C for 2hrs prior to use. This was done to remove all organic lipids and surface active impurities from the glassware as previously discussed (Keough *et al* 1988). Water used in this study was doubly distilled, with the second distillation done from dilute potassium permanganate to remove all organic surface active impurities (Keough *et al* 1988; Nag *et al* 1998).

2.2. Preparation of DPPC vesicles

Required amounts of DPPC were weighed using an electronic balance and carefully transferred to a small round bottomed flask. To this 500 μ L of chloroform-methanol mixture (3:1 v/v) was added. The contents in the flask was vacuum evaporated using a rotary evaporator for 15 minutes at 37°C to remove the solvents. Traces of the solvent were removed by drying under nitrogen followed by desiccating overnight. The required volume of double distilled water was added to the flask and vigorously vortexed for 5 min at 46°C. This temperature was chosen since it is above the phase transition temperature of DPPC (41°C). Under such conditions multi-lamellar vesicles are formed as discussed previously (Chapman and Collin, 1965; Veldhuizen *et al*, 1998).

2.3. Methods

For all the studies conducted in this project, viz. monolayer, adsorption, FTIR, Raman, DSC, and AFM, Fbg was dissolved in saline at a concentration of 10 mg/ml (10 mg/ml is the maximum solubility of fibrinogen in saline). The dissolved fibrinogen was then mixed with BLES after appropriate dilution at (0.1:1 to 5:1, Fbg: BLES, wt/wt). These desired amounts of Fbg added to BLES were physiologically/pathologically relevant to what was observed in injured lungs for soluble proteins. Panda *et al* (2004) observed a phosphatidylcholine to protein ratio of 1:1 in injured lungs as compared to 4:1 in normal lungs. Also high protein concentrations (up to 5:1 to 10:1) were studied as models of *in-vitro* studies which exhibited maximum inhibitions. These high

concentrations used in the laboratory are to demonstrate and equate the inhibitory effects of proteins *in vitro* as done by others (Holm *et al.*, 1999 and 1985a).

The buffer used in the study was prepared by adding 150mM NaCl (equivalent to 9 grams) and 5mM Trizma hydrochloride (equivalent to 0.08 grams) to 1 liter of double distilled water, mixed well and the pH was adjusted to 7 using 0.1 M NaOH.

2.3.1 Surface Balance (Monolayer)

A modified Langmuir- Wilhelmy surface balance (Langmuir Mini Trough, Applied Imaging, England) with a teflon ribbon barrier was used, the design and construction of which has been described previously (Taneva and Keough, 1997). The dimensions of the Teflon trough gave a surface area of approximately 500 cm², which is used as 100% of monolayer area in the isotherms. Surface tension as a function of monolayer surface or pool area was used in all studies, as accurate area/molecule information can not be calculated for adsorbed films. The area/per molecule determination for adsorbed Langmuir films does not lead to systematically reproducible results. This is due to different amount of adsorption of different samples, giving non-equivalent surface tensions, and only a variable and apparent estimate based on the assumption that every lipid molecule inserted under the air-water interface reaches the surface to form monolayer (Panda *et al*, 2004). Most surfactant studies of adsorbed films are thus performed using surface tension – area curves (Fuchimukai *et al*, 1987; Holm *et al*, 1988; Keough *et al*, 1989). Surface tension is measured by a roughened Wilhelmy platinum dipping plate hanging from a force transducer (Nag *et al.*, 1990). A motorized

Teflon barrier operated by a FWD-RVS (forward-reverse) switch located on the instrument was used to compress and expand the monolayer.

Initially, NaCl-Trizma.HCl buffer, pH 7 was used to fill the teflon trough as the subphase representing an air-water interface and having a surface tension of around 72mN/m. Bovine lipid extract surfactant dispersed in buffer containing either no Fbg (control) or varying weight percentages of Fbg were adsorbed using a Hamilton syringe just under the air-water interface of the subphase. One hour was allowed for equilibration of the films. Unlike the samples which are organic solvent spread, with the monolayer formed by evaporation of the organic solvent over the subphase, our samples which are adsorbed in buffer have been shown to have similar characteristics previously described to solvent spread films previously (Nag *et al.*, 1996; Panda *et al.*, 2004). After equilibration, compression and expansion of the films was initiated by movement of the barrier and the isotherms were obtained at an ambient room temperature of $23 \pm 1^\circ\text{C}$. By compressing and expanding the monolayer, the transition of the surfactant from fluid to condensed (gel-like) phase can be initiated and monitored by the inflexion in lipid isotherms (Nag *et al.*, 1998).

2.3.2 Adsorption Experiments

Studies of surface tension as a function of time adsorption isotherms were carried out in a 6.28 ml small cylindrical teflon cup. Measurements were made at room temperature ($23 \pm 1^\circ\text{C}$) with a 6mL subphase of NaCl-Trizma.HCl buffer, pH 7, which was stirred continuously to minimize diffusion resistance. Adsorption experiments were

initiated by injecting 400 μL of BLES or BLES-Fbg dispersions to the clean surface, stirred, surfactant-free subphase to give a final volume of 6 mL. Adsorption to the surface (determined by surface tension drop) was then measured as a function of time in seconds, using a Wilhelmy plate as discussed in detail in a previous study (Nag *et al.*, 1998).

2.3.3. Atomic Force Microscopy (AFM)

The Atomic force microscope works by scanning with a fine ceramic or semiconductor tip (2-20 nm to single atom in diameter) on a surface. This is similar to a phonograph needle scanning a gramophone record. The tip is positioned at the end of a cantilever beam shaped much like a diving board. As the tip is repelled by or attracted by the corrugation of a surface, the cantilever beam deflects. The magnitude of the deflection is captured by a laser that reflects at an oblique angle from the very end of the cantilever. A plot of the laser deflection versus tip position on the sample surface provides the resolution of the hills and valleys that constitute the topography of the surface. The AFM can work with the tip touching the sample (contact mode), or the tip can tap across the surface (tapping mode) much like the cane of a blind person (Binnig *et al.*, 1986).

A Langmuir surface balance was used to deposit preformed monolayers of BLES-fibrinogen films on mica or glass slides to study the structures in the films using AFM. The substrate (teflon holder carrying a round shaped mica sheet, equivalent in diameter to a microscopic cover slip) was submerged into the ring well of the surface balance before film formation. Compression to a desired surface tension ($\gamma = 52 \text{ mN/m}$, 42 mN/m or 32

mN/m, etc) was performed. Following a slow compression ($7.3 \text{ cm}^2/\text{sec}$) and a few minutes waiting time, the surface film was deposited onto the mica by raising it vertically at a rate of 0.22 mm/sec at the desired surface tension. The films were compressed at the three different surface tensions mentioned above for all the samples. Details of such AFM methodology to study LS films are discussed elsewhere (Nag *et al.*, 2004b). The Langmuir-Blodgett deposit on mica was mounted on the magnetic steel disk of the AFM scanner (Scanner J) where the samples were imaged within 1 hr of deposition by a Nanoscope® Scanning Probe Microscope (Veeco Instruments, Nanoscope IIIa). The image field sizes scanned were $5 \mu\text{m} \times 5 \mu\text{m}$, $10 \mu\text{m} \times 10 \mu\text{m}$, and some times $20 \mu\text{m} \times 20 \mu\text{m}$ at various regions of the sample using a piezoelectric J – scanner. The measurements were in contact mode using a silicon nitride tip on a cantilever having a force constant of 0.38 N/m or 0.06 N/m . The $2.5 \mu\text{m} \times 2.5 \mu\text{m}$ images of the samples were flattened using the Nanoscope IIIa software and analysed to determine the height differences (by section analysis) between the observed domains (Nag *et al.*, 2004b; Harbottle *et al.*, 2003). Also, in order to compare the AFM image of the BLES film alone to that of BLES+Fbg film with respect to shape of the domains and height differences, parameters such as field size, Z-scale, compression surface tensions at which the films were deposited were kept constant for all experiments. At least 3-5 areas of a typical deposit were scanned and a representative image was displayed.

2.3.4 Differential Scanning Calorimetry (DSC)

In DSC the sample and inert reference are heated independently in such a way that their temperatures remain equal. In the absence of phase transition the differential heat flow between the sample and reference is zero or constant. As phase transition takes place, heat has to be applied to or withdrawn from the sample in order to maintain the same temperature in sample and reference compartments. The differential heat flow is recorded as a function of temperature to produce a peak shaped trace known as an endotherm. The term 'Scanning' implies that the temperature of both sample and reference is varied at a programmed rate. It has been previously realized that the phospholipids of the cell membrane exist as bilayers and are crucial in maintaining the structure and function of a cell. In the pioneering work of Chapman and Collin (1965), it was demonstrated that the phospholipid dispersions exhibited thermotropic mesomorphism i.e a number of phase changes occurred during melting. Thermotropic mesomorphism indicates that these compounds do not pass directly from a crystalline state to an isotropic liquid, but that, at intermediate temperatures, they exist in a liquid-crystalline state. The transitions from gel to a liquid-crystalline state and from liquid-crystalline to an isotropic liquid are endothermic processes (Chapman and Collin, 1965). In the gel state, the hydrocarbon chains of the phospholipids are in fully extended, *all-trans* configuration. At the first transition (transformation to the liquid-crystalline state) the hydrocarbon chains in the bilayer 'melt', their mobility increases and they are no longer in the fully extended state. The number of gauche conformations increases and the chains display 'kinks' with increasing temperature. The chain 'melting' requires quite an appreciable investment of

energy, whereas the transformation from the liquid-crystalline state to an isotropic fluid state, which occurs at higher temperatures (capillary melting) is accompanied by small changes in the enthalpy and entropy, as it involves only the breakdown of the polar lattice.

DSC endotherms (heating thermograms) over a temperature range of 10 °C-50 °C were obtained for BLES and DPPC using a commercially available DSC (MC-2 Differential Scanning Calorimeter, Serial No. 025, Microcal, LLC Inc., Northhampton, Massachusetts) by methods discussed by others (Keough and Kariel, 1987). A sharp transition of 41°C was observed for DPPC vesicles, whereas BLES showed a broad transition between 10°C-35°C with maximal heat flow (T_{max}) occurring at 27°C.

Endotherms of DPPC/or BLES plus varying percent by weight of Fbg were obtained over a temperature range of 10°C-45°C. This range was chosen so as to include the main transition in DPPC which occurs at 41°C (Chapman and Collin, 1965; Keough and Kariel, 1987) and to avoid thermal denaturation of Fbg which happens at 50°C. A scanning rate of 30°C/hr was used throughout the DSC experiments unless otherwise stated. A total of 3-scans were taken for each sample, with a 60 min break in between for the phospholipid to cool back to the starting temperature of 10°C (Keough and Kariel, 1987). The scans obtained were later baseline normalized (to kcal/mole of phospholipids) using the MicroCal Origin data analysis software. Normally the second or third scan out of the 3-cycles was shown in the data, as previously described by others (Keough and Kariel, 1987). All DSC samples were studied at least 3 times (n=3) and a representative endotherm of one experiment is shown in the results.

2.3.5 Raman Spectroscopy

The Raman spectroscopic technique is a vibrational molecular spectroscopy which derives from an inelastic light scattering process. With Raman spectroscopy, a laser photon is scattered by a sample molecule and loses (or gains) energy during the process. The amount of energy lost is seen as a change in energy (frequency in wavenumbers) of the irradiating photon. This energy change is characteristic for a particular bond in the molecule. It is a technique which can be used for the analysis of solids, liquids and solutions and can even provide information on physical characteristics such as crystalline phase and orientation, polymorphic forms, and intrinsic stress.

Temperature dependence of BLES dispersions with respect to the various bond stretches was studied at different temperatures. The influence of Fbg on BLES at a ratio of 1:1 by weight was studied for any changes that are brought about in the position and shape of the bands at 28°C.

The C-H stretching bands in the 2800 – 3100 cm^{-1} region have been chosen as one of the regions of interest as the CH_2 symmetric stretching and asymmetric stretching modes in Raman at 2850 cm^{-1} and 2890 cm^{-1} respectively, are generally the strongest bands in the spectra of lipids. The frequencies of these bands are conformation-sensitive and also respond to changes of the *trans/gauche* ratio in acyl chains. This is also the case, although to a lesser extent, for the vibrational frequency changes due to the terminal CH_3 groups found at 2930 cm^{-1} (symmetric stretch) and 2960 cm^{-1} (asymmetric stretch).

The C–C stretching of the acyl chain backbone which exists either in *all-trans* or *all-gauche* form is the second marker used in our study. Typically, the lipid Raman peaks at approximately 1064 cm^{-1} and approximately 1128 cm^{-1} , respectively, have been assigned to the symmetric and asymmetric *all-trans* C-C stretching vibrations. The random C-C stretch (*trans-gauche-trans*) appears at around 1089 cm^{-1} (Lippert and Peticolas, 1971; Spiker and Levin, 1975).

The Raman spectra were obtained using a LABRAM confocal microscope (Horiba Jobin Yvon Inc, Edison, NJ, USA) with a grating (1800 groves/mm), a Leica microscope equipped with a long-working distance objective with magnification factor of 50X, and a Peltier CCD detector. The spectra were obtained by using the 532 nm green laser (Ar ion laser) line for excitation. The D_0 filter (no attenuation) and acquisition times of 30 seconds were used in acquiring the spectra. Spectra were also obtained from 15 min to 2 hrs acquisition times without any major changes observed from the 30 sec spectra. The short time period was chosen to avoid drying effects. The Raman spectra of BLES with and without fibrinogen at different temperatures were obtained by placing the sample chamber (small glass cuvette covered by a brass jacket) on a heating-cooling stage which, in turn, was placed on the microscope stage of the Raman confocal microscope.

2.3.6. Fourier Transform Infrared Spectroscopy

Infrared Spectroscopy is an absorption technique in which the intensity of absorption is measured. The position of absorption bands depend on the energy

difference between resonance states of specific vibrational modes of the molecule. These energy differences are in turn affected by intra- and intermolecular conformations and interactions, leading to changes in the absorption maxima. The frequency shift of the incident light occurs due to the molecular vibrations of the C-H, C-C etc. bonds of the phospholipids of the sample (Dluhy and Mendelsohn, 1988). All the IR spectra were obtained in absorbance mode for our studies.

FTIR experiments were carried out with a Bruker Tensor 27 Infrared Spectrometer (Bruker, Billerica, Massachusetts). This instrument is equipped with a MIRacle Attenuated Total Reflection (ATR) accessory allowing rapid and easy Fourier transform analysis of liquid and solid samples.

Previous experiments in our laboratory of BLES dispersions with different concentrations of BSA (bovine serum albumin) were performed in this instrument by allowing an infrared beam to reflect from the sample laid on the surface of a zinc crystal (Vidyasankar, 2004). This method of handling our sample (BLES) i.e. placing it on the zinc crystal and analyzing, resulted in extremely weak signals for the supposedly intense lipid C-H vibrations of the fatty chains. Because the infrared beam in ATR was reflected off the sample surface laid on the zinc crystal from below, signals were obtained only from the groups (particularly the polar head groups in BLES) which were exposed to the evanescent field of IR beam. This resulted in weak signals for all the lipids present in multilamellar vesicles which normally yield the strongest signals in a surfactant due to the presence of numerous C-H bonds in the two fatty chains, and the method was not utilized in our study. In this work, a demountable FTIR liquid cell (Pike Technologies,

Madison, WI) has been used to rectify the problem (which occurred only with our sample-BLES). Initially, the two disc-shaped window materials (made up of CaF₂) were sealed in place using the aluminum needle plate and Teflon alignment posts as guides. This sealed assembly is placed in a demountable liquid cell holder which can eventually be placed in any commercial Bruker IR instrument. BLES dispersion is then injected in-between the window materials through an inlet port located in the cell. The sample volume between the windows is controlled by using appropriate pathlength spacers. A pathlength spacer of 0.05mm thickness, capable of holding a maximum volume of 200 μ L was used. BLES dispersion (sandwiched between windows materials) interacts uniformly with the IR beam as the holder is placed in its path and the beam passes directly through the sample. Spectra (intensity Vs wavelength) were obtained at 28°C for BLES, BLES + fibrinogen, and BLES + BSA dispersions. The data was then treated to subtract the unwanted large water peak (appearing at 1640 cm^{-1}) in the spectra. The absorbance values of the background solvent were subtracted from those of the corresponding numbers of the sample-containing-solvent to obtain a solvent subtracted spectrum.

2.3.7 Transmission Electron Microscopy

Transmission electron micrographs were obtained for BLES/Fbg dispersions by methods discussed elsewhere (Nag *et al*, 1999a). Samples were fixed in 4% glutaraldehyde and water, stained with 1% OsO₄, pelleted by centrifugation and left overnight. The sample was then dehydrated with acetone, and embedded in an epoxy

TAAB 812 resin. This was followed by ultrathin (100nm) sectioning of the resin block using a Reichert 0 mU2 ultra microtone to 90 nm thicknesses. It was then counterstained with uranyl acetate and lead citrate, and examined with a Zeiss EM109 transmission electron microscope, and photographs of the images were ultimately obtained. Details of such methods applied to LS were discussed previously (Nag *et al.*, 1999a).

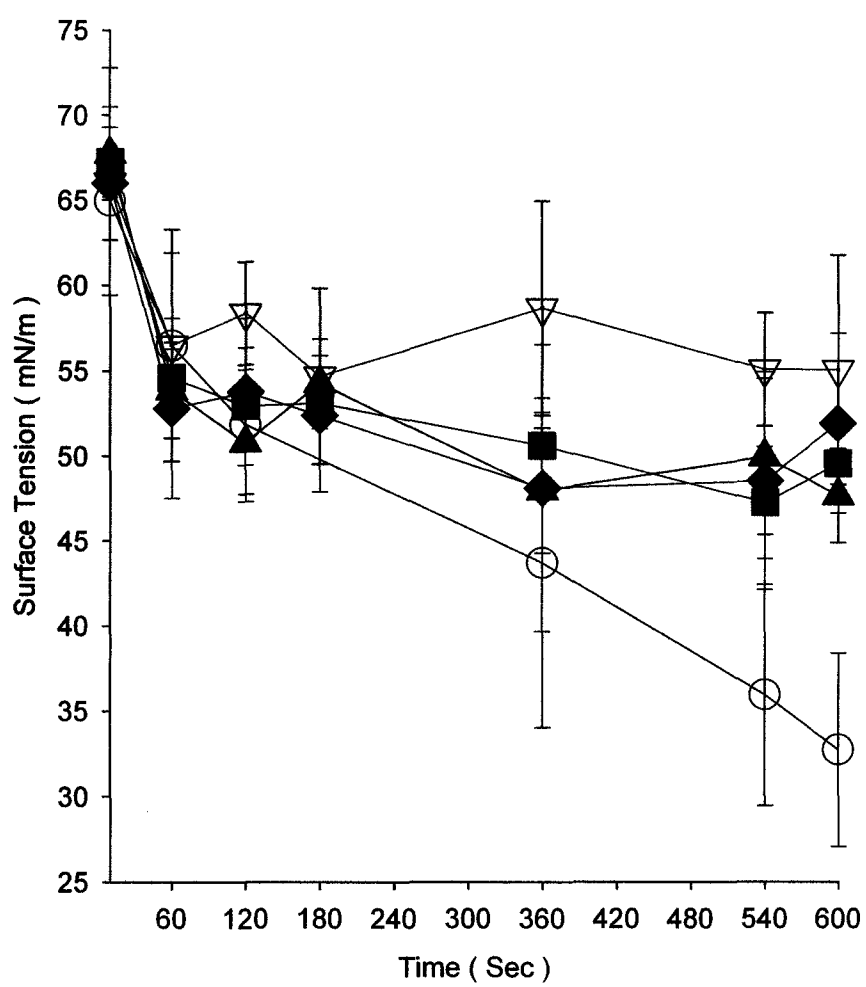
Chapter – 3

RESULTS

3.1 Adsorption Isotherms

Adsorption experiments were carried out in which BLES (6.75mg/ml) or BLES+Fbg dispersions (in which the concentration of BLES was similar to that in BLES alone) were injected beneath the clean air-buffer interface. The adsorption of materials to the surface was measured as a function of time (in seconds), monitored by a change in surface tension (γ). Fbg at various percentages by weight was added to BLES dispersions (6.75 mg/ml) and studied. BLES: Fbg mixtures (1:0, 1:0.5, 1:1, 1:10, and 0:1) were incubated at 37°C for one hour before the experiment. Figure 3 shows the adsorption curves for BLES alone and BLES with Fbg. These experiments were repeated three times, and each curve is an average of three independent experiments, with the standard deviations noted by the error bars. After 120 seconds, BLES alone adsorbed rapidly to a minimum γ of 30 mN/m (near the equilibrium γ of 25 mN/m), whereas in mixtures with Fbg, a decrease in the magnitude of the drop in γ in the same time period was observed. Pure Fbg adsorbed to a γ of about 50 mN/m and BLES: Fbg (1: 10, wt/wt) showed the lowest decrease in γ . A final equilibrium γ of approximately 55 mN/m, significantly higher than the equilibrium γ of 30 mN/m for BLES was obtained with Fbg. This suggests that Fbg does not allow the BLES to adsorb rapidly to an air-water interface. Statistically however there was no significant difference between the adsorption data (as indicated by the large error bars) of BLES: Fbg and those of BLES alone at 360 seconds.

Figure 3: Adsorption isotherms (surface tension vs. time) of BLES dispersion in buffer (6.75 mg/ml) and with varying amounts of Fbg in the dispersions at $23 \pm ^\circ\text{C}$ is shown. The curves are an average of $n=3$ sets of experiments, with standard deviations, shown by error bars. Pure fibrinogen adsorbed to a γ of only 50 mN/m, whereas BLES reached $\sim 30\text{mN/m}$ after 600 seconds.



- BLES
- Fibrinogen
- ▲ BLES : Fibrinogen (1 : 0.5 , wt/wt)
- ◆ BLES : Fibrinogen (1 : 1, wt/wt)
- ▽ BLES : Fibrinogen (1 : 10, wt/wt)

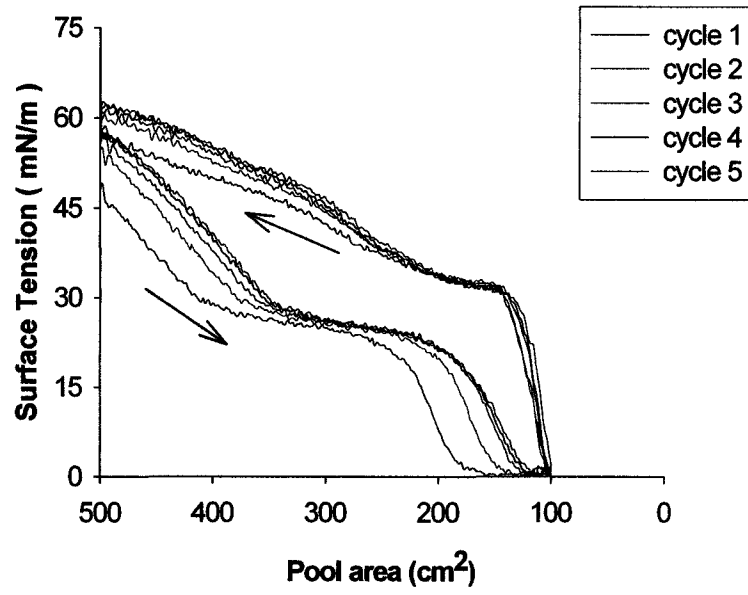
3.2 Monolayer (Surface balance) experiments

Figure 4 compares multiple compression-expansion cycles of adsorbed films of BLES in buffer (a) with multiple cycles of BLES: Fbg (1:1, wt/wt) (b). Compression-expansion cycles were carried out at a speed of 7.3 cm²/sec. The amount of BLES (1.62 mg) used to form the adsorbed monolayer was kept constant. BLES films showed a reduction of γ to a minimum of ~ 0 mN/m, whereas, when Fbg was present in the BLES dispersion, as in (b), there was a rise in γ to around 27 mN/m. This suggests that in the BLES dispersions containing Fbg, the protein interfered with the films reaching a surface tension of near zero.

The change in compressibility of the films of BLES with increasing percent by weight of Fbg in BLES is shown in the bar graph [Figure 5 (a)]. Film compressibility is defined as the ability of the film to be compressed at a fixed surface tension and is expressed as the percent change in film area compressible with a fixed drop in γ of 15 mN/m. It has been calculated using intercepts of total monolayer area reduction in 15 mN/m of γ as shown in Figure 5(b), as previously performed by others using captive bubble surfactometry (Nag *et al*, 2004c and Schurch *et al*, 1992). The films are considered less compressible, the larger the area required to drop the surface tension, as also previously found by others using serum proteins such as CRP for BLES (Nag *et al*, 2004c). The percent change in pool area increases with increasing Fbg in BLES: Fbg mixtures (1:0, 1:0.5, 1:1, 1:10, 0:1 wt/wt). This trend was observed for cycle 2 (shown in blue) and cycle 5 (Green) as shown in Figure 5 (a).

Figure 4: Surface tension vs. Pool area isotherms for compression-expansion cycles of BLES in buffer **(a)** and BLES: Fbg (1: 1, w/w) **(b)** adsorbed onto a buffer subphase. Total monolayer area (100%) was 500 cm² and 5 - cycles were performed for each sample. The amount of BLES in forming the monolayer was kept constant in the both the above dispersions. All experiments were performed at an ambient but monitored room temperature of 23 ± 1°C. All compression-expansion experiments were repeated 3 times for reproducibility, and only a representative plot is shown for clarity. The average of three sets of data is shown in Figure 5 (a).

(a)



(b)

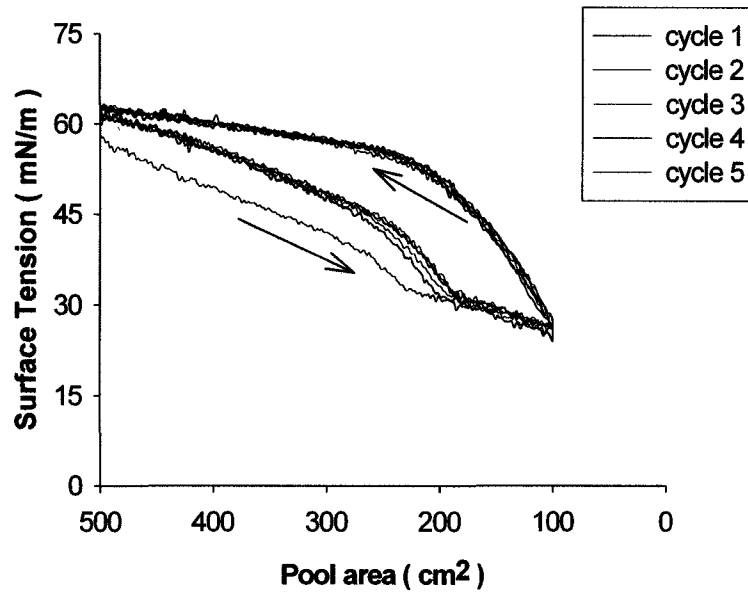
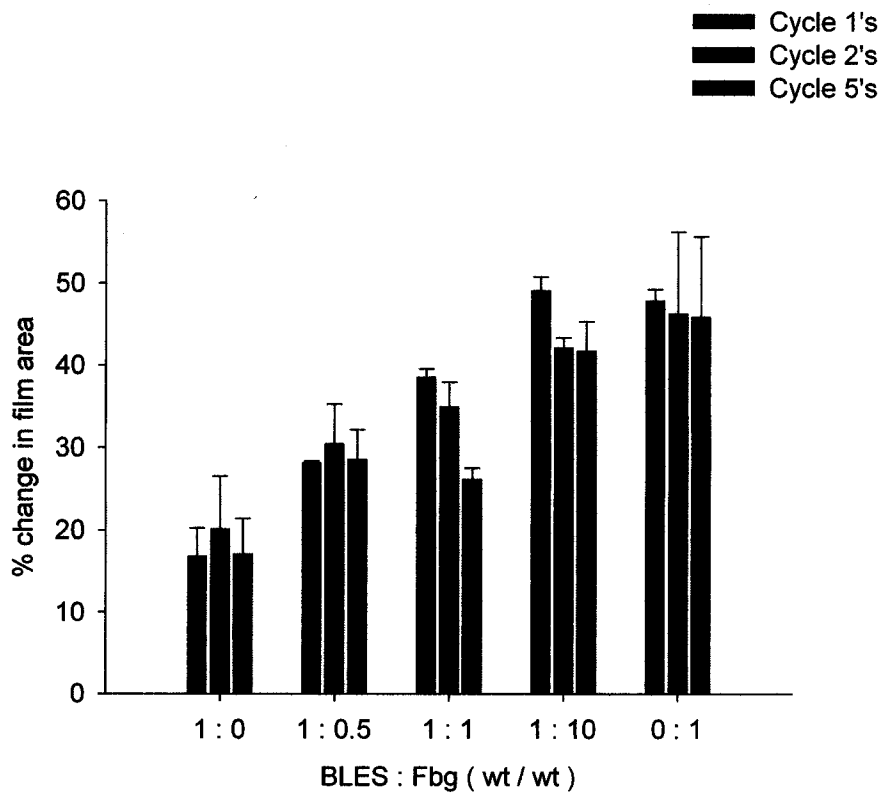
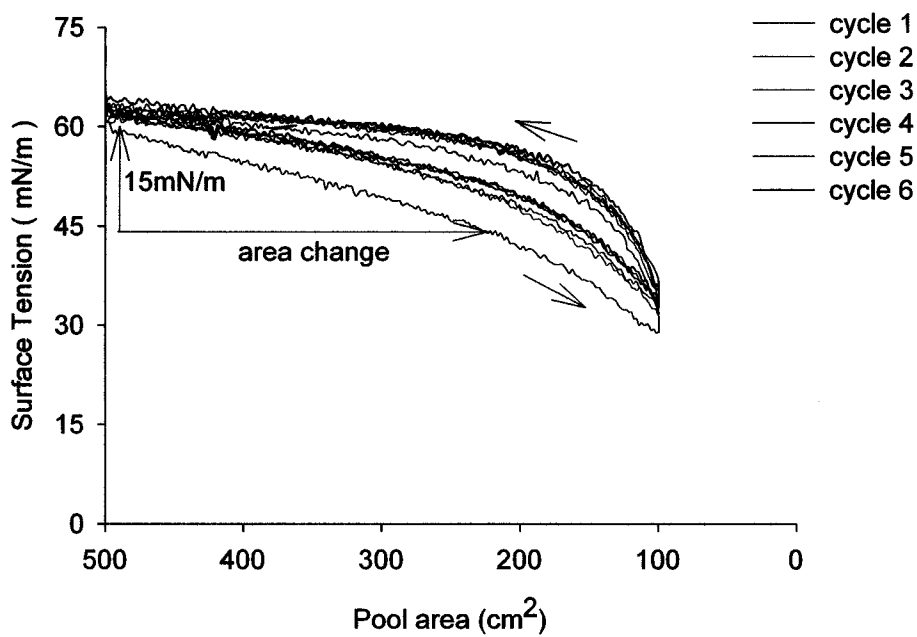


Figure 5: (a) Percent change in film area at increasing weight of fibrinogen in BLES. For all the cycles, the number of experiments at each BLES: Fbg by weight was n=3 and the standard deviation is shown by error bars. (b) Surface tension Vs. Pool area isotherm for compression-expansion cycles of pure fibrinogen adsorbed onto a buffer subphase. This isotherm was repeated 3 times for reproducibility, and only a representative plot is shown for clarity. The areas in (a) are calculated using intercepts of total area reduction in 15 mN/m as shown in (b).

(a)



(b)



3.3 Atomic Force Microscopic Studies

Langmuir-Blodgett films of the samples used in monolayer studies, prepared on a freshly cleaved mica surface were examined using AFM. Representative AFM images of BLES, Fbg, and different amounts of Fbg in BLES are shown in Figure 6 for a film compressed to $\gamma = 52$ mN/m before deposition. The images show that the films undergo a transition from liquid expanded state (fluid) to liquid condensed state (gel-like) with compression (Nag *et al*, 2004a and 2004b). The liquid condensed (LC) or gel-like domains (formed when films were compressed to $\gamma = 52$ mN/m) of BLES in the image are observed as bright greater height circular domains. This is due to a perpendicular tilt of the molecule compared to the plane of the film and the surrounding liquid expanded phase (LE). The isotropic darker background surrounding the gel domains corresponding to the LE phase are lower in height. These LC domains in BLES have approximately a height difference of 1.5 nm (15 Å) as determined by the section analysis of representative images [Figure 8 (a)].

Pure Fbg film images, obtained similarly unlike BLES, did not form domains but rather was deposited more homogeneously as a continuous film (Figure 7). The three dimensional view of the image shows that it has several sharp peaks with an average height of ~ 1.6 nm. Addition of Fbg (at 1:1, wt/wt) in the BLES dispersion showed film structures resembling ribbon-like domains and LC domains [Figure 6 (c)].

Figure 6: Atomic force microscopic images of deposits of films on mica taken at a γ of 52 mN/m for BLES : Fbg dispersions (wt/wt) – (a) 1 : 0 (b) 1 : 0.5 (c) 1 : 1 (d) 1 : 10 (e) 0 : 1. The adsorbed films were compressed at a speed of $7.3 \text{ cm}^2/\text{sec}$. All the Images have field sizes of $2.5 \mu\text{m} \times 2.5 \mu\text{m}$. Appropriate height differences of the domains are indicated by the scale shown using a color bar (2.5 nm). The higher condensed domains in the images are about 1.5 nm higher than the surrounding darker fluid regions.

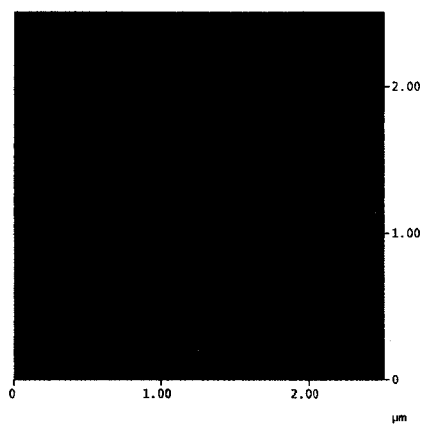
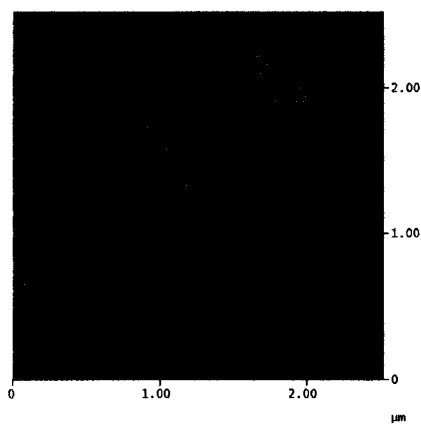
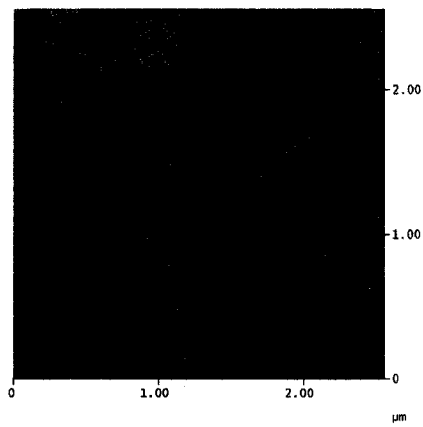
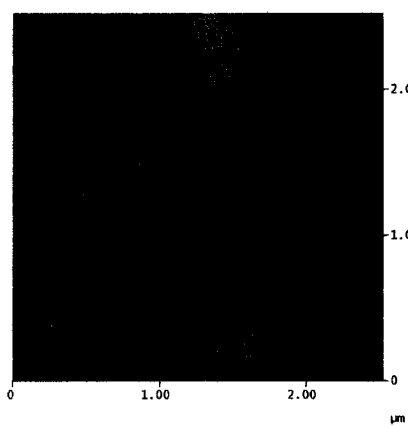
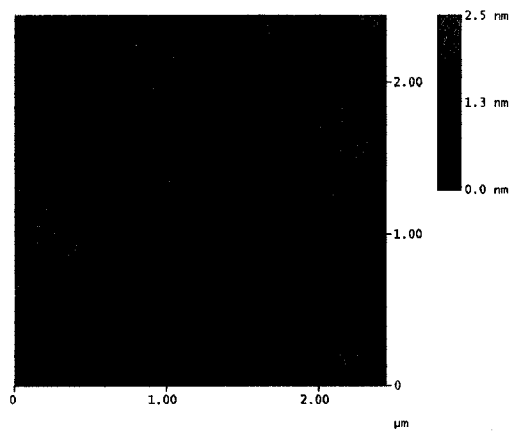
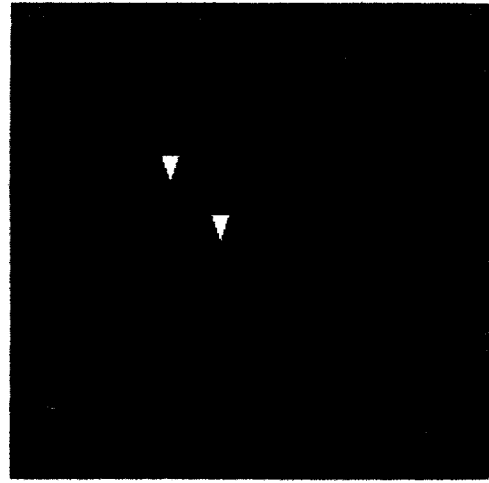
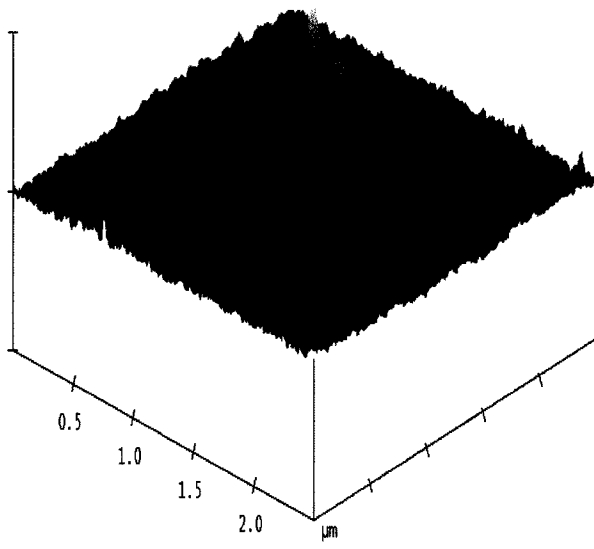
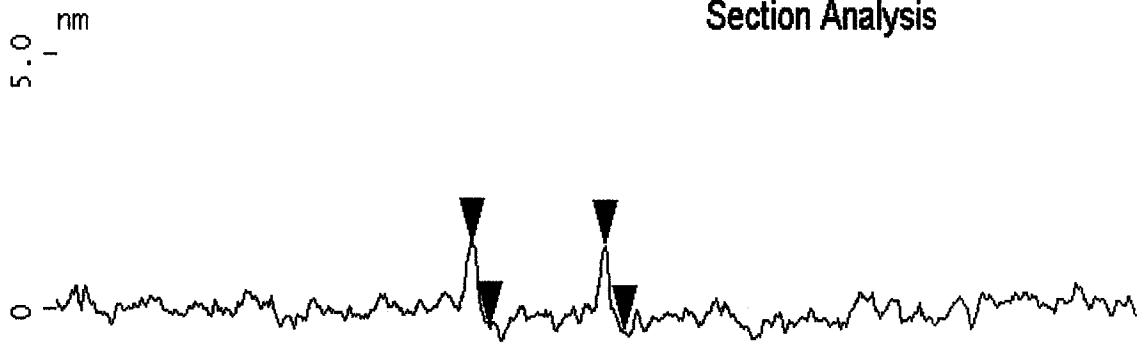


Figure 7: AFM height difference section analysis and three dimensional view of Fbg film deposited on mica taken at a γ of 52 mN/m. The bright regions correspond to the higher topography and the darker areas correspond to the lower height regions. The peaks in the image are about 1.6 nm higher than the surrounding fluid phase.

Section Analysis



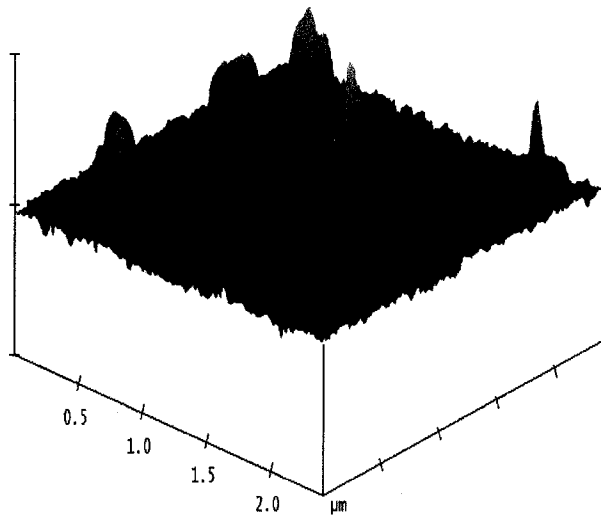
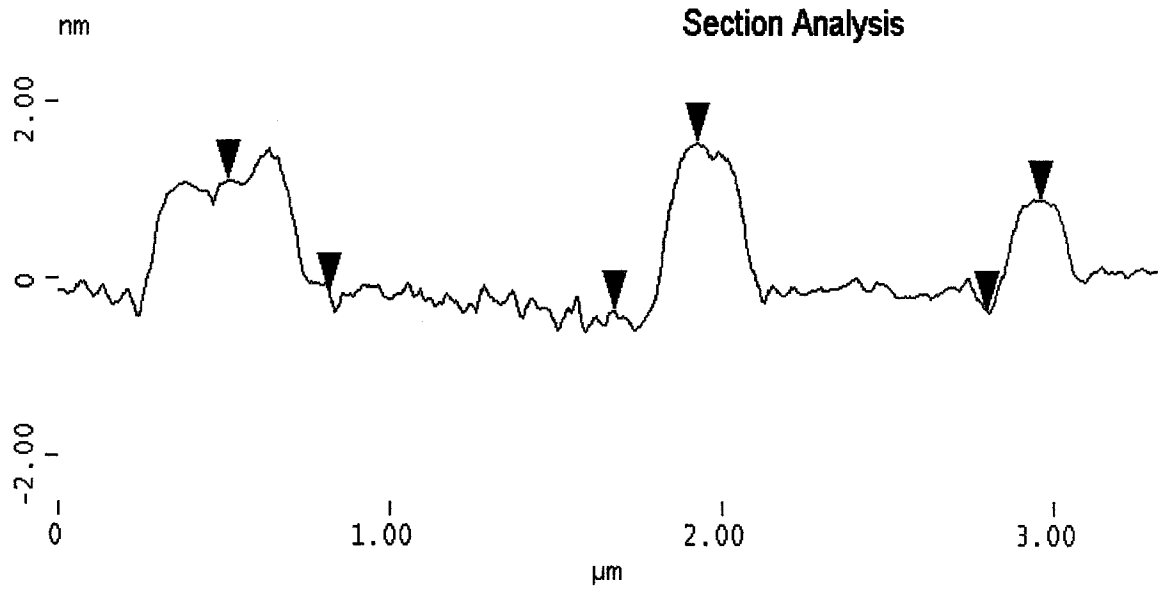
In Figure 8 (a), the BLES condensed domains were observed as clear and distinct structures. Section analysis of these condensed domains showed that they are ~ 1.5 nm above the surrounding fluid phase. In BLES: Fbg (1:1, wt/wt) [Figure 8 (b)], the BLES domains (formed at a $\gamma = 52$ mN/m) were still intact and distinct with a slight reduction in height from 1.5 nm (as seen in BLES alone) to 1.1 nm. Other structures seen in the image as continuous stream of peaks (height of the peaks = ~ 1.2 nm) surrounding the BLES gel domains may be fibrinogen or its aggregates.

The condensed domains were no more isolated in films of BLES alone [Figure 8 (a)] and, conversely, seem to associate into the so called ribbon-like network of possibly the protein. The other observation from such films is that Fbg has no direct effect on the condensed BLES domains and, possibly, the protein is inserted in the fluid phase. These effects are seen in three-dimensional view as in Figure 8 (b) which shows that the ribbon-aggregate network of the protein is found only in the fluid (expanded) phase, although some of the aggregates seem to be in contact with the condensed domains.

The films of BLES [Figure 9 (a)] and BLES with Fbg (1:1, wt/wt) [Figure 9 (b)] deposited on mica and taken at a $\gamma = 42$ mN/m, showed similar features as in the previous images. BLES gel domain was seen as adhering to the surrounding Fbg aggregates even at lower surface tension (high surface pressure).

Figure 8: AFM height difference section analysis and three dimensional view of deposited films on mica taken at a γ of 52 mN/m - **(a)** BLES; the condensed domains in the image are 1.3nm (red cursor), 1.9 nm (green cursor) and 1.3 nm (black cursor) higher than the surrounding darker area; **(b)** BLES: Fbg (1: 1, w/w); the condensed domain in the image is 1.1 nm (Red cursor) higher than the surrounding darker area. The peaks surrounding the domains are 1.4 nm (green cursor), and 1.4 nm (black cursor) higher than the surrounding darker area.

(a)



(b)

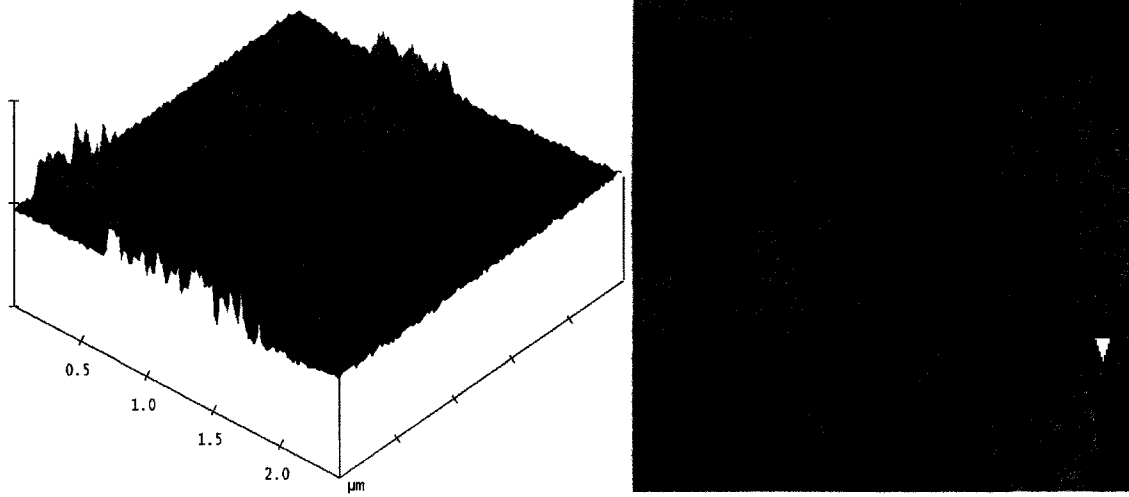
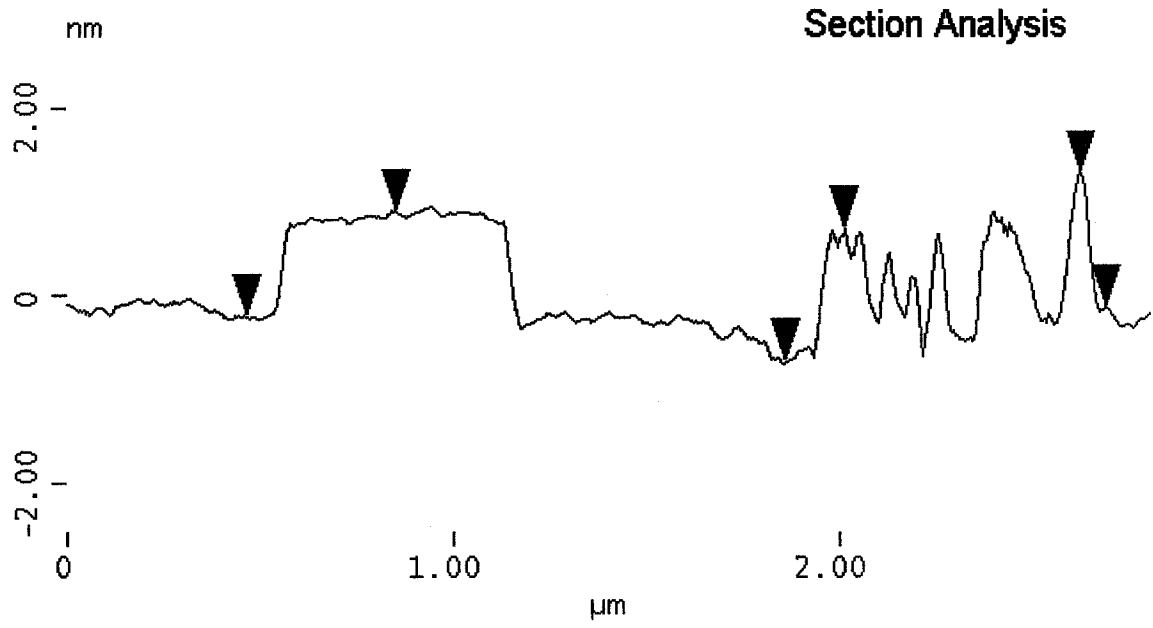
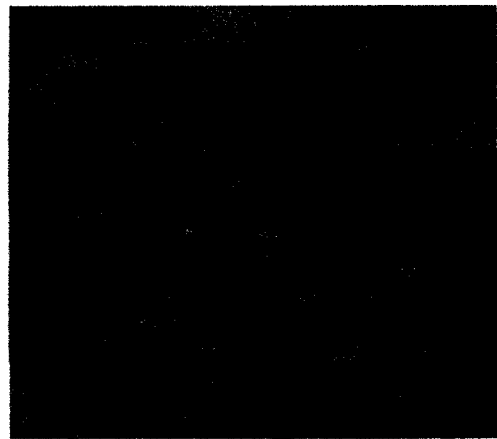
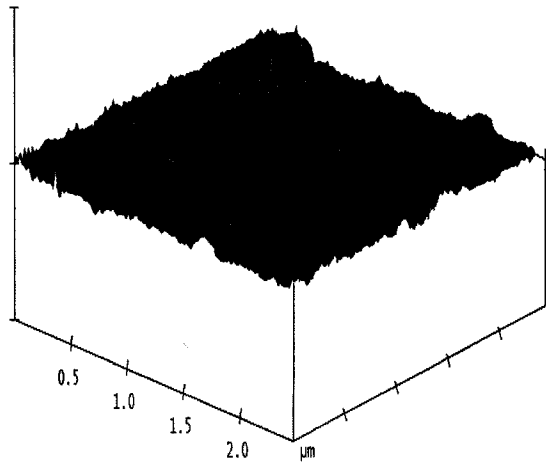
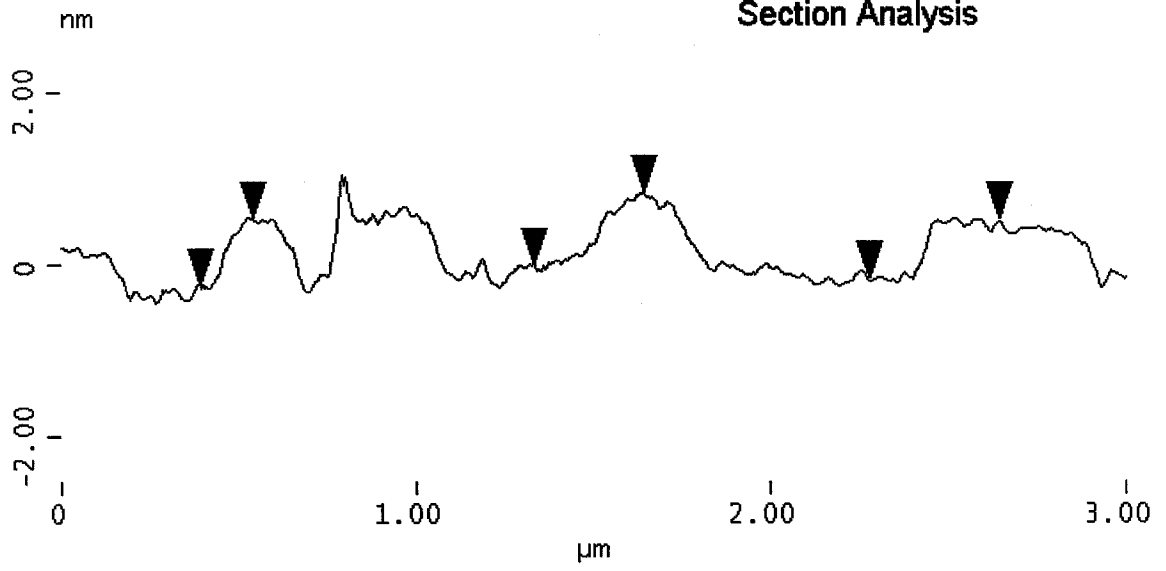


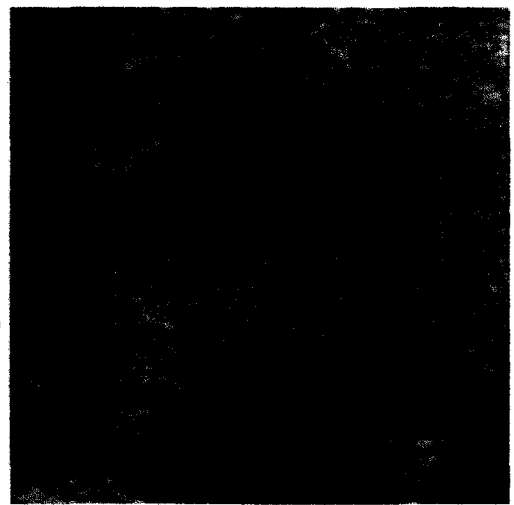
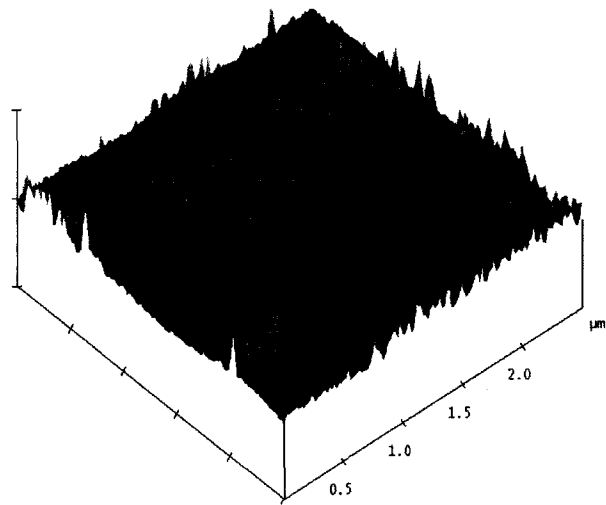
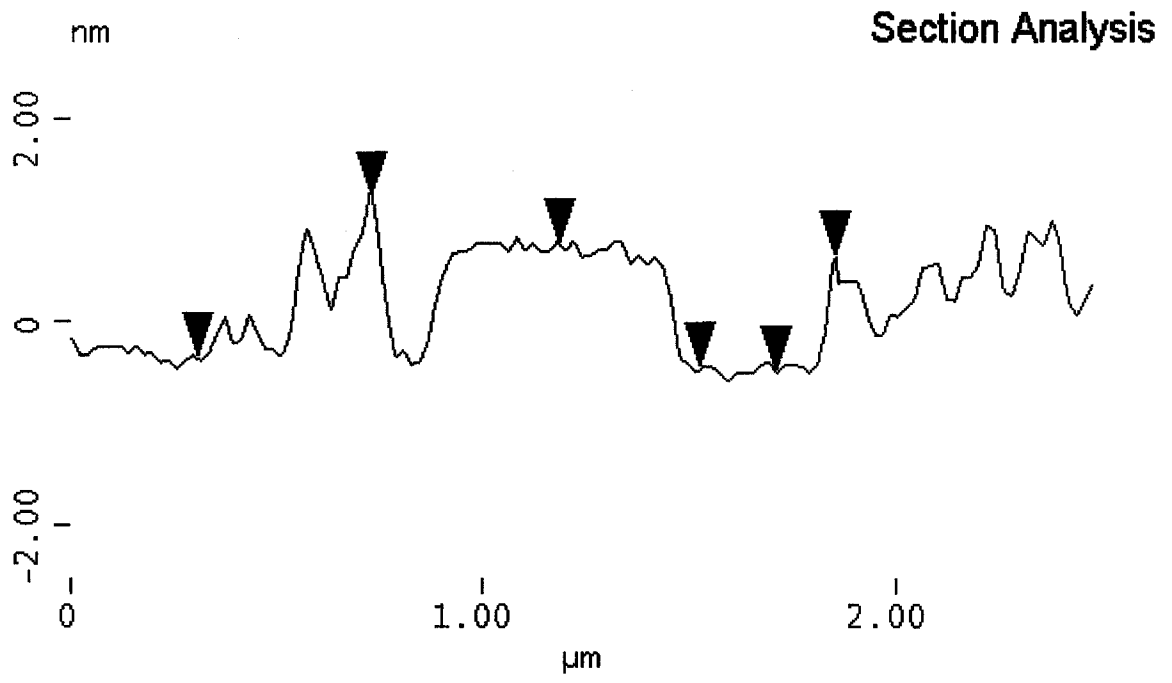
Figure 9: AFM height difference section analysis and three dimensional view of deposited films on mica taken at a γ of 42 mN/m - (a) BLES; the condensed domains in the image are 0.85 nm (Green cursor), 0.8 nm (Red cursor), and 0.74 nm (Black cursor) higher than the surrounding darker area; (b) BLES : Fbg (1 : 1, w/w); the condensed domain in the image is 1.2 nm (red cursor) and 1.6 nm (green cursor), and 1.1 nm (black cursor) higher than the surrounding fluid (or darker) areas.

(a)

Section Analysis



(b)



3.4 Differential Scanning Calorimetric studies

Differential scanning calorimetric heating endotherms of multilamellar dispersions of DPPC alone and with Fbg (1: 10, wt/wt) are shown in Figure 10. Figure 10 (a) illustrates the typical sharp phase transition of DPPC at 41°C in all the three cycles. With DPPC: Fbg at 1:10, wt/wt [Figure 10 (b)], the transition was slightly broadened. Moreover, moving from cycle 1 to cycle 3 [bottom to top in Figure 10 (b)], the main transition peak observed in cycle 2 and cycle 3 were split. A shift in second peak of the transition by $\pm 1^\circ\text{C}$ was observed from that of pure DPPC at 41°C. This result clearly shows that Fbg affects the gel-fluid phase transition of DPPC by interacting with the bilayer to broaden the transition and splitting of peaks when compared to pure DPPC.

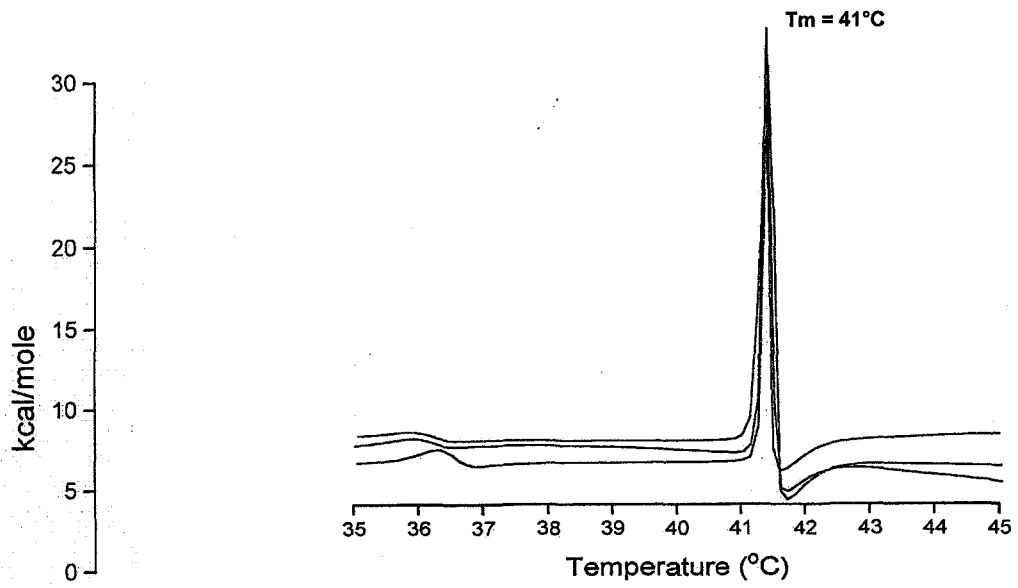
Figure 11 shows the first scan of the heating-cooling endotherms for a pure BLES dispersion and dissolved pure Fbg over a temperature range of 10 °C to 70 °C. BLES showed a broad transition at 28 °C and the Fbg denaturation peak was observed at 50 °C. The three heating scans of BLES were reproducible with all the scans showing a broad transition at 28 °C. This suggested that the gel to liquid-crystalline transition in BLES was reversible. However, the melting or denaturation peak of pure Fbg was not reversible as a flat line was obtained in scan 2 and 3 in DSC.

Figure 12 shows the thermal melting behavior for BLES (a) and with various amounts of Fbg by weight added to the BLES dispersion. For all the DSC curves shown in Figure 12, three scans were obtained but only third scan is shown for clarity. The transitions from scan to scan (3 heating and cooling cycles) were reversible. BLES alone displayed a broad transition and a T_{max} of 27°C which shifted to higher values (34°C)

with increasing amounts of Fbg in BLES. With 1: 0.1 [Figure 12 (b)] and 1: 0.5 [Figure 12 (c)] BLES: Fbg weight by weight, the phase transition was delayed only by 1°C. On the other hand the T_{\max} was moved from 27 °C to 34 °C with added Fbg (1:1) [Figure 12 (d)] and from 27 °C to 35 °C with 1: 1.4 [Figure 12 (e)]. This shift in T_{\max} of BLES with increasing amounts of Fbg clearly shows that Fbg probably is interacting with BLES and allowing the lipids present in it to melt only at higher temperatures. Figure 13 clearly shows this shift in the T_{\max} .

Figure 10: DSC thermograms of DPPC dispersion **(a)** and with fibrinogen at (1: 10, w/w) dispersion **(b)**. Three-cycles of heating and cooling were performed on these dispersions at a scan rate of 30°C/h. All the scans were normalized to kcal/mole of phospholipids with baseline correction (Keough and Kariel, 1997). The curves have been shifted upwards along the y-axis to display all three cycles in the same figure. The transition temperature for DPPC bilayer dispersion was seen at 41.5°C and two peaks were observed at 41.5°C and 42°C for dispersions with fibrinogen.

(a)



(b)

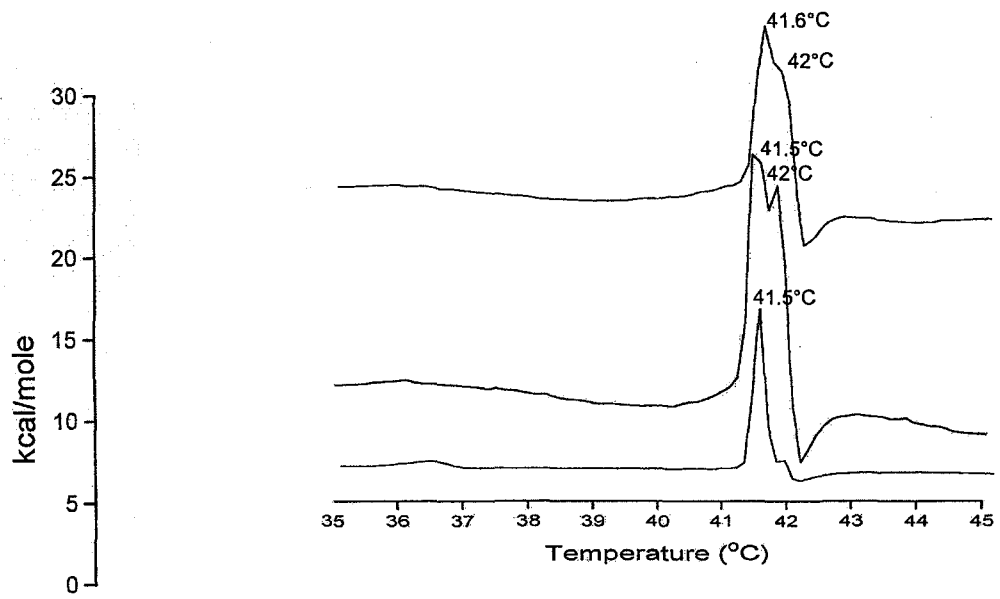


Figure 11: DSC thermograms (cycle 1's) of BLES dispersion and human fibrinogen are shown. Scans were performed at a scan rate of 30 °C/h. The transition temperature for BLES is seen at 28 °C in the graph. The denaturation peaks of Fbg are noted at 50 °C and 53 °C.

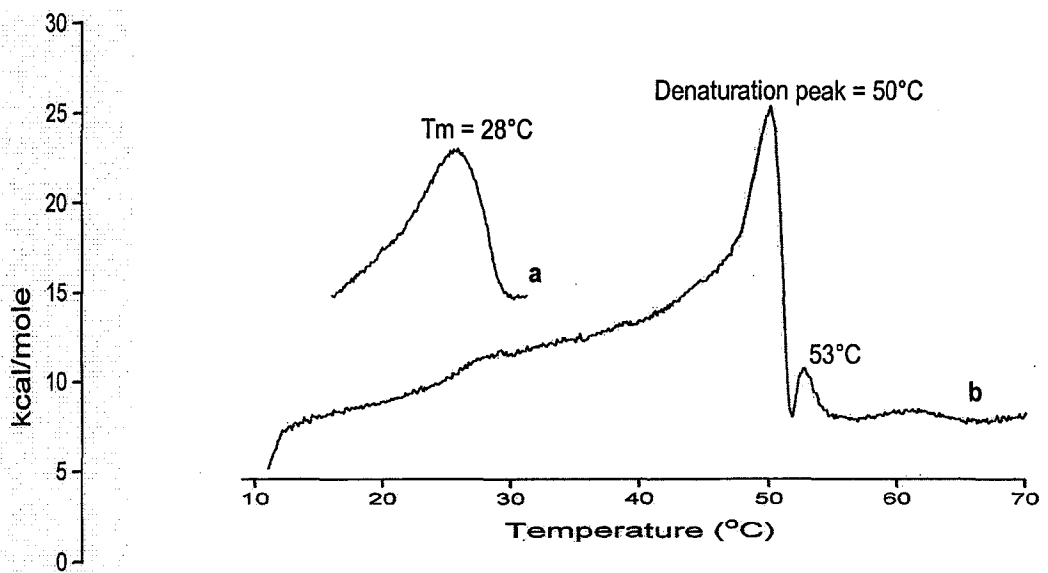


Figure 12: DSC melting profiles of BLES: Fbg (wt/wt) dispersions – **(a)** 1: 0 ($T_{\max} = 27^{\circ}\text{C}$), **(b)** 1: 0.1 ($T_{\max} = 28^{\circ}\text{C}$), **(c)** 1: 0.5 ($T_{\max} = 28^{\circ}\text{C}$), **(d)** 1: 1 ($T_{\max} = 34^{\circ}\text{C}$), **(e)** 1: 1.4 ($T_{\max} = 35^{\circ}\text{C}$). Scan rate was 30°C/hr and scans were normalized to kcal/mole of BLES phospholipids with baseline correction. Three separate sets of experiments were performed for these BLES/Fbg mixtures with 3 individual scans per experiment, and scan 3 of the endotherms is shown for clarity.

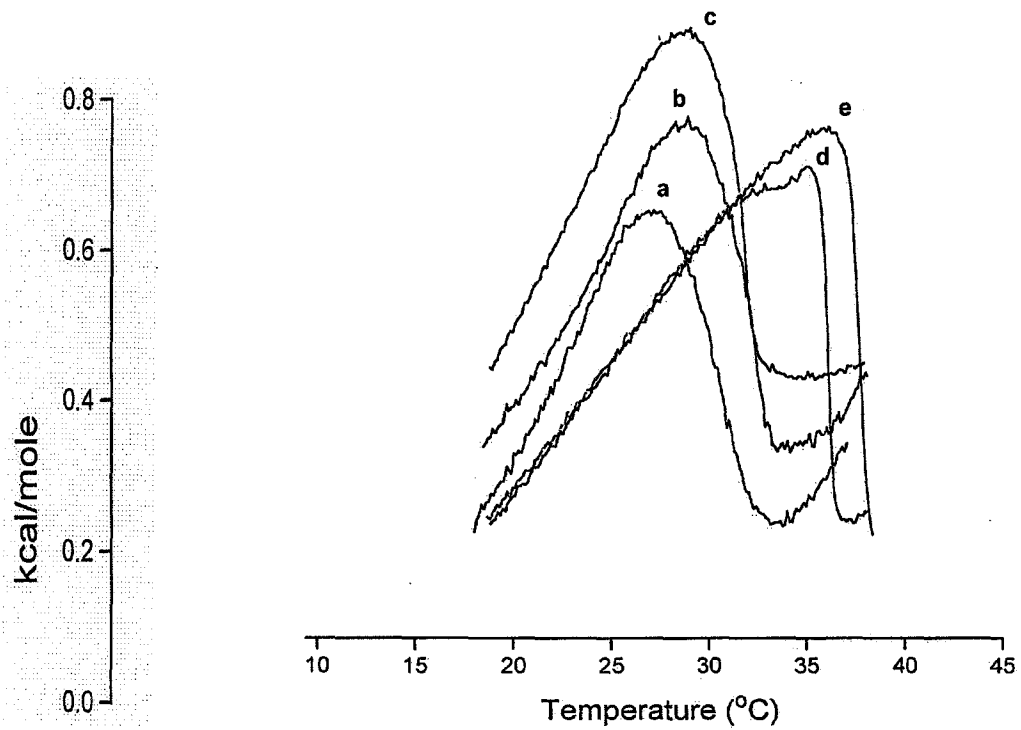
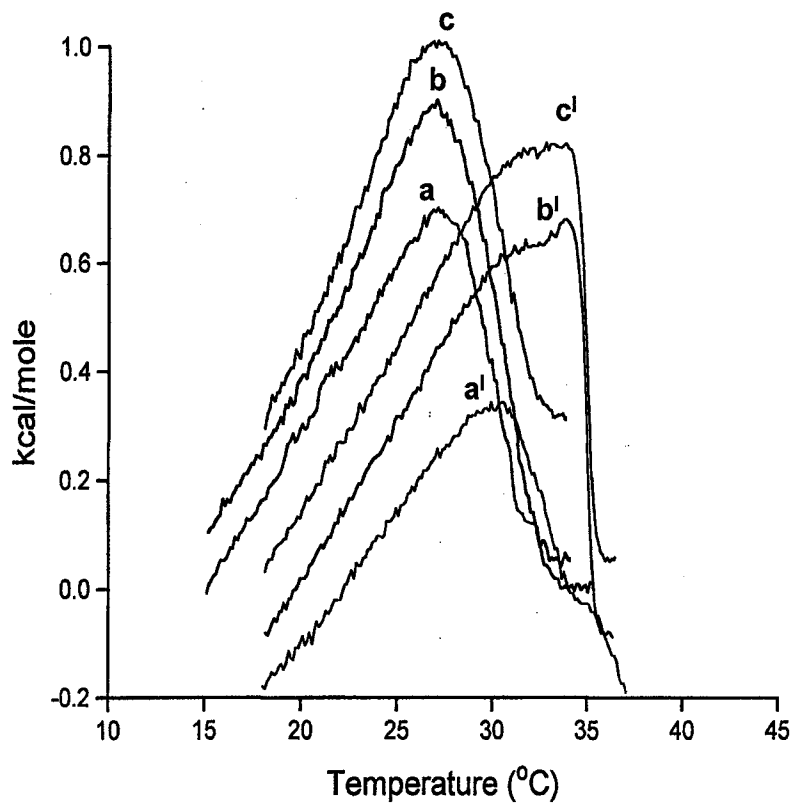


Figure 13: DSC melting profiles of BLES: Fbg (wt/wt) dispersions – cycle 1 ($T_{\max} = 28^{\circ}\text{C}$) (**a**), cycle 2 ($T_{\max} = 27^{\circ}\text{C}$) (**b**), and cycle 3 ($T_{\max} = 27^{\circ}\text{C}$) (**c**) for 1:0 (wt/wt) and Cycle 1 ($T_{\max} = 31^{\circ}\text{C}$) (**a**¹), cycle 2 ($T_{\max} = 33^{\circ}\text{C}$) (**b**¹), and cycle 3 ($T_{\max} = 34^{\circ}\text{C}$) (**c**¹) for 1:1 (wt/wt); Scan rate was 30°C/hr and scans were normalized to kcal/mole of BLES phospholipids with baseline correction. Three separate sets of experiments were performed for these samples with 3 individual scans per experiment, and all the three scans are compared here.



3.5 Transmission Electron Microscopy

Figure 14 shows the transmission electron micrograph (TEM) of BLES dispersion (a) and BLES with Fbg (1: 1, w/w) (b). These dispersions were consistently used for all the DSC, Raman, FTIR, and monolayer studies and are representative of the bulk bilayer phase structures. With BLES alone, the dispersions appeared to be multi-lamellar and the vesicles appeared tightly packed. However, when Fbg was added, the vesicles had appearances in some cases that seemed to show more loosely packed lamellas. Further image analysis is required to confirm such appearances, as only 2-3 samples of this mixture were analyzed and only one representative image is shown.

3.6 Fourier Transform Infrared Spectroscopic studies

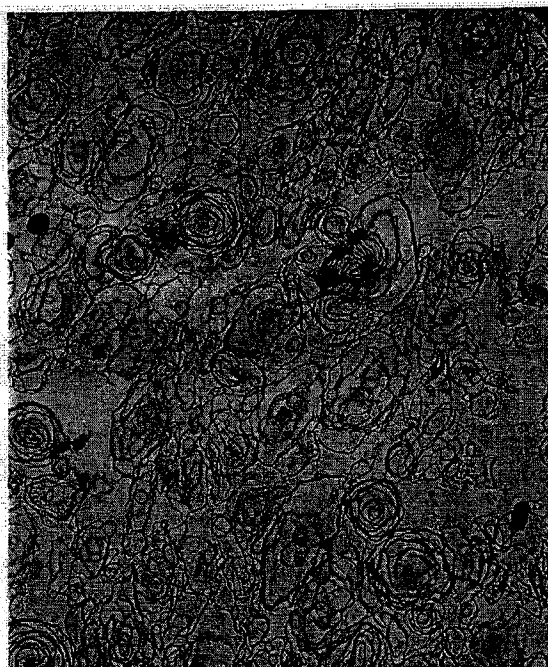
The structure of the phospholipid molecule (the backbone structure of DPPC and BLES) with the major bond vibrations is shown in figure 15. The alterations in some of these vibrational stretches (CH_2 , CH_3 , PO_4^- , etc) with the addition of Fbg were studied using Fourier transform infrared spectroscopy (FTIR) and Raman spectroscopy. Figure 16 shows the complete spectra (with the various vibrations) of BLES taken using FTIR and Raman.

Figure 14: TEM of (a) BLES dispersion and (b) with fibrinogen (1: 1, w/w), where Fbg was added to the preformed BLES MLV dispersion. Samples were prepared and embedded according to materials and methods (Section 2.3.7), and they were positively stained with uranyl acetate and lead citrate. Scale bar applies to both images.

a



b



6 μm

Figure 15: A typical Phospholipid molecule showing the various group vibrations in the acyl chains and in the headgroup region. A comparison of the band frequencies in the FTIR and Raman spectra of BLES (having the basic phospholipid skeleton) is shown in Figure 16.

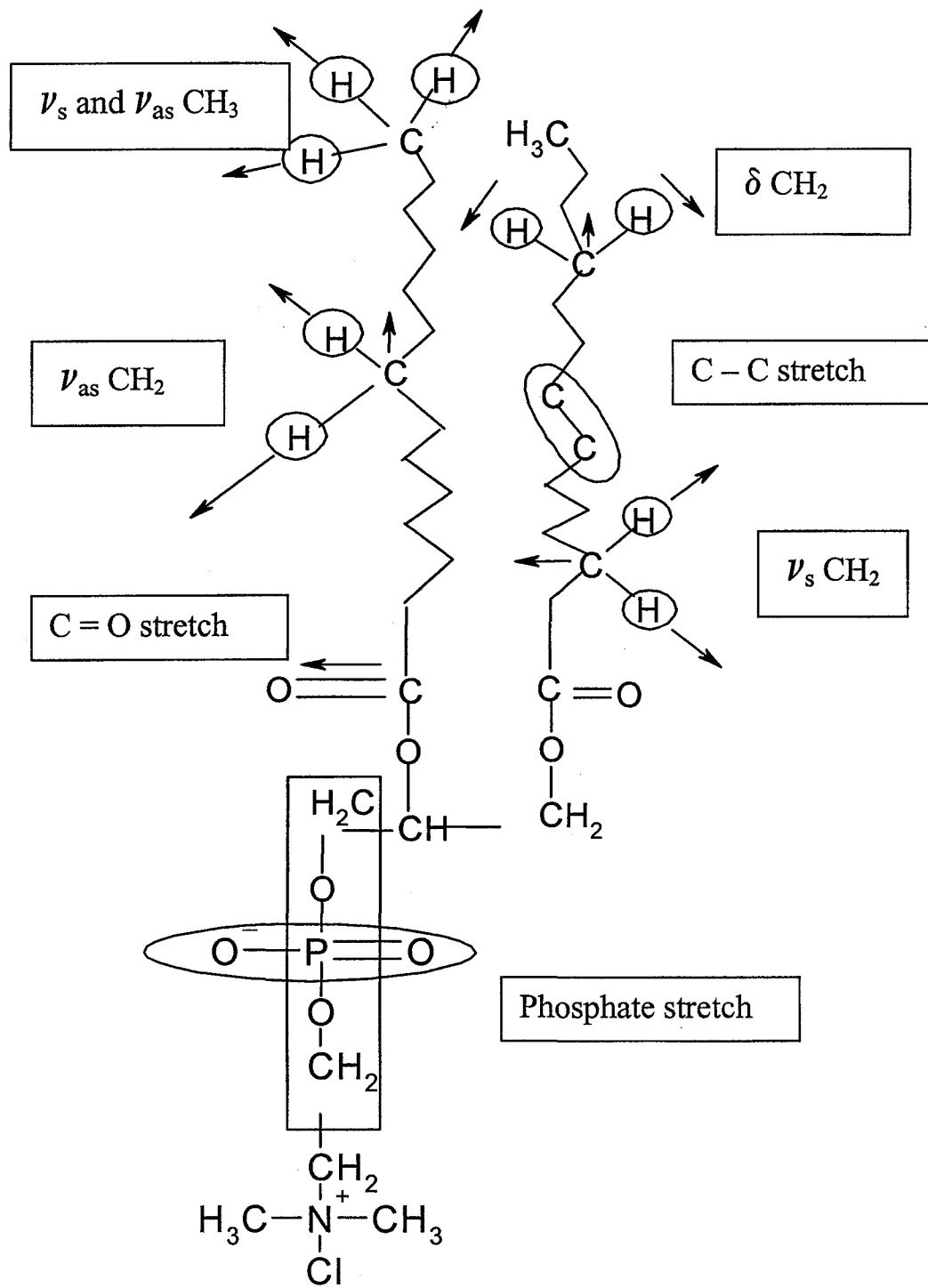


Figure 16: Complete spectra of 27mg/ml BLES dispersion (a) FTIR (b) Raman.

Corresponding peaks have been assigned in the figure.

FTIR bands and their peak assignments for BLES dispersion [typical phospholipid bands have been assigned previously by others (Casal and Mantsch, 1984; Fringeli and Gunthard, 1981; Lee and Chapman, 1986)].

CH₂ stretching, symmetric (ν_s) at 2852 cm⁻¹

CH₂ stretching, asymmetric (ν_{as}) at 2922 cm⁻¹

CH₃ stretching, symmetric (ν_s) at 2872 cm⁻¹

CH₃ stretching, asymmetric (ν_{as}) at 2955 cm⁻¹.

Symmetric phosphate stretch (ν_s PO₂⁻) doublet 1066/1087 cm⁻¹

Asymmetric phosphate stretch (ν_{as} PO₂⁻) at 1224 cm⁻¹

Symmetric methyl bending mode (δ_s CH₃) at 1378 cm⁻¹

CH₂ deformation mode of acyl chain at 1467 cm⁻¹

C=O stretching, esters at 1741 cm⁻¹

Figure 16: Complete spectra of 27mg/ml BLES dispersion (a) FTIR (b) Raman. Corresponding peaks have been assigned in the figure.

Raman bands and their peak assignments for BLES dispersion [phosphatidylcholine Raman bands have been assigned previously by others (Lippert and Peticolas, 1971; Spiker and Levin, 1975)]. Note the absence of large water peak at around 1600 cm^{-1} in the Raman (b) compared to FTIR (a), which was subtracted.

Symmetric phosphate and random (*all-gauche*) hydrocarbon stretch at 1091 cm^{-1} ;

Symmetric (ν_s) and asymmetric (ν_{as}) *all-trans* hydrocarbon stretch (C-C) at 1064 and 1129 cm^{-1} respectively;

Amide III (40% C-N stretch) and CH_2 twisting mode at 1298 cm^{-1}

CH_2 scissoring mode of acyl chain at 1439 cm^{-1}

Amide I (80% C=O stretch) at 1658 cm^{-1}

CH_2 stretching, symmetric (ν_s) at 2852 cm^{-1}

CH_2 stretching, asymmetric (ν_{as}) at 2886 cm^{-1}

CH_3 stretching, symmetric (ν_s) at 2937 cm^{-1} .

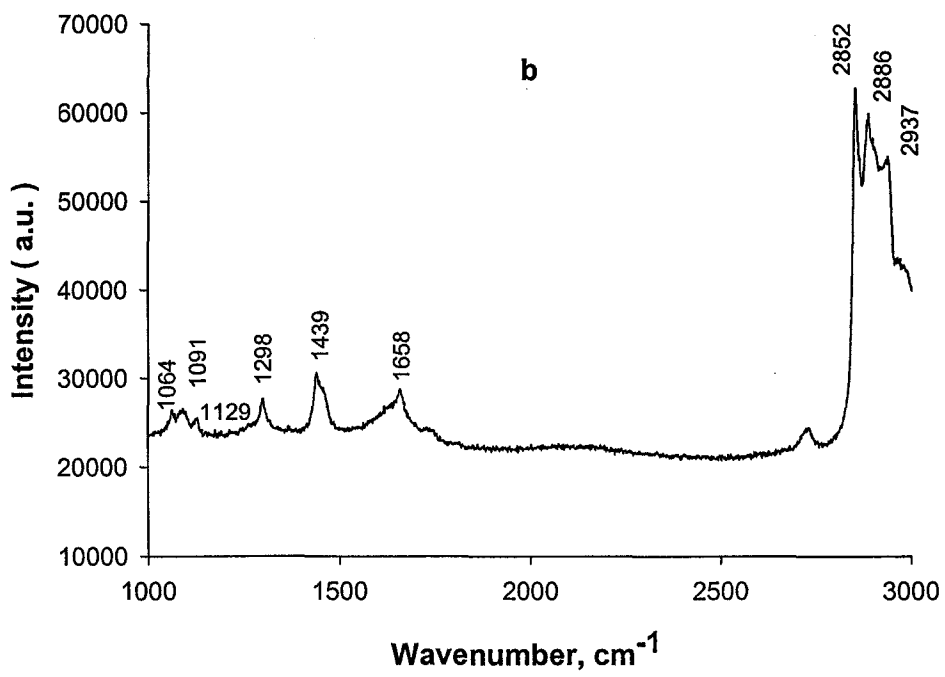
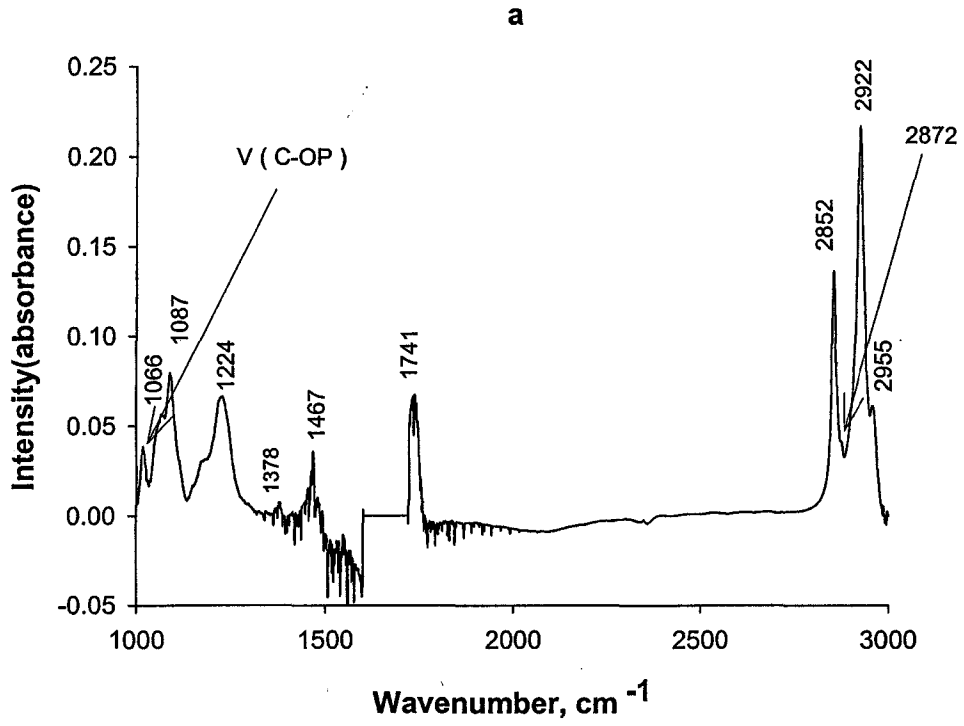
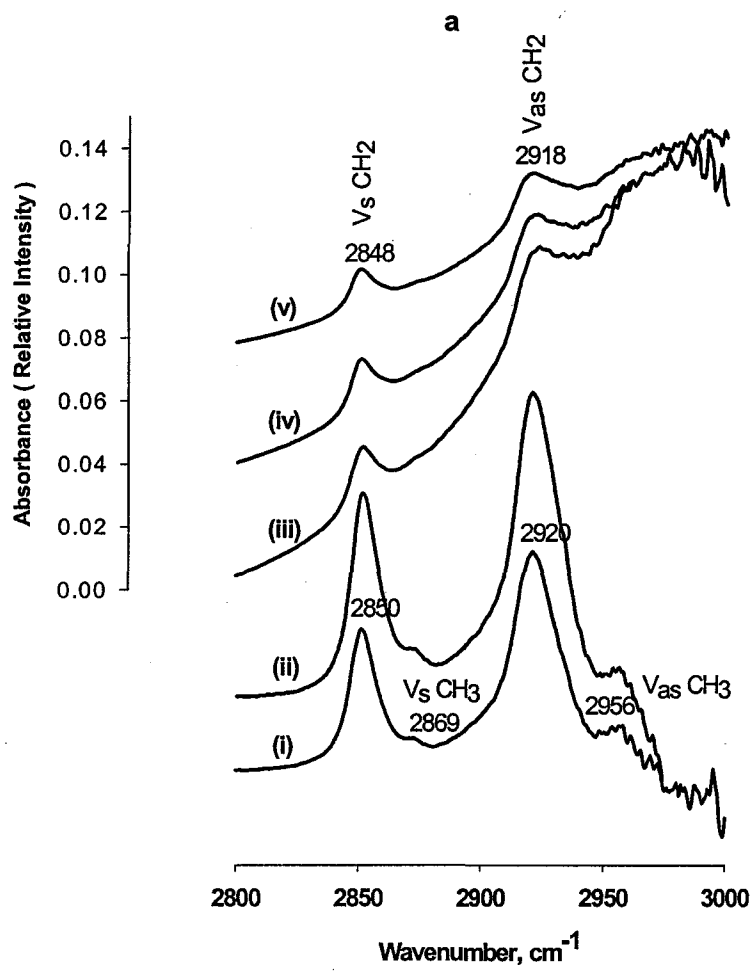
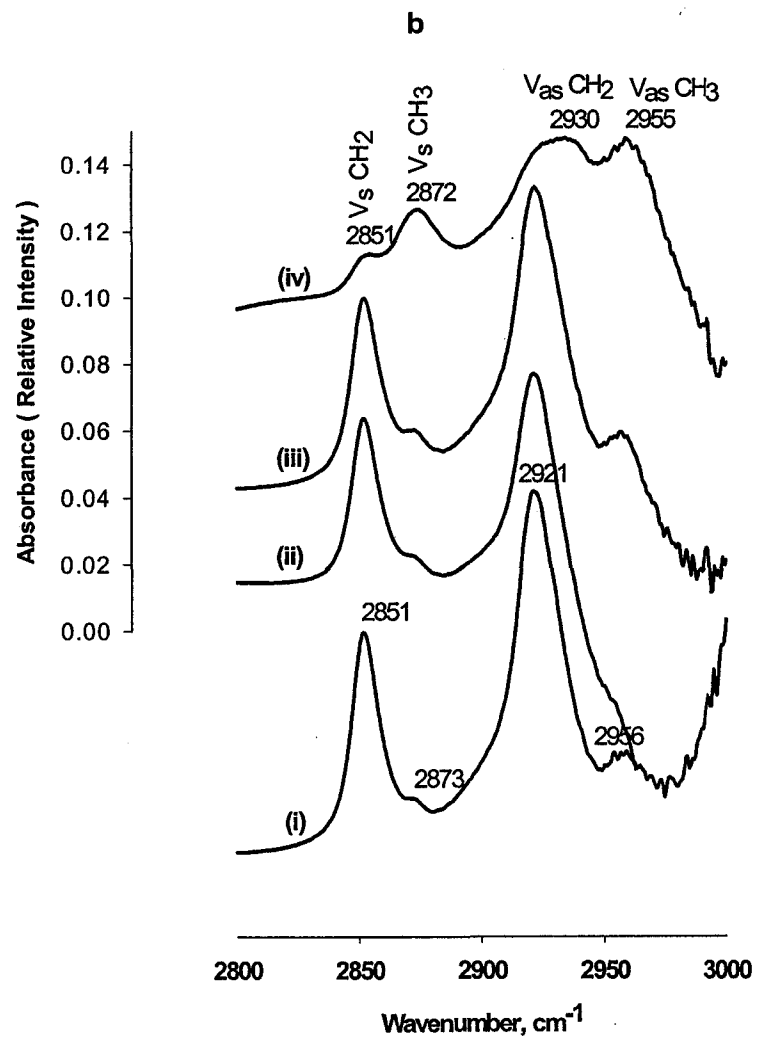


Figure 17 (a) shows how the FTIR spectra of the C-H stretching spectral region (2800 – 3000 cm^{-1}) particularly the symmetric (ν_s) and asymmetric (ν_{as}) methylene/methyl stretching modes in BLES are influenced with various amounts by weight of Fbg in BLES. The symmetric methylene stretch in BLES which appears at 2850 cm^{-1} is broadened gradually with increasing weight of Fbg in BLES as shown in Figure 17 (a). This broadening can be seen clearly with BLES: Fbg (wt/wt) - 1: 0.5 (iii), 1: 1 (iv), and 1: 1.4 (v). Also there seems to be no drastic shift in the wavenumber for symmetric methylene stretch ($\nu_s \text{CH}_2$) with increasing amounts of Fbg. The same effect was observed even with the asymmetric methylene stretch ($\nu_{as} \text{CH}_2$) in BLES which appears around 2920 cm^{-1} . The other prominent effect observed in this region is with the terminal methyl stretches. Both these modes i.e. the symmetric and asymmetric methyl stretches in BLES which appear at 2869 cm^{-1} and 2956 cm^{-1} respectively, was suppressed with increasing amounts of Fbg as shown by the decrease of intensity of these peaks in BLES.

A similar study was also conducted using bovine serum albumin (BSA). BSA, like Fbg, was shown to broaden the symmetric methylene peak but did shift the peaks in wavenumber with increasing amounts of BSA in BLES [Figure 17 (b)]. At 1: 10 (BLES: BSA, wt/wt) (iv), the symmetric methyl ($\nu_s \text{CH}_3$) peak intensity was found to be higher than the symmetric methylene peak ($\nu_s \text{CH}_2$). This effect was, however, not seen with low amounts of BSA. An unusual effect observed was that the asymmetric methylene ($\nu_{as} \text{CH}_2$) peak appearing in BLES (i) at 2920 cm^{-1} was shifted to 2930 cm^{-1} with BLES: BSA (1: 10, wt/wt) dispersion (iv). Also, the asymmetric methyl ($\nu_{as} \text{CH}_3$) peak intensity was found to increase to an equal extent in intensity to that of the asymmetric methylene peak

Figure 17: FTIR spectra of the C-H stretching spectral region ($2800 - 3000\text{cm}^{-1}$) showing the Symmetric (ν_s) and Asymmetric (ν_{as}) methylene/methyl stretches in (a) dispersions of BLES : Fbg (wt/wt) – (i) 1:0 (ii) 1: 0.25 (iii) 1: 0.5 (iv) 1: 1 and (v) 1: 1.4 and (b) dispersions of BLES : BSA (wt/wt) – (i) 1:0 (ii) 1: 0.5 (iii) 1: 1 and (iv) 1: 10. Due to low solubility of Fbg in water, a 1: 10 (BLES: Fbg, wt/wt) mixture could not be prepared [as signals from lower amount of BLES ($< 6 \text{ mg/ml}$) is not significantly observed or feasible for FTIR].





($\nu_{\text{as}} \text{CH}_2$). Again this increase in intensity of $\nu_{\text{as}} \text{CH}_3$ was not even close to the $\nu_{\text{as}} \text{CH}_2$ at lower amounts of BSA in BLES [Figure 17 (b)].

The phosphate group vibrations have the most characteristic stretching in the phospholipid headgroup (polar) region of hydrated DPPC bilayers as noted by Arrondo *et al* (1984). The effect on these phosphate bond stretches of BLES with various amounts of Fbg has been studied in this work [Figure 18 (a)]. The asymmetric phosphate stretching mode ($\nu_{\text{as}} \text{PO}_2^-$) appeared around 1224 cm^{-1} in BLES (i), and this shifted to a lower wavenumber of 1219 cm^{-1} with BLES : Fbg (1: 1.4, wt/wt) dispersion (v). The symmetric phosphate stretching doublet which appeared in BLES around 1087 cm^{-1} and 1070 cm^{-1} were also moved to lower wavenumbers at 1082 cm^{-1} and 1051 cm^{-1} respectively. The other prominent effect observed in this polar region was a greater shift towards higher wavenumbers of the methyl symmetric deformation mode around 1373 cm^{-1} of BLES (i) to 1397 cm^{-1} in BLES: Fbg (1: 1.4, wt/wt) (v).

The change of phosphate vibrations of BLES was also studied with bovine serum albumin (BSA) [Figure 18 (b)]. Unlike Fbg, albumin shifted the asymmetric phosphate stretching in BLES appearing at 1222 cm^{-1} (i) to 1243 cm^{-1} (iv) with 1: 10 (BLES : BSA, wt/wt). This effect was also seen with BLES : BSA (1: 1, wt/wt) as shown in (iii). Similar to Fbg, the symmetric phosphate stretching doublet which appeared in BLES around 1088 cm^{-1} and 1064 cm^{-1} was shifted to lower wavenumbers, 1080 cm^{-1} and 1047 cm^{-1} with BLES : BSA (1: 10, wt/wt) (iv). Also, the methyl symmetric deformation mode around 1377 cm^{-1} in BLES (i) was shifted to 1399 cm^{-1} with BLES : BSA (1: 10, wt/wt) (iv).

Figure 18: FTIR spectra of the polar (PO_2^- stretching) region ($1000 - 1500\text{cm}^{-1}$) showing the Symmetric (ν_s) and Asymmetric (ν_{as}) phosphate stretches in **(a)** dispersions of BLES : Fbg (wt/wt) – (i) 1:0 (ii) 1: 0.25 (iii) 1: 0.5 (iv) 1: 1 and (v) 1: 1.4 and **(b)** dispersions of BLES : BSA (wt/wt) – (i) 1:0 (ii) 1: 0.5 (iii) 1: 1 and (iv) 1: 10

Vibrational modes and their peak assignments as observed in BLES dispersion [typical phospholipid bands have been assigned previously by others (Casal and Mantsch, 1984; Fringeli and Gunthard, 1981; Lee and Chapman, 1986)]

Symmetric phosphate stretch ($\nu_s \text{PO}_2^-$) doublet at $1070/1087 \text{ cm}^{-1}$

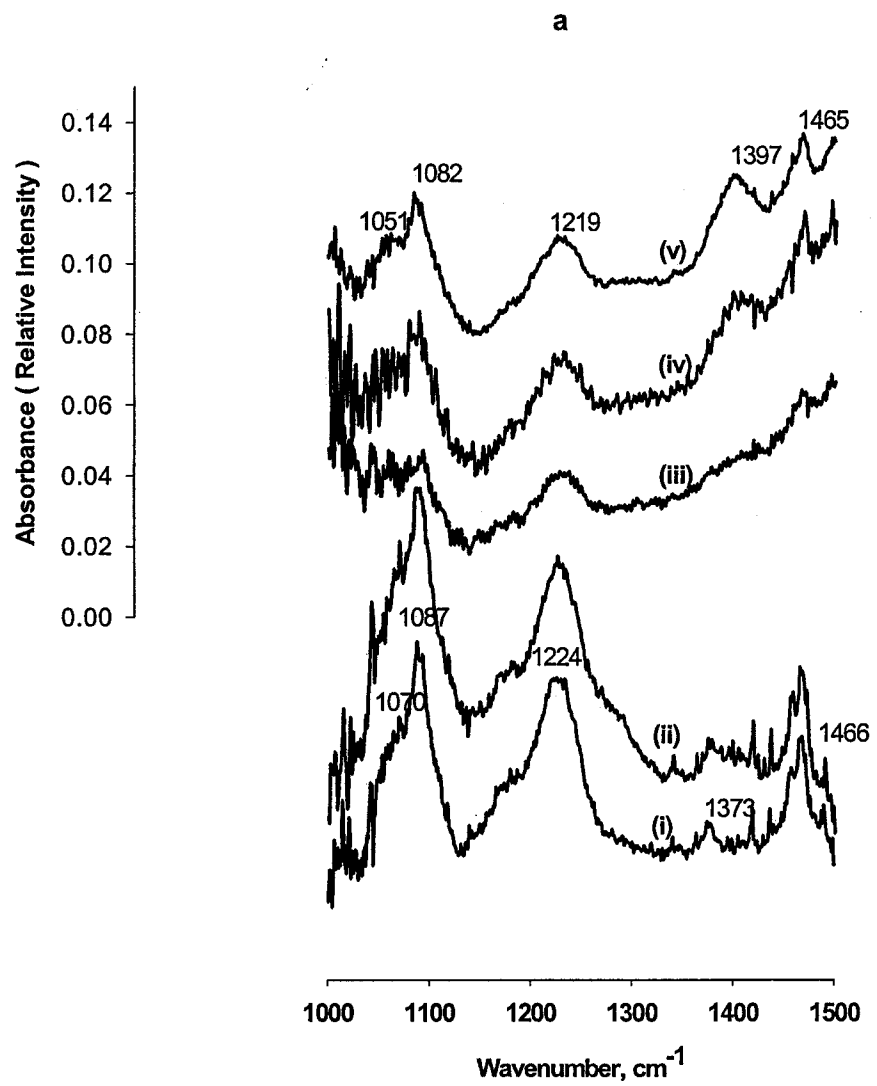
Asymmetric phosphate stretch ($\nu_{as} \text{PO}_2^-$) at 1224 cm^{-1}

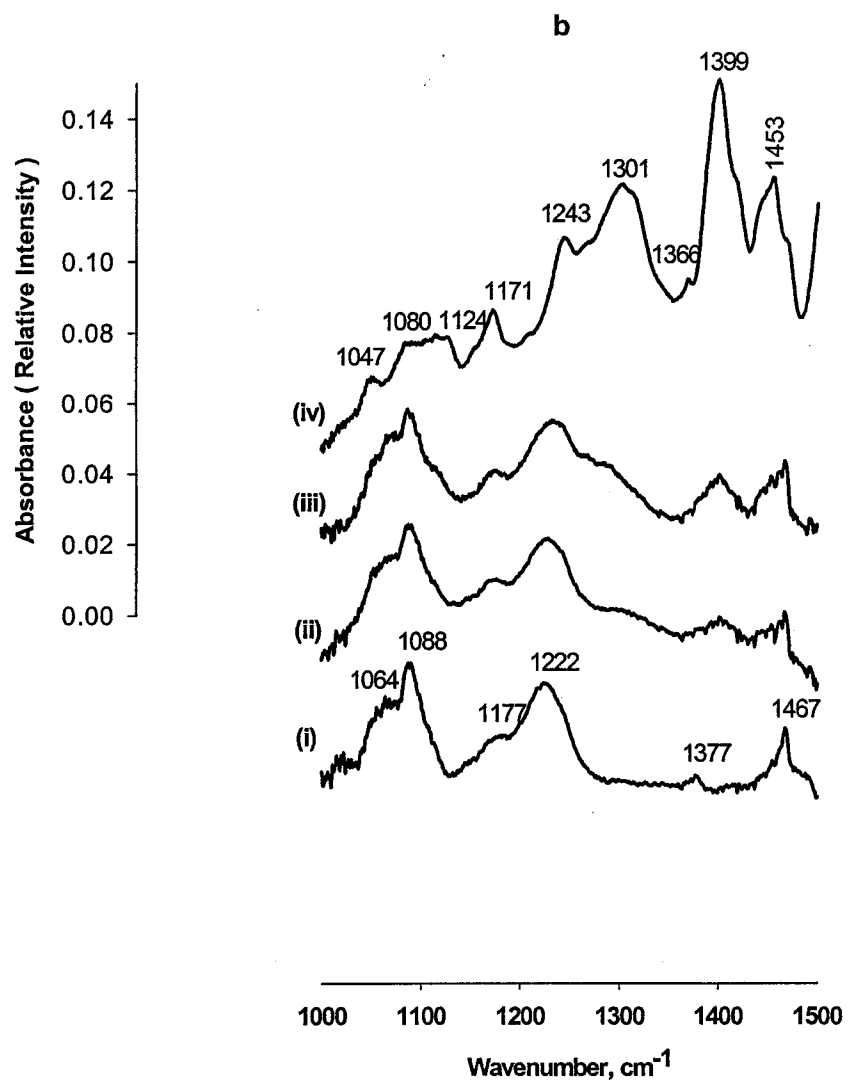
Symmetric methyl bending mode ($\delta_s \text{CH}_3$) at 1373 cm^{-1}

CH_2 deformation mode of acyl chain at 1466 cm^{-1}

Symmetric *all-trans* backbone hydrocarbon stretch ($\nu_s \text{C-C}$) at $\sim 1124 \text{ cm}^{-1}$

Random *all-gauche* backbone hydrocarbon stretch at $\sim 1087 \text{ cm}^{-1}$.





3.7 Raman Spectroscopy of BLES with Fibrinogen

The Raman scattering technique is a vibrational molecular spectroscopy which derives from an inelastic light scattering process. With Raman spectroscopy, a laser photon is scattered by a sample molecule and loses (or gains) energy during the process. The amount of energy lost is seen as a change in energy (frequency in wavenumbers) of the irradiating photon. This energy change is characteristic for a particular bond in the molecule. It is a technique which can be used for the analysis of solids, liquids and solutions and can even provide information on physical characteristics such as crystalline phase and orientation, polymorphic forms, and intrinsic stress. It has an added advantage over FTIR as water is Raman inactive in the region of interest ($2800 - 3100 \text{ cm}^{-1}$) and biological samples can be studied with ease.

The C-H stretching bands in the $2800 - 3100 \text{ cm}^{-1}$ region have been chosen as one of the regions of interest as the CH_2 symmetric stretching and asymmetric stretching modes in Raman at 2850 cm^{-1} and 2890 cm^{-1} , respectively, are generally the strongest bands in the spectra of lipids. The frequencies of these bands are conformation-sensitive and also respond to changes of the *trans/gauche* ratio in acyl chains.

This is also the case, although to a lesser extent, for the vibrational frequency changes due to the terminal CH_3 groups found at 2930 cm^{-1} (symmetric stretch) and 2960 cm^{-1} (asymmetric stretch).

The C-C stretching of the acyl chain backbone which exists either in *all-trans* or *all-gauche* form is the second marker used in our study. Typically, the lipid Raman peaks at approximately 1064 cm^{-1} and approximately 1128 cm^{-1} respectively have been

assigned to the hydrocarbon backbone symmetric and asymmetric all-trans C-C stretching vibrations. The random C-C stretch (*all-gauche*) appears at around 1089 cm^{-1} (Lippert and Peticolas, 1971; Spiker and Levin, 1975).

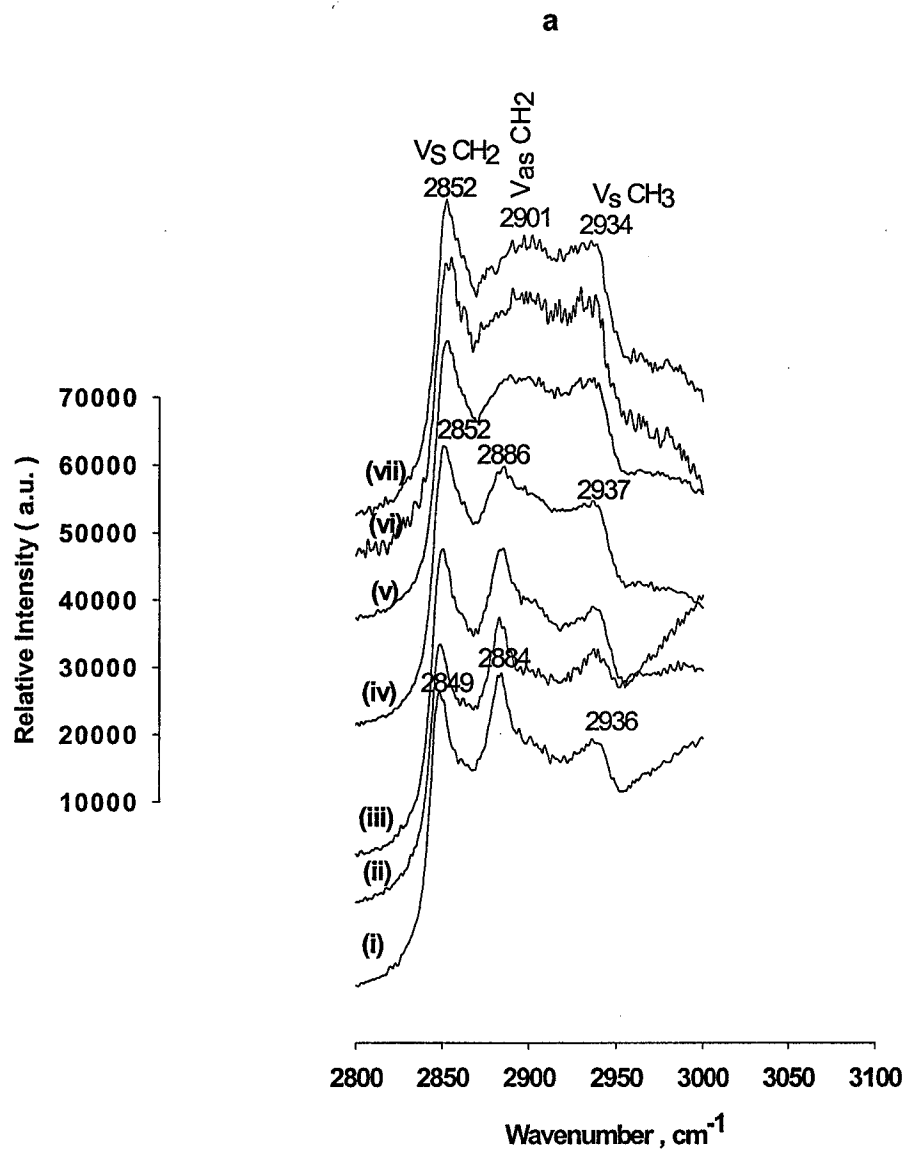
The Raman spectra of BLES in the $2800\text{-}3100\text{ cm}^{-1}$ region at different temperatures are shown in Figure 19a. Raman peaks in this region have been assigned previously by others for saturated phosphatidylcholine (Spiker and Levin, 1975). The 2850 cm^{-1} for the symmetric CH_2 stretch ($\nu_s \text{CH}_2$); 2890 cm^{-1} for the asymmetric CH_2 stretch ($\nu_{as} \text{CH}_2$); approx. 2930 cm^{-1} for the symmetric CH_3 stretch ($\nu_s \text{CH}_3$), and approx. 2960 cm^{-1} for the asymmetric CH_3 stretch ($\nu_{as} \text{CH}_3$) and are shown in Figure 19a for BLES.

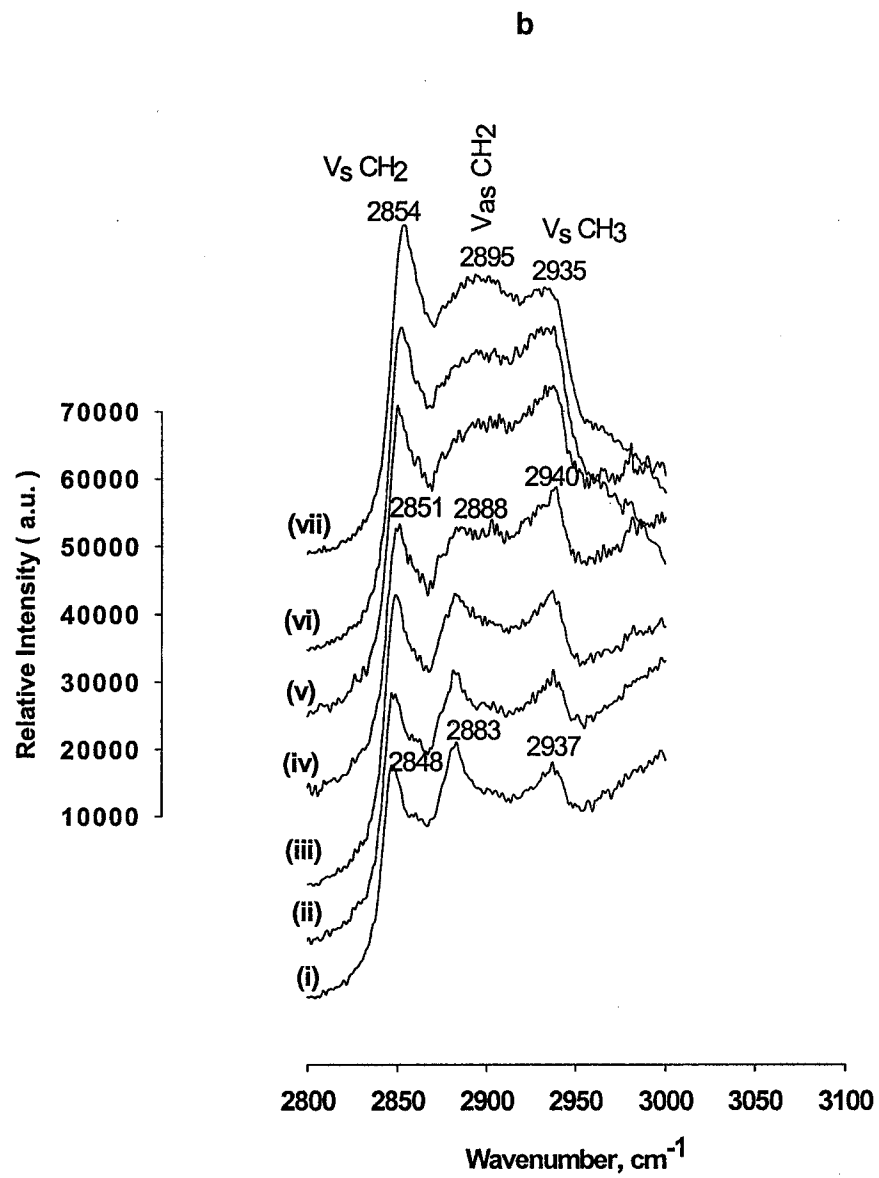
A broadening of the asymmetric CH_2 ($\nu_{as} \text{CH}_2$) stretch with increase in temperature from 25°C (iv) to 45°C (vii) and a narrowing in the peak with decrease in temperature from 25°C (iv) to 13.7°C (i) was observed with BLES (Figure 19a). Apart from this broadening, the $\nu_{as} \text{CH}_2$ peak appearing at 2886 cm^{-1} at 25°C , as seen in (iv) is shifted to higher wavenumbers with increase in temperature to 2900 cm^{-1} at 40°C as in (vi) and to 2901 at 45°C as in (vii). The peak intensity of the $\nu_{as} \text{CH}_2$ stretch which was lesser than the $\nu_s \text{CH}_2$ peak at 25°C , increased with a drop in temperature, and was of higher intensity than the $\nu_s \text{CH}_2$ peak at 13.7°C (Figure 19a). The other effect observed as shown in Figure 19a was that the intensity of the $\nu_s \text{CH}_3$ peak (appearing at 2937 cm^{-1}) which was less than the $\nu_{as} \text{CH}_2$ peak (2886 cm^{-1}) at 25°C increased in intensity with increase in the temperature and was commensurate with it at 45°C (vii). All the above effects observed in Raman spectra of dispersions of BLES (Figure 19a) show that the

acyl chains underwent a conformational change and that an increase in the hydrocarbon chain fluidity (increase in gauche conformers) occurred around 25-30 °C or at the T_{\max} observed using DSC.

A broadening of the ν_{as} CH₂ stretch with an increase in temperature from 25°C (iv) to 45°C (vii) and a narrowing in the peak with a drop in temperature from 25°C (iv) to 10°C (i) was noticed with BLES: Fbg (1 :1, wt/wt) dispersion (Figure 19b). Again, apart from this broadening, the ν_{as} CH₂ peak appearing at 2888 cm⁻¹ at 25°C, as seen in (iv) is shifted to higher wavenumber with increase in temperature to 2895 cm⁻¹ at 45°C as in (vii). The peak intensity of the ν_{as} CH₂ stretch which was equal to the ν_{s} CH₂ peak at 25°C (iv), started increasing with a drop in temperature, and was higher than the ν_{s} CH₂ peak at 10°C (Figure 19b). This effect was similar to that of BLES in Figure 19a. The peak intensity of the ν_{s} CH₂ stretch which was less than the ν_{s} CH₃ peak at 25°C (iv), was greater in intensity at 45°C (vii) (figure 19b).

Figure 19: Raman spectra of the 2800 – 3100 cm^{-1} region of (a) BLES at (i) 13.7°C, (ii) 15°C, (iii) 20°C, (iv) 25°C, (v) 30°C, (vi) 40°C, (vii) 45°C and (b) BLES : Fbg (1: 1, wt/wt) at the same temperatures.





From the general distribution and intensity of the peaks in BLES and the ones with Fbg, it is clear that the protein did not affect the gel or the fluid phase of BLES significantly. However, previous studies have shown (Cameron et al, 1981; Mendelsohn and Mantsch, 1986) that by accurately plotting the shift of the ν_s CH₂ peak as a function of temperature, small conformational changes may be observed.

In Figure 20, using such a method of plotting, the effect of Fbg on BLES is clearly shown. The frequency of the ν_s CH₂ stretching mode of the acyl chains near 2850 cm⁻¹ is plotted as a function of temperature for three such independent experiments, and the average points are plotted. The thermotropic behavior of BLES monitored through temperature induced alterations in the frequency of ν_s CH₂ stretching bands of the lipid acyl chains near 2850 cm⁻¹ is shown by the open circles in figure 20. A broad phase transition between 10-35°C with an onset temperature of 15°C and a completion temperature of about 35°C is observed. The midpoint of the transition is around 27°C which is close to the T_{max} obtained by DSC. When Fbg was added to BLES at 1:1 (wt/wt), the CH₂ frequency was decreased by 1 cm⁻¹ for all the temperatures (as shown by triangles in Figure 20) with no change in the onset and completion temperatures. The Raman spectra of BLES at various temperatures in the 1000-1200 cm⁻¹ region are shown in Figure 21 (a). A continuous decrease in the intensity of the Raman bands at 1062 cm⁻¹ and 1128 cm⁻¹ that are due to a vibration of the extended *all-trans* structure is observed as the temperature is increased from 10°C to 45°C. At the same time an increase in the intensity of the 1091 cm⁻¹ band assigned to random lipid configuration (*all-gauche*) is observed. An abrupt rise in the intensity of the 1091 cm⁻¹ band assigned to

random liquid like configuration and a corresponding decrease in the Raman bands at 1062 cm^{-1} and 1128 cm^{-1} (as reflected in the I_{1091}/I_{1062} ratio) is observed in Figure 18 (c) at 30°C and 35°C . These changes correspond to the gel-liquid crystalline phase transitions taking place in BLES and that these transitions involve a change in the C-C or carbon skeletal backbone of the phospholipid acyl chains of BLES from *all-trans* to a more *trans-gauche* conformation. Figure 21 (b) shows the effect of Fbg on BLES (1:1, wt/wt) Raman bands in the $1000\text{-}1200\text{ cm}^{-1}$ region at various temperatures. A similar effect as seen in Figure 21 (a) was observed. The I_{1091}/I_{1062} ratio was similar to that of BLES alone [Figure 21 (c)].

Figure 20: A comparison between thermotropic behaviors of vibrational shift of Raman frequency for (a) BLES from 10°C to 50°C (open circles) and (b) BLES with Fbg (1: 1, w/w) (triangles), in the same temperature range . The parameter monitored is the frequency of the CH₂ symmetric stretching mode (ν_s CH₂) of the acyl chains near 2850 cm⁻¹. For samples with Fbg the lower frequencies are observed for all temperatures except at 50°C. Lower wavenumbers are indicative of higher number of *trans* bonds or condensations (Mendelsohn and Mantsch, 1986).

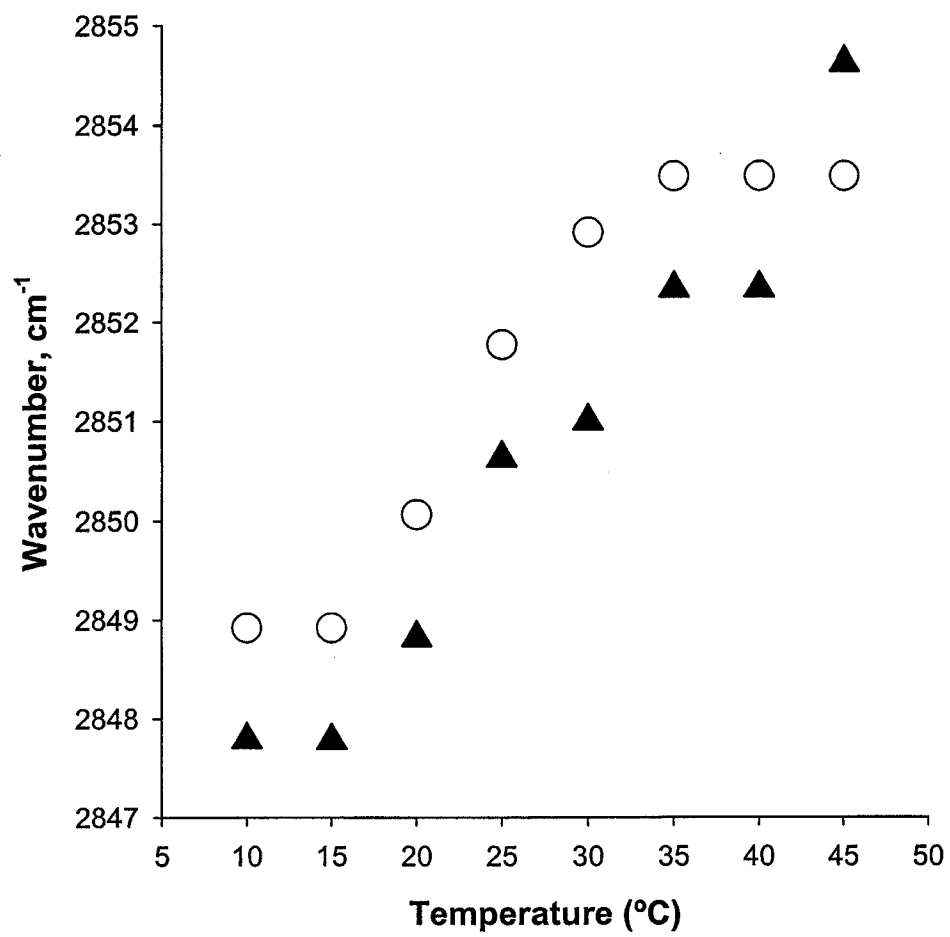
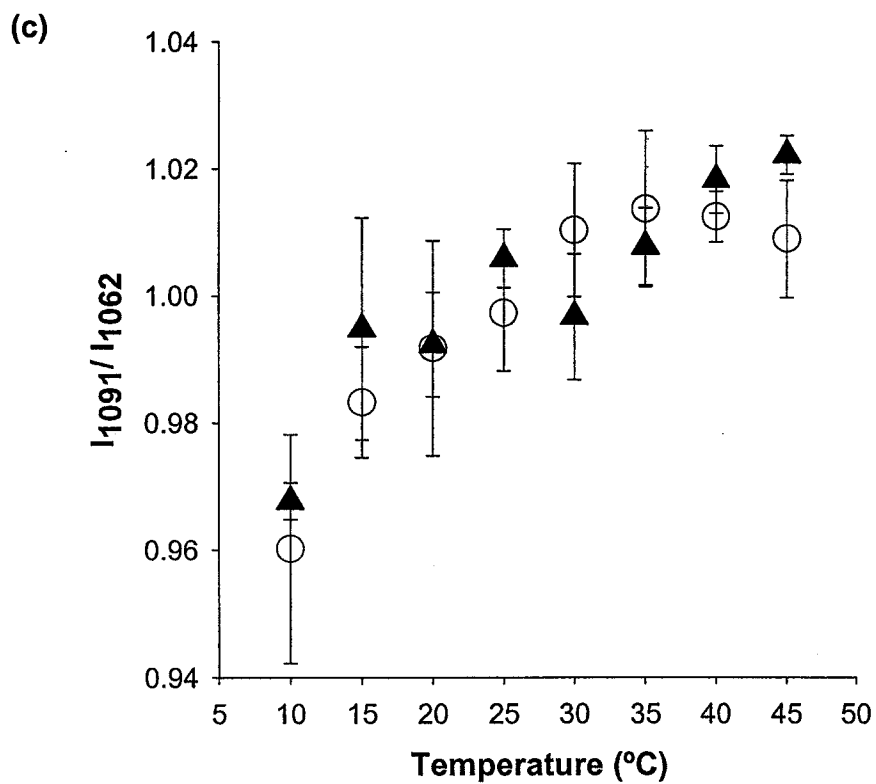
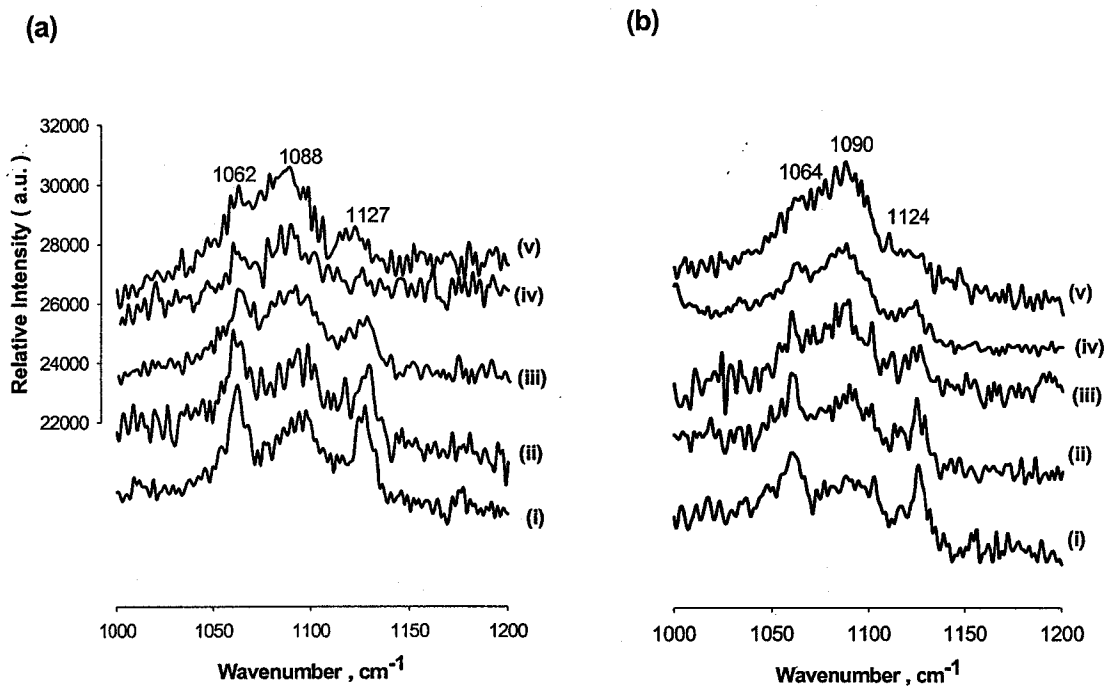


Figure 21: Raman spectra of the 1000-1200 cm^{-1} region of (a) BLES at (i) 10°C, (ii) 15°C, (iii) 25°C, (iv) 40°C, (v) 45°C and (b) BLES : Fbg (1: 1, wt/wt) at the same temperatures; (c) Changes with temperature in the ratio of Raman peak intensities (I_{1091}/I_{1062}). BLES (Open circles) and BLES: Fbg (1: 1, w/w) (Triangles). The intensity ratios at each temperature are an average of $n=3$, with standard deviation shown by error bars.



At 25°C (Figure 22-panel A), Fbg : BLES (wt/wt) at both 1:1 (b) and 10:1 (c) caused the lipid CH₂ band at 2886 cm⁻¹ in BLES to broaden and at the same time, the lipid terminal methyl band (at 2937 cm⁻¹) intensity was increased indicating that Fbg interacts with BLES lipids and changes their conformation. This effect was also observed at 40°C where the lipid chains are in random configuration, Figure 22 (panel B). Due to limitations of fibrinogen solubility in water, only one set of high amounts of Fbg: BLES mixture was attempted in the Raman study. We assume the concentration of BLES: Fbg is 1: 10, however, the concentration was definitely higher than that of 1: 1.4 as used in most studies. This study was conducted mainly to follow up other studies done at high concentrations of albumin, however the solubility of albumin in water was very high as seen in the FTIR experiments.

The gel conformation of BLES (a) at 15°C (Figure 22-panel C) can be rationalized by the following arguments. First, the ν_{as} CH₂ stretch is falling at a lower wavenumber (2884 cm⁻¹) compared to the ν_{as} CH₂ stretch of BLES appearing at 2900 cm⁻¹ at 40°C when the lipids in BLES are in fluid conformation (Figure 22-panel B). Second, the ν_s CH₃ peak intensity (near 2936 cm⁻¹) relative to the ν_{as} CH₂ peak intensity (near 2884 cm⁻¹) is lower when compared to BLES at 40°C and 25°C, suggesting that the acyl chains of BLES are in gel-state or more *all trans* conformations. The ratio of intensity changes of the symmetric methyl vibration with respect to the asymmetric C-H band is indicative of random-fluid configuration of acyl chains as demonstrated previously by Larsson and Rand (1973) by conducting studies employing Raman spectroscopy. Interestingly, when the temperature was lowered to 15°C (Figure 22-panel

C), Fbg at both 1:1 (b) and 10:1 (c) by weight in BLES, caused the lipid C-H band at 2884 cm^{-1} in BLES (a) to broaden and at the same time, the lipid terminal methyl band (at 2936 cm^{-1}) intensity increased relative to the $\nu_{\text{as}}\text{ CH}_2$ band. This shows that Fbg is somehow interacting with BLES and changing its conformation even when the lipids in BLES are in gel states or tightly packed. The symmetric methyl vibrations relative to the $\nu_{\text{as}}\text{ CH}_2$ band as a function of temperature for BLES dispersion and with fibrinogen (1:1, wt/wt) in BLES is shown in Figure 23.

Figure 22: Raman spectra of the 2800-3100 cm^{-1} region of BLES: Fbg (wt/wt) dispersions, **(a)** 1: 0; **(b)** 1:1 and **(c)** 1: 10 showed at 25°C (panel A); 40°C (panel B); 15°C (panel C).

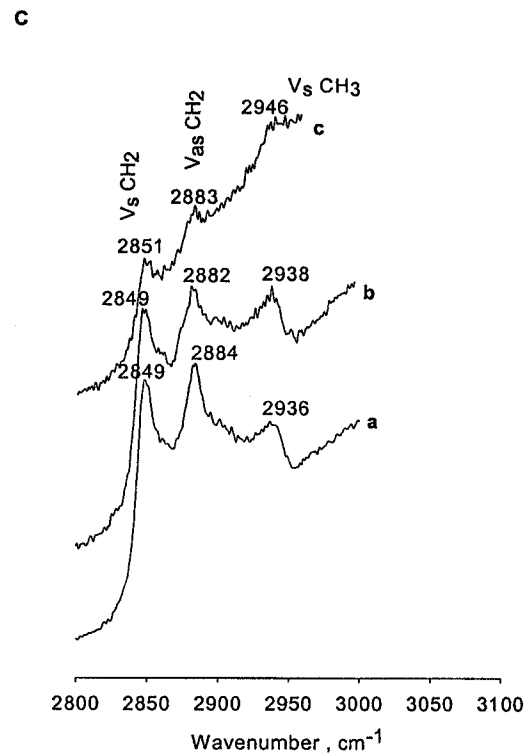
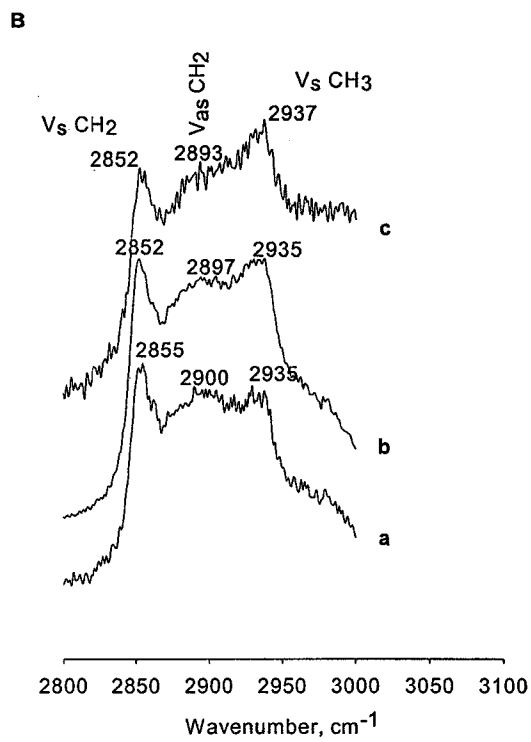
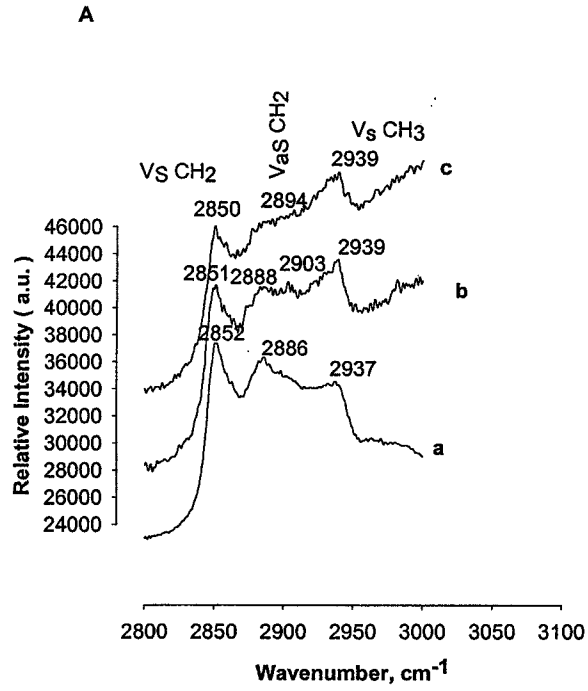
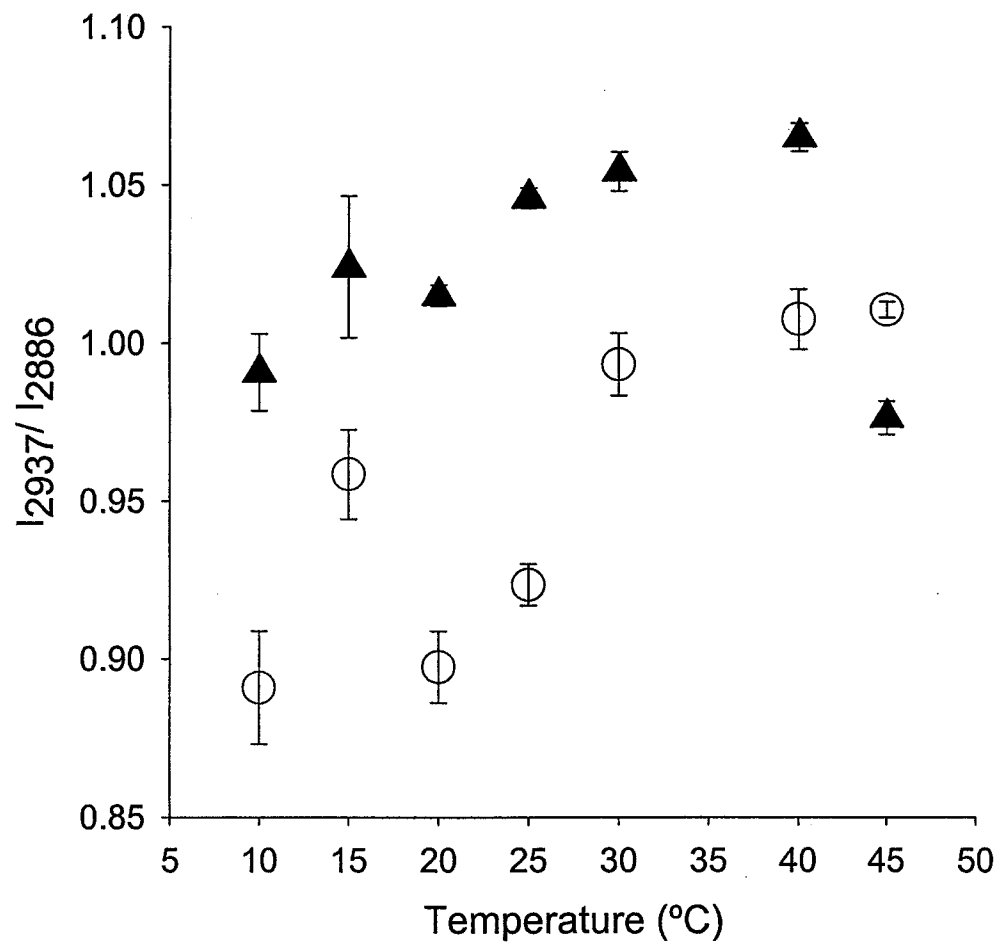


Figure 23: Changes with temperature in the ratio of Raman peak intensities (I_{2937}/I_{2886}).
(a) BLES (Open circles) and (b) BLES: Fbg (1: 1, w/w) (Triangles). The intensity ratios at each temperature are an average of $n=3$, with standard deviation shown by error bars.



Chapter – 4

DISCUSSION

A number of previous studies on surfactant inhibition by serum proteins, and the possible mechanisms involved in such inhibitions have been performed *in vitro* (Enhorning, 1977; reviewed by Griese, 1999; Holm *et al.*, 1999; reviewed by Holm, 1992; Holm *et al.*, 1988; Keough *et al.*, 1989; Panda *et al.*, 2004;). Also, some of these studies have looked at the effects of changes such as ions, pH, and temperature fluxes, as well as serum protein on the function and inhibition of various surfactant preparations (reviewed by Holm, 1992). Many serum proteins have been studied such as albumin, Fbg, C-reactive protein (CRP), and globulin, among others, and all have been shown to inhibit LS function, by preventing the reduction of γ (mN/m) in the lipid-protein films to near 0 mN/m (Amirkhanian and Tausch, 1993; Casals *et al.*, 1998; Fuchimukai *et al.*, 1987; Holm, 1992; Holm *et al.*, 1988; Keough *et al.*, 1989; Liu and Chang, 2002; McEachren and Keough, 1995; Nag *et al.*, 2004c). These studies have shown that LS films could reduce γ only to 25-30 mN/m in the presence of serum protein, and adsorption to the equilibrium γ values of 20 mN/m was increased to 45 mN/m. However the concentrations of the proteins tested have been quite varied and in most cases non-physiological or non-pathological, and various different surfactant preparations have been used (Reviewed by Holm, 1992).

In a recent study, Panda *et al.* (2004) examined large aggregate LS from normal, ventilated, and hyper-ventilated injured lungs of rats, and had noticed a 3 fold increase in

the amounts of soluble (serum) protein associated with surfactant in the injured lungs compared with normal. The soluble proteins were approximately 280 $\mu\text{g}/\text{lung pair}$ in normal lungs versus 830 $\mu\text{g}/\text{lung pair}$ in injured lungs, whereas the total LS phospholipid levels were similar in both. This means that the lipid:protein ratio of 3:1 in normal lungs had decreased to 1:1 in injured lungs, showing a possibility that serum protein inhibitions can occur at much lower values. The LS extracted from such lungs was completely dysfunctional. However, most previous studies had not examined such small ratios when testing inhibition in the laboratory. Studies on Fbg, albumin and on other serum proteins have been done using extremely high concentrations of protein, such as 1: 5 (surfactant lipid: protein, wt/wt) (Enhorning *et al.*, 2000), and others with 1:10, 1:15, and 1:20 lipid:protein ratios (Holm, 1992; Notter, 2000; Otsubo and Takei, 2002). These have shown LS inhibition in varying degrees. However, some studies have tested lower concentrations of proteins similar to the physiological concentrations (Amirkhanian and Taeusch, 1993; Casals *et al.*, 1998; Liu and Chang, 2002). They have found that Fbg and CRP have a much greater inhibitory effect than albumin (Enhorning *et al.*, 2000, Nag *et al.*, 2004c). Also, in one such study it was suggested that there may be specific protein-ligand interactions such as CRP with PC headgroups (McEachren and Keough, 1995; Nag *et al.*, 2004c). However all these studies are difficult to compare considering the varying amounts of proteins used, composition of surfactant, and the fact that only a single type of surface tension measurement was performed (reviewed by Holm, 1992). As well, these studies used different types of model lipid- protein (different levels of SP-B/C) surfactants and very different surface-activity techniques such as the capillary

surfactometer, which measures the upper respiratory air-flow (Enhorning *et al.*, 2000). Also, such studies did not examine the effect of the proteins in the bulk-phase and were limited to the surface activity of monolayers. Our study attempted to determine the interaction of LS with Fbg at physiological concentrations as well as higher concentrations, in a monolayer and bilayer system of a defined extracted bovine lung surfactant (BLES), and some general interactions could be noted at 1:1 (BLES: Fbg) levels.

Different but complementary techniques used in this project, such as Langmuir-Blodgett dynamic compression-expansion, adsorption, and AFM to study the interaction of Fbg with BLES in monolayers, and DSC, Raman, FTIR and TEM with BLES in bulk-phase yielded correlated information at the molecular level of these systems. Through these complementary studies, we can suggest possible molecular mechanisms of the different ways that Fbg may interact with LS lipids. In this study, interactions were examined with a focus only on the lipid components of bovine surfactant, however, the presence of SP-B/SP-C in BLES could have also mediated such interactions.

4.1. Film adsorption and Isotherm studies

Monolayer studies have been conducted to qualitatively comprehend the inhibition of surface activity of BLES by Fbg, to come up with a tentative mechanism for inhibition of the surface activity of BLES related to structure and phase transitions of the lipids at an air-water interface. Adsorption of BLES and BLES+Fbg mixtures (Figure 3) to the air-buffer interface showed that both, BLES and BLES+Fbg mixtures adsorbed to

the interface quite similarly initially. In 120 seconds, BLES reached a surface tension of around 30 mN/m (which is close to the equilibrium surface tension of 25 mN/m) whereas BLES+Fbg mixtures achieved a surface tension of approximately 50 mN/m. Although the standard deviation of the data for adsorption does not show any significant differences between the various BLES: Fbg mixtures used, a general inhibitory trend at 600 seconds between BLES and the mixtures to achieve $\gamma_{\text{equilibrium}}$ could be observed. These mixtures did not show any further lowering of surface tension even after 120 seconds. This clearly shows that the final adsorption of BLES to the surface to reach equilibrium γ of ~ 30 mN/m is impaired in all BLES+Fbg mixtures. This could probably happen by Fbg occupying part of the surface by competing with the adsorption of BLES molecules to the surface and thereby preventing the surface tension reduction ability of the adsorbed BLES to form a compact monolayer. A similar trend of adsorption inhibition was observed in previous studies with other serum proteins (Fuchimukai *et al.*, 1987; Holm *et al.*, 1988; Holm *et al.*, 1987; Holm *et al.*, 1985a; Keough *et al.*, 1989; McEachren and Keough, 1995; Wang and Notter, 1998). In a number of these studies inhibition of adsorption was somewhat similar to the ones observed here and an equilibrium surface tension ($\gamma = \sim 25$ mN/m) was never reached under high serum protein concentration.

Wang and Notter (1998) and Holm *et al.* (1988) studied CLSE obtained from excised lungs. CLSE varies in composition from BLES in that it contains all the neutral lipid components of natural LS, whereas BLES has the neutral lipids removed, however adsorption to γ of around 25 mN/m are similar for BLES and CLSE in 120 seconds.

Other studies were done with different soluble proteins, which are known to exhibit varied levels of inhibitory effects on LS (Fuchimukai *et al.*, 1987). Although different techniques such as the pulsating bubble surfactometer, and an adsorption apparatus were used in those studies, there seems to be a general trend in that adsorption was inhibited in all those studies as also reported here. However our studies on adsorption did not show any significant effect due to the change of concentration of (see error bars in Figure3) Fbg from 1:0.5 to 1:1 (BLES: Fbg). This is possible either due to lack of sensitivity of the adsorption apparatus, or some mechanisms may be at play which do not discriminate between low and high amounts of proteins.

Compression-expansion experiments were carried out in a Langmuir- Wilhelmy surface balance. The dimensions of the Teflon trough gave a surface area of approximately 500 cm², which is used as 100% of monolayer area in the isotherms. Surface tension as a function of pool area was used in all studies, as accurate area/molecule information can not be calculated for adsorbed films (Panda *et al*, 2004). Surface tension is measured by a roughened Wilhelmy platinum dipping plate hung on a force transducer (Nag *et al.*, 1990). A motorized Teflon barrier operated by a FWD-RVS (forward-reverse) switch located on the instrument was used to compress and expand the monolayer.

Initially, NaCl-Trizma.HCl buffer, pH 7 was used to fill the teflon trough as the subphase representing an air-water interface and having a surface tension of around 72mN/m. Bovine lipid extract surfactant dispersed in buffer containing either no Fbg (control) or varying weight percentages of Fbg were adsorbed using a Hamilton syringe

at various points below the air-water interface on the subphase as previously done by others (Nag *et al*, 1998; Panda *et al*, 2004). One hour was allowed for equilibration of the films. After equilibration, the compression and expansion of the films was initiated by movement of barrier and the isotherms were obtained at an ambient temperature of $23\pm 1^\circ\text{C}$. By compressing and expanding the monolayer, the transition of the surfactant from fluid to condensed (gel-like) phase was initiated and monitored by the isotherm in our studies as previously performed on porcine LS extract (Nag *et al.*, 1998) and rat LS (Panda *et al*, 2004).

Compression-expansion isotherms of adsorbed monolayer films of BLES and BLES: Fbg (1:1, w/w) are shown in Figure 4. BLES achieved a minimum surface tension of around 1 mN/m as in typical lung surfactant, whereas with Fbg in BLES, the surface tension of BLES minimized at 27 mN/m. This suggests that Fbg does not allow the lipids in LS films to reach low surface tension. Normally, when LS monolayer is compressed, the fluid lipids in the films are presumed to be squeezed out and the gel lipids, being able to pack tightly upon compression, attribute to the achieving of lower surface tension values, close to zero (Goerke, 1998). Fbg probably, is either directly or indirectly interacting with these gel lipids and altering their packing in reaching low γ .

However, since the AFM images (Figures 8 and 9) did not show major disruption of gel domains, another mechanism is possible. It is possible that Fbg occupying space at the interface prevents the BLES gel lipids occupying this space in the monolayer to be compressed and reach low surface tension. This incompressibility of the BLES monolayer in the presence of Fbg (at various amounts by weight in BLES) is seen as an

increase of the pool area required [Figure 5 (a)] for a 15 mN/m drop of γ . Also, the difficulty in compressing the BLES films with an increase in the amount of Fbg in such films suggests that Fbg may be occupying the space with BLES molecules for the space at the surface and that this competition is proportionally enhanced with increasing Fbg. As in the case of pure Fbg films [Figure 5 (b)], the area compressibility of the protein is seen to be minimal, and in such films γ minimizes at 30 mN/m even at maximal compression [Figure 5 (b)]. This suggests that if fibrinogen occupies a large area in the BLES films, these films would behave more like the pure protein system rather than those of the surfactant or BLES lipids. A related possibility is that if Fbg binds the gel phase lipids of BLES in the bulk phase, the monolayer films formed from such aggregated material may not be able to reduce γ as efficiently.

4.2. Atomic Force Microscopic studies

Atomic force microscopy is emerging as a promising tool for investigating the topography or structures of biological samples (Baro *et al*, 1985). It has been previously used to study various model lung surfactants (Flanders and Dunn, 2002; Nag *et al*, 2002; Nag *et al*, 1999a; Von Nahmen *et al*, 1997; Panaiotov *et al*, 1996). Our lab is the first to apply AFM of surfactant to study interactions of serum proteins such as albumin (Vidyasankar, 2004), as well as this study of interaction of Fbg with LS. To the best of our knowledge, only a single study has employed AFM to image structures in dysfunctional LS film (Panda *et al*, 2004). At a surface tension of 52 mN/m and 42 mN/m, in BLES: Fbg (1:1, wt/wt) films [Figures 8 (b) and 9 (b)], Fbg was seen to be

inserted in the lipids in fluid phase while also somewhat aggregating the gel domains. Firstly, this shows that Fbg interacts with the lipids of BLES and allows us to interpret the surface balance and adsorption data structurally. In our surface balance studies, BLES monolayer reached a surface tension of ~ 1 mN/m, whereas in the presence of Fbg at all the amounts studied, the surface tension did not reach such low values [Figures 4 (b) and 5 (a)]. This was also true from our adsorption experiments (Figure 3) that BLES alone adsorbed to a minimum γ of 30 mN/m (near the equilibrium γ of 25 mN/m), whereas in mixtures with Fbg, a decrease in the magnitude of the drop in γ in the same time period was observed. Pure Fbg adsorbed to a γ of about 50 mN/m and BLES: Fbg (1: 10, wt/wt) showed the least drop in γ , with a final γ of approximately 55 mN/m (Figure 3). This was significantly higher than the equilibrium γ of 30 mN/m for BLES alone. The AFM images of the BLES: Fbg (1:1, wt/wt) were similar to those of Fbg alone, suggesting that Fbg not only penetrates the fluid phase of the films, but a higher concentration abolishes any remnants of gel phase. It is possible that such films are mostly made of Fbg (smooth AFM features) alone.

Secondly, the Fbg is seen to induce two sets of domains, one with the gel lipids and the other with fluid lipids in AFM. This could probably explain the broadening and splitting of the DPPC peak appearing at 41°C [Figure 10 (a) and 10 (b)] in the presence of Fbg in our DSC study. Fbg interacts with a certain number of DPPC molecules and these Fbg-DPPC complexes require melting at a slightly higher temperature. However, while the DSC of BLES with Fbg did not show any major peaks, the main transition peak (T_{\max}) was shifted to slightly higher temperatures (Figure 12). In the case of BLES

(unlike DPPC) Fbg probably has a cumulative effect on its overall transition or interacts with the gel and fluid lipids additively in BLES. This interaction can be seen in the AFM images where Fbg occupied the fluid phase but aggregated the condensed-gel domains [Figure 6 (c) and 8 (b)]. Such aggregates may be difficult to compress to obtain low γ of the films.

4.3. Differential scanning calorimetric studies

The effect of proteins on the enthalpy change and T_{\max} of the transition has been used previously to characterize the interaction of proteins with the lipid bilayer (Papahadjopoulos *et al.*, 1975). Thermotropic behavior of DPPC vesicles reconstituted with the glycoprotein of stomatitis virus has been studied by Petri *et al.* (1980). Alteration of the thermodynamic properties of the phospholipid bilayer by surfactant proteins, SP-B and SP-C have also been studied using DSC (Shiffer *et al.*, 1993). In the present study, Fbg added to the preformed vesicular dispersion of DPPC had some effect on the gel-liquid-crystalline phase transition. DPPC vesicles in the absence of Fbg underwent a sharp phase transition at 41°C [Figure 10 (a)]. With the addition of Fbg at various amounts by weight to preformed DPPC vesicles, a slight broadening in the typical sharp transition occurring in DPPC and splitting of the peak into two peaks with the daughter peak appearing at a slightly higher temperature was observed. This effect was more pronounced in DPPC: Fbg (1: 10, wt/wt), and is shown in Figure 10 (b). The split in the transition peaks of DPPC by Fbg may be due to its aggregation of certain fraction of DPPC molecules in the outer layers of multilamellar vesicles which melt at high

temperature. The other population of DPPC was probably the ones not in contact with Fbg in the inner layers of the MLV's, which melts at the usual phase transition of DPPC. This assumption is based on the fact that Fbg was added to the MLV dispersions after the preparation of the vesicles were complete, as appropriate to those events in the lung, where lamellar bodies come in contact with serum materials only in the outside bilayer. From this observation, one can speculate that Fbg has a slight chain ordering effect by aggregating a certain fraction of DPPC molecules. Shiffer *et al* (1993) observed a broadening of the DPPC gel to liquid-crystalline phase transition in DSC and a shift in the peak transition temperature to a higher value in the presence of surfactant proteins SP-B and SP-C and concluded that both the proteins formed at least two different lipid phases. Petri *et al* (1980) have studied the thermotropic behavior of DPPC vesicles reconstituted with a glycoprotein and explained the broadening in the gel to liquid-crystalline phase transition because of the protein altering the interaction energies between lipids required for melting. However, our studies show instead of broadening of the transition, Fbg acts as a condenser or induces two sets of domains in BLES and DPPC bilayers. Others have, however, seen condensation of acidic phospholipid bilayers by positively charged proteins using DSC (Papahadjopoulos *et al.*, 1975).

The results of the DSC studies reported in this work i.e. influence of Fbg on BLES dispersion had a similar outcome as that noted above for DPPC vesicles. As noted in Figure 12, the broad gel to liquid-crystalline phase transition which appeared in BLES at 27°C had shifted to higher temperatures with fibrinogen. This shift was more pronounced at 1:1 and 1: 1.4 of BLES: Fbg (wt/wt). This delay in the gel-liquid

crystalline phase transition occurring in BLES with Fbg clearly indicates that Fbg interacts and hence condenses the lipids in BLES. It is not possible to conclude from our results whether fibrinogen binds to any specific lipid or non-specifically to various lipids in BLES. However, since the main transition as a whole was being affected, the interaction with the major lipid DPPC is not being ruled out. Fbg bears a negative charge at pH 7 (Mihalyi, 1950) and may interact via electrostatic interactions with the positively charged SP-B and SP-C proteins, which may further condense the films.

4.4. Transmission Electron Microscopy

Experiments undertaken in this work were designed to observe the effect of Fbg on the multilamellar vesicles of BLES using TEM. BLES vesicles appeared concentric and tightly packed. When Fbg was added to BLES (1:1 wt/wt), the vesicles appeared slightly distorted with loosely packed lamellae. This may suggest that Fbg somehow disrupts the tight inter-bilayer compact packing of BLES multilamellar vesicles (Figure 14).

There have been previous studies done on electron micrographs of BLES, however only one study has looked at the effect of a serum protein (CRP) on BLES using this technique (Nag *et al.*, 2004c). In that study no significant changes in the MLV's with serum protein was noted by these authors (Nag *et al.*, 2004c). Thus TEM may not be a sensitive technique by which to judge LS/serum protein interaction, but can be used for general information on the status of the MLV dispersions used in our study. In the diseased and dysfunctional lung, such structures as defined MLV and TM are diminished.

It appears that the serum proteins may disrupt the organization of LS bilayers in lamellar bodies, or even possibly the secretory form of LB *in vivo* during disease (Fig. 14). This, in turn, may not allow such vesicles to undergo a transformation to TM, or the most surface active form, as suggested by others (Larsson *et al.*, 2003).

4.5. Fourier Transform Infrared Spectroscopic (FTIR) studies

Fourier transform infrared spectroscopy is a valuable and emerging technique in probing the lipid-protein interaction at molecular level. This technique, apart from having the advantage of requiring microgram quantities of material, has the potential to measure the lipid acyl chain configuration and phospholipid head group interactions without the use of any probe molecules which could disturb the physico-chemical properties of the system. In the FTIR studies, the peak intensities and the wavenumber shifts of various bands in BLES alone and BLES + Fbg/bovine serum albumin were monitored. The regions of interest were mainly the asymmetric and symmetric bands in the C-H stretching region (2800-3000 cm^{-1}) and the asymmetric and symmetric phosphate bands appearing at 1224 cm^{-1} and 1087 cm^{-1} respectively of the headgroup region (1000-1500 cm^{-1}).

Fbg at the selected amounts by weight in BLES tested (1: 0.5, 1: 1, and 1: 1.4) slightly broadened the symmetric (2850 cm^{-1}) and asymmetric (2920 cm^{-1}) peaks with no major shift in the frequency of these vibrations. The symmetric and asymmetric terminal methyl vibrations in BLES became more intense when the acyl chains are in a fluidized state. The observations reported in the results section demonstrate that the intensity

pattern of the vibrations were suppressed indicating that Fbg was somehow increasing the acyl chain order with the effect of suppressing the terminal methyl vibrations [Figure 17 (a)].

The asymmetric and symmetric phosphate bands in BLES shifted to a lower frequency with Fbg indicating that the environment surrounding the headgroup region of BLES was more hydrated [Figure 18 (a)]. This was in consensus with Arrondo *et al* (1984) who observed the asymmetric phosphate band appeared at 1220 cm^{-1} with hydrated DPPC, and 1240 cm^{-1} with DPPC in 'dry' state. They concluded that the phosphate group of the headgroup of the DPPC forms more hydrogen bonds with the surrounding water molecules in its fully hydrated state with a wavenumber of 1220 cm^{-1} being monitored. Whether Fbg further hydrates the headgroup region by forming more hydrogen bonds with water, or binds to some groups in the headgroup region of BLES phospholipids and eventually enhances the H-bonding network, could not be explained from our FTIR data. However, that Fbg does affect the headgroup region and makes the lipid more polar has been suggested in other studies using Raman spectroscopy of dimyristoyl phosphatidylcholine (DMPC) (Lis *et al*, 1976). However, Fbg can interact with the headgroup of BLES as evidenced by the changes in the frequencies of the symmetric and asymmetric phosphate bands of the headgroup.

To determine if the effect of Fbg was specific to the system under study in this work, another serum protein, albumin (BSA) was studied using FTIR with BLES [Figures 17 (b) and 18 (b)]. In the C-H stretching region ($2800\text{-}3000\text{ cm}^{-1}$), BSA at lower amounts by weight in BLES (1: 0.5 and 1: 1) did not have any appreciable influence on

the symmetric and asymmetric stretches of BLES. At BLES: BSA (1: 10, wt/wt), the intensity of symmetric methyl vibrations was increased relative to the symmetric methylene peak. The asymmetric CH₃ band which appears at 2956 cm⁻¹ in BLES as a shoulder to the $\nu_{\text{as}}\text{CH}_2$ band (appearing at 2920 cm⁻¹) increased in intensity with increased BSA, and was almost equal in intensity to that of the $\nu_{\text{as}}\text{CH}_2$ band. Also, there was a large shift in the $\nu_{\text{as}}\text{CH}_2$ band towards higher energy [Figure 17 (b)]. This trend is quite different from what was observed from our BLES: Fbg spectra.

In the phosphate stretching region, BSA (unlike Fbg) shifted the asymmetric phosphate stretching band to a higher frequency indicating that it was dehydrating the headgroup region in BLES as also described previously by Arrondo *et al* (1998). According to these authors, proteins that interact mainly with the polar moiety of phospholipids, tend to bind negatively-charged phospholipids, modifying the network of hydrogen bonds at the bilayer surface, so that the phospholipid polar headgroups exchange H-bonds with the protein, rather than with water leading to partial dehydration at the bilayer surface.

Similarly, we found that BSA may be dehydrating the BLES bilayer surface by interacting with the headgroup and this interaction probably was reflected deep into the bilayer core where it changed the conformation of acyl chains (increase in fluidity). This was evident from the shift in the $\nu_{\text{as}}\text{CH}_2$ band towards a higher frequency and an increase in the intensity of symmetric and asymmetric terminal methyl vibrations (Figure 17b). This FTIR study with BSA proving its lipid fluidizing nature is in agreement with the

previous bilayer studies conducted in our laboratory employing this protein and correlated with DSC results (Vidyasankar, 2004).

4.6. Raman spectroscopic studies

Raman spectroscopy has been one of the most powerful techniques widely used to study the membrane systems, as the Raman spectra can be obtained without the use of any probe molecules which would perturb the system under investigation. It has been successfully applied by others to investigate interactions of model phospholipid membrane systems with peptides and proteins (Carrier and Pezolet, 1984; Levin, 1984; Mushayakarara and Levin, 1984; Vincent *et al*, 1993). Also, Raman has the added advantage that water, being Raman inactive in the region of interest (1000 to 3000 cm^{-1}), the spectra requires no subtraction as in FTIR. The C-H stretching bands in the 2800-3000 cm^{-1} region and the ratio of their intensities have been found to reflect the order/disorder properties of the membrane systems (Levin, 1984). Gaber and Peticolas (1977) have shown that the lower the I_{2850}/I_{2880} ratio, the more ordered the hydrocarbon chains are. The I_{2935}/I_{2880} ratio is sensitive to intermolecular chain interactions and the mobility of the terminal methyl groups of hydrocarbon chains of phospholipids. Thus, the lower the ratio, the higher the conformational order of the lipid hydrocarbon chains and the lower the mobility of the terminal methyl group (Yellin and Levin, 1977).

At 25°C (Figure 22-panel A), the peak intensity of the asymmetric CH_2 stretch appearing at 2886 cm^{-1} was observed to be increasing relative to the symmetric CH_2 stretch (at 2852 cm^{-1}) with an increase in the amount of Fbg by weight present in BLES.

The I_{2852}/I_{2886} ratio was decreased, indicating increased acyl chain order, which was in agreement with the observations of Gaber and Peticolas (1977). Presumably, Fbg directly or indirectly interacts with certain lipids in BLES and thereby stabilizes the acyl chain packing or order. This effect was observed in the gel phase (panel C) as well as the fluid phase (panel B) of BLES.

The shift of the frequency of the $\nu_s\text{CH}_2$ stretch of BLES to lower energy in the BLES: Fbg (1:1, wt/wt) samples at all the temperatures suggested the lipids in BLES to be in more ordered conformation compared to BLES alone (Figure 20). Thus, more heat was required to melt the chains as also seen in the DSC results, where the T_{max} of BLES was shifted to 34°C. This lipid chain ordering effect, monitored through the temperature induced alterations in the frequency of the $\nu_s\text{CH}_2$ stretch, has been suggested previously on other systems containing synthetic phospholipids undergoing thermotropic transitions (Cameron et al, 1981; Mendelsohn and Mantsch, 1986).

The symmetric terminal methyl peak intensity relative to the intensity of the asymmetric CH_2 stretch was seen to increase with increasing amounts by weight of Fbg. The I_{2937}/I_{2886} ratio increased indicating the increase in the terminal methyl vibrations similar to what observed by Yellin and Levin, (1977). This effect was also observed at 40°C (the temperature above the gel to liquid-crystalline phase transition occurring in BLES at 27°C) as in figure 22-panel B and at 15°C (the temperature below the gel to liquid-crystalline phase transition of BLES) as in Figure 22-panel C.

The conclusion that can be drawn from Raman experiments is that Fbg slightly affects (condenses) the acyl chain of phospholipids in BLES. Although a water soluble

protein, this interaction is observed even inside the core of the bilayer from the changes of the terminal methyl vibrations.

Summary and Conclusions

LS play a vital role in the normal functioning of the lungs normally. It stabilizes the alveoli during normal respiration by reducing the surface tension of the alveolar air-water interface during expiration preventing the alveolar collapse. During ARDS, and in other lung diseases, serum proteins gets flooded into the alveolar space and inhibit the dynamic surface tension lowering effect of the Lung Surfactant. Interaction of serum fibrinogen with the bulk bilayer phases and films of BLES was studied in this project employing various biophysical techniques. Several studies have looked at effects of different plasma proteins (at various concentrations) on LS surface activity, however, to the best of our knowledge, the effect of small and large concentrations of serum fibrinogen (more physiological), with monolayers as well as LS bilayers have not been examined in detail.

In this study, several experiments were done on BLES monolayers and bilayers, and some possible inter-molecular interactions of fibrinogen with LS is suggested. Adsorption studies showed that Fbg competed with BLES molecules for the space at the surface and hence prevented the surface tension reduction of such BLES monolayers. Compression-expansion isotherms of adsorbed films of BLES in the presence of Fbg suggested that Fbg significantly altered the surface activity of such films. The difficulty in compressing the BLES films with an increase in the amount of Fbg in such films also

suggests that Fbg may be occupying the space with BLES molecules at the surface and that this competition is proportionally enhanced with increasing Fbg. From AFM studies, Fbg was seen to be inserted in the lipids in fluid phase while also somewhat aggregating the gel domains. This showed that Fbg interacted with the lipids of BLES and somewhat allowed the structural interpretation of the surface activity data. Also, it was seen that Fbg formed two sets of domains and interacted with the gel and fluid lipid domains of LS. This explained the shift of the main transition peak (T_{max}) of BLES towards slightly higher temperatures in the presence of fibrinogen as seen from our DSC studies. The influence of Fbg on DPPC, as noted from DSC studies has shown that the sharp gel-liquid crystalline phase transition of DPPC which appeared as a single peak at 41°C was split and some domains melted at slightly higher temperatures (Figure 10).

Raman and Fourier Transform Infrared Spectroscopy (FTIR) of the bulk dispersions suggested that fibrinogen altered the CH_2 , CH_3 , and PO_4^- vibrational modes of the BLES lipids at 1:1 (BLES: Fbg, wt/wt) ratios. This effect was very different from that of BSA with BLES. The vibrational shifts of frequencies were consistent with slight increase in hydration of the headgroups (PO_4^-) as well as increased ordering of the hydrocarbon chains (CH_2 and CH_3) of BLES. This result was in direct contrast to the disordering effects of BLES observed with another serum protein, albumin and suggest some specific LS lipid-Fbg interactions.

In conclusion, this project, through various biophysical studies, revealed that fibrinogen interacts with lung surfactant at the molecular level as monitored by structural and functionality changes in the system. This may lead to the LS inefficiency in reducing

the alveolar air-water interface surface tension, thus inhibiting the prevention of alveolar collapse. This interaction is accomplished by fibrinogen affecting the lipid chains and the headgroup of bilayers of the lung surfactant.

Future directions

To further probe the interaction of Fbg with LS and to come up with a definite molecular mechanism of how Fbg inhibits LS function, complete LS from native lungs needs to be studied. Wang and Notter (1998), have shown supplementation with large amounts of exogenous CLSE would be effective in reversing inactivation by the mixtures of blood proteins. Also SP-A in LS can reverse the activity of inhibitory proteins, as suggested by others (Casals *et al*, 1998; Cockshutt *et al*, 1990; Nag *et al*, 2004c). Similarly, for future experiments, large amounts of BLES+SP-A can be used to determine if Fbg can still inhibit the surface activity of such LS.

To find effectively how and where in the lipids of BLES, Fbg interacts (using Raman and FTIR), substitution of hydrogen by deuterium could be performed. By inserting small amounts of per-deuterated DPPC into BLES, the interaction of Fbg with a specific C-D bond can be monitored using Raman and FTIR. In deuterated acyl chains, the asymmetric and symmetric bands appear around 2195 and 2090 cm^{-1} , respectively different from the positions obtained for the $-\text{CH}_2$ at around 2920 and 2850 cm^{-1} .

Since Fbg can form clots, future study with use of thrombin in the BLES: Fbg mixtures may suggest other relative modes of interaction of the main blood clotting agent in the lung.

REFERENCES

- Abrams, M. E. (1966). Isolation of quantitative estimation of pulmonary surface-active lipoprotein. *J. Appl. Physiol.*, 21: 718-720.
- Amirkhanian, J.D., and Taeusch, H.W. (1993). Reversible and irreversible inactivation of preformed pulmonary surfactant surface films by changes in subphase constituents. *Biochim. Biophys. Acta*, 1165: 321-326.
- Arrondo, J. L. R., Goni, F. M., Macarulla, J. M. (1984). Infrared spectroscopy of phosphatidylcholines in aqueous suspension. A study of the phosphate group vibrations. *Biochim. Biophys. Acta*, 794: 165-168.
- Arrondo, J.L.R., and Gofii, F.M. (1998). Infrared studies of protein-induced perturbation of lipids in lipoproteins and membranes. *Chem. Phys. Lip.* 96: 53-68.
- Ashbaugh, D.G., Bigelow, D.B., Petty, T.L., and Levine, B.E. (1967). Acute respiratory distress in adults. *Lancet.* 2(7511): 319-323.
- Avery, M.E., Mead, J. (1959) Surface properties in relation to atelectasis and hyaline membrane disease. *Amer. Med. Assoc. J. Dis. Child* 97(5 Part 1): 517-523.
- Avery, M. E., Taeusch, H. W and Floros, J. (1986). Surfactant replacement. *N. Engl. J. Med*, 315: 825-826.
- Balis, J. U., Shelley, S. A., McCue, M. J., and Rappaport, E. S. (1971). Mechanisms of damage to the lung surfactant system. *Exp. Mol. Pathol*, 14: 243-262.
- Baro, A.M., Miranda, R., Alaman, J., Garcia, N., Binnig, G., Rohrer, H., Gerber, C., and Carrascosa, J.L. (1985). Determination of surface topography of biological specimens at high resolution by scanning tunneling microscopy. *Nature*, 315(6106): 253-254.
- Batenburg, J. J., and Haagsman, H. P. (1998). The lipids of pulmonary surfactant: dynamics and interaction with proteins. *Prog. Lipid. Res.* 37:235-276.
- Bernard, G.R., and Brigham, K.L. (1986). Pulmonary edema: Pathophysiologic mechanisms and new approaches to therapy. *Chest.* 89(4):594-600.
- Binnig, G., Quate, C.F., and Gerber, Ch. (1986). Atomic force microscope. *Phys. Rev. Lett*, 56 (9), 930-933.

- Cameron, D. G., Kauppinen, J. K., Moffatt, D. J., and Mantsch, H. H. (1981). *Biochemistry*, 20: 4496-4500.
- Carrier, D., Pezolet, M. (1984). Raman spectroscopic study of the interaction of poly-l-lysine with dipalmitoylphosphatidylglycerol bilayers. *Biophys. J.* 46: 497-506.
- Casal, H. L., Mantsch, H. H., (1984). Polymorphic phase behavior of phospholipid membranes studied by infrared spectroscopy. *Biochim. Biophys. Acta.* 779: 381-401
- Casals, C., Varela, A., Ruano, M.L.F., Valiño, F., Pérez-Gil, J., Torre, N., Jorge, E., Tendillo, F., and Castillo-Olivares, J.L. (1998). Increase of C-reactive protein and decrease of surfactant protein A in surfactant after lung transplantation. *Amer. J. Respir. Crit. Care Med.* 157: 43-49.
- Chapman, D and Collin, D. T. (1965). Differential thermal analysis of phospholipids. *Nature*, 206: 189.
- Clark, J. M., and Lambertsen, C. J. (1971). Pulmonary oxygen toxicity: a review. *Pharmacol. Rev.* 23: 37-133.
- Clements, J.A. (1957). Surface tension of lung extracts. *Proc. Soc. Exper. Biol.* 95:170-172.
- Cockshutt, A.M., Weitz, J., and Possmayer, F. (1990). Pulmonary surfactant-associated protein A enhances the surface activity of lipid extract surfactant and reverses inhibition by blood proteins in vitro. *Biochem.* 29(36): 8424-8429.
- Colacicco, G., and Basu, M. K. (1978). Effect of serum albumin on dynamic force-area curve of dipalmitoyllecithin. *Respir. Physiol.* 32: 265-279.
- Curstedt, T., Jornvall, H., Robertson, B., Bergman, T., and Berggren P. (1987). Two hydrophobic low molecular-mass protein fractions of pulmonary surfactant. Characterization and biophysical activity. *Eur J Biochem.* 168: 255-262.
- Danesh, J., Collins, R., Appleby, P., and Peto, R. (1998). Association of Fbg, C-reactive protein, albumin, or leukocyte count with coronary heart disease: meta-analyses of prospective studies. *JAMA.* 279:1477-82.
- Dluhy, R.A., and Mendelsohn, R. (1988). Emerging techniques in biophysical FT-IR. *Anal. Chem.* 60(4): 269-278.
- Enhorning, G. Surfactant replacement in adult respiratory distress syndrome. (1989). *Am. Rev. Respir. Dis.* 140: 281-283.

- Enhorning, G. Pulsating bubble technique for evaluating pulmonary surfactant. *J. Appl. Physiol.* 43: 198-203, 1977.
- Enhorning, G., Hohlfeld, J., Krug, N., Lema, G., and Welliver, R.C. (2000). Surfactant function affected by airway inflammation and cooling: possible impact on exercise-induced asthma. *Eur. Respir. J.* 15: 532-538.
- Flanders, B.N., and Dunn, C. (2002). A near-field microscopy study of submicron domain structure in a model lung surfactant monolayer. *Ultramicroscopy.* 91: 245-251.
- Fringeli, U. P., Gunthard, H. H., (1981). Infrared membrane spectroscopy. In: Grell, E. (Ed.), *Membrane Spectroscopy.* Springer, Berlin, pp. 270-332.
- Fuchimukai, T., Fujiwara, T., Takahashi A and Enhorning, G. (1987). Artificial pulmonary surfactant inhibited by proteins. *J. Appl. Physiol.* 62 (1), 429-437.
- Fujiwara, T., Maeta, H., Chida, S., Morita, T., Watabe, Y., and Abe, T. (1980). Artificial surfactant therapy in hyaline membrane disease. *Lancet.* 1: 55-9.
- Gaber, B. P and Peticolas, W. L. (1977). On the quantitative interpretation of biomembrane structure by Raman spectroscopy. *Biochim. Biophys. Acta*, 465, 260-274.
- Goerke J. (1974). Lung surfactant. *Biochim Biophys Acta.* 344 (3-4): 241-261.
- Goerke, J. (1998). Pulmonary surfactant: functions and molecular composition. *Biochim. Biophys. Acta.* 1408:79-89.
- Griese, M. (1999). Pulmonary surfactant in health and human lung diseases: state of the art. *Eur. Respir. J.* 13:1455-1476.
- Gross, N.J. (1995). Extracellular metabolism of pulmonary surfactant: the role of a new serine protease. *Annu. Rev. Physiol.* 57: 135-150.
- Haagsman, H. P., Van Golde, L. M. G (1991). Synthesis and assembly of lung surfactant. *Ann Rev Physiol*, 53: 441-464.
- Hagwood, S., Benson, B. J., Schilling, J., Damm, D., Clements, JA., White, RT. (1987). Nucleotide and amino acid sequences of pulmonary surfactant protein SP-18 and evidence for cooperation between SP-18 and SP-28-36 in surfactant lipid adsorption. *Proc. Natl. Acad. Sci. USA.* 84: 66-70.

- Hall, C. E., Slayter, H. S. (1959). The Fbg molecule: Its size, shape and mode of polymerization. *J. Biophys. Biochem. Cytol.* 5:11-15.
- Hallman, M., Spragg, R., Harell, J. H., and Moser, K. M. (1982). Evidence of lung surfactant abnormality in respiratory failure. Study of bronchoalveolar lavage phospholipids, surface activity, phospholipase activity, and plasma myoinositol. *J. Clin. Invest.* 70, 673-683.
- Harbottle, R.R., Nag, K., McIntyre, S., Possmayer, F., and Peterson, N.O. (2003). Molecular organization revealed by time-of-flight secondary ion mass spectrometry of a clinically used extracted pulmonary surfactant. *Langmuir.* 19(9): 3698-3704.
- Hoepflich, P. D and Doolittle, R. F. Dimeric half-molecules of human Fbg are joined through disulfide bonds in an antiparallel orientation. *Biochemistry.* 22: 2049-2055, 1983.
- Holm, B.A., Notter, R.H., and Finkelstein, J.H. (1985a). Surface property changes from interactions of albumin with natural lung surfactant and extracted lung lipids. *Chem. Phys. Lip.* 38: 287-298.
- Holm, B. A., Notter, R. H., Siegle, J., and Matalon, S. J. (1985b). Pulmonary physiological and surfactant changes during injury and recovery from hyperoxia. *Appl. Physiol.* 59: 1402-1409.
- Holm, B.A., and Notter, R.H. (1987). Effects of hemoglobin and cell membrane lipids on pulmonary surfactant activity. *J. Appl. Physiol.* 63: 1434-1442.
- Holm, B.A., Enhorning, G., and Notter, R.H. (1988). A biophysical mechanism by which plasma proteins inhibit lung surfactant activity. *Chem. Phys. Lip.* 49: 49-55.
- Holm, B.A. (1992). Chapter 27: Surfactant Inactivation in Adult Respiratory Distress Syndrome. *Pulmonary Surfactant: from molecular biology to clinical practice.* Ed.B. Robertson, L.M.G. Van Golde, and J.J. Batenburg. Elsevier Science Publishers: Oxford, England.
- Holm, B. A., G. Enhorning, and R. H. Notter. (1998). A biophysical mechanism by which serum proteins inhibit lung surfactant activity. *Chem. Phys. Lipids* 49: 49-55.
- Holm, B. A., Wang, Z., and Notter, R. H. (1999). Multiple mechanisms of lung surfactant inhibition. *Pediatr. Res.* 46:85-93.
- Ikegami, M., Jobe, A., and Glatz, T. (1982). Surface activity following natural surfactant treatment in premature lambs. *J. Appl. Physiol.* 51: 306-312.

- Ikegami, M., Agata, Y., Elkady, T., Hallman, M., Berry, D., and Jobe, A. (1987). Comparison of four surfactants: in vitro surface properties and responses of preterm lambs to treatment at birth. *Pediatrics*. 79: 39-46.
- Ikegami, M., Jobe, A., Jacobs, H., and Lam, R. (1984). A protein from airways of premature lambs that inhibits surfactant function. *J. Appl. Physiol.*, 57:1134-1142.
- Jacobson, W., Park, G.R., Saich, T., and Holcroft, J. (1993). Surfactant and adult respiratory distress syndrome. *Brit. J. Anaesth.* 70: 522-526.
- Johansson, J., and Curstedt, T. (1997). Molecular structures and interactions of pulmonary surfactant components. *Eur. J. Biochem.* 244:675-693.
- Keough, K. M. W., and Kariel, N. (1987). Differential scanning calorimetric studies of aqueous dispersions of phosphatidylcholines containing two polyeoic chains. *Biochim. Biophys. Acta.* 902:11-18.
- Keough, K. M. W., Parsons, C. S., Phang, P. T., and Tweedale, M. G. (1988). Interactions between serum proteins and pulmonary surfactant: surface balance studies. *Can. J. Physiol. Pharmacol.* 66: 1166-1173.
- Keough, K. M. W., Parsons, C. S., and Tweedale, M. G. (1989). Interactions between serum proteins and pulmonary surfactant: pulsating bubble studies. *Can. J. Physiol. Pharmacol.* 67: 663-668.
- Larsson, K and Rand, R. P. (1973). Detection of changes in the environment of hydrocarbon chains by Raman spectroscopy and its application to lipid-protein systems. *Biochim. Biophys. Acta* 326: 245-255.
- Larsson, M., Larsson, K., Nylander, T., and Wollmer, P. (2003). The bilayer melting transition in lung surfactant bilayers: the role of cholesterol. *Eur. Biophys. J.* 31: 633-636.
- Lee, D. C., and Chapman, D. (1986). Infrared spectroscopic studies of biomembranes and model membranes. *Biosci Rep.* 6: 235-256.
- Levin, I. W. (1984). Vibrational spectroscopy of membrane assemblies. *Advances in infrared and Raman spectroscopy.* Wiley Heyden, 11: 1-48.
- Lewis, J., and Jobe, A. (1993). State of the art: Surfactant and the adult respiratory distress syndrome. *Amer. Rev. Respir. Dist.* 147: 218-233.

- Lippert, J. L., and Peticolas, W. L. (1971). Laser Raman investigation of the effect of cholesterol on conformational changes in dipalmitoyl lecithin multilayers. *Proc. Natl. Acad. Sci. U.S.* 68: 1572-1576.
- Lis, J.S., Kauffman, J.W., and Shriver, D.F. (1976). Raman spectroscopic detection and examination of the interaction of amino acids, polypeptides, and proteins with the phosphatidylcholine lamellar structure. *Biochim. Biophys. Acta.* 436: 513-522.
- Liu, Y., and Chang, C. (2002). Inhibitory effects of Fbg on the dynamic surface tension-lowering activity of dipalmitoyl phosphatidylcholine dispersions in the presence of tyloxapol. *Coll. Polym. Sci.* 280: 683-687.
- Lorand, L. (1983). New approaches to old problems in the clotting of Fbg. *Ann. N. Y. Acad. Sci.* 408:226-232.
- Lowe, G., Rumley, A., Norrie, J., Ford, I., Shepherd, J., Cobbe, S., Macfarlane, P., and Packard C. (2000). Blood rheology, cardiovascular risk factors, and cardiovascular disease: the West of Scotland Coronary Prevention Study. *Thromb. Haemost.* 84:553-8.
- Lumb, R. H (1989). Phospholipid transfer proteins in mammalian lung. *Am. J. Physiol.* 257: L190-L194.
- Matalon, S., Benos, D.J., and Jackson, R.M. (1996). Biophysical and molecular properties of amiloride-inhibitable Na⁺ channels in alveolar epithelial cells. *Amer. J. Physiol.* 271: L1-L22.
- McEachren, T. M., and Keough, K. M. W. (1995). Phosphocholine reverses inhibition of pulmonary surfactant adsorption caused by C-reactive protein. *Amer. J. Physiol. (Lung Cell Mol. Physiol.)*. 13: L492-497.
- Mendelsohn, R., and Mantsch, H.H. (1986). Fourier transform infrared studies of lipid-protein interaction. *In Progress in Protein-Lipid Interaction*. 2. A. Watts and J. J. H. H. M. de Pont, editors. Elsevier Science Publishers BV (Biomedical division), Amsterdam.
- Mihalyi, E. (1950). Electrophoretic investigation of fibrin and Fbg dissolved in urea solutions. *Acta. Chem. Scand.*, 4: 351-358.
- Mingyao, L., Liman, W., Li, E, and Enhorning, G. (1991). Pulmonary surfactant will secure free airflow through a narrow tube. *J. Appl. Physiol.* 71(2): 742-748.
- Mushayakarara, E and Levin, I. W. (1984). Effects of polypeptide-phospholipid interactions on bilayer reorganizations. Raman spectroscopic study of the binding

of polymixin B to dimyristoylphosphatidic acid and dimyristoylphosphatidylcholine dispersions. *Biochim. Biophys. Acta*, 769: 585-595.

- Mutafchieva, R., Panaiotov, I., and Dimtrov, D. S. (1984). Surface pressure hysteresis of mixed lipid/protein monolayers: applications to the alveolar dynamics. *Z. Naturforsch. C Biosci.* 39: 965-972.
- Nag, K., Boland, C., Rich, N., and Keough, K.M.W. (1990). Design and construction of an epifluorescence microscopic surface balance for the study of lipid monolayer phase transitions. *Rev. Sci. Instrum.* 61: 3425-3430.
- Nag, K. (1996). Association and interactions of lipids and proteins of pulmonary surfactant in model membranes at the air-water interface. *Ph.D. Thesis*, Department of Biochemistry, Memorial University of Newfoundland, St. John's, Newfoundland, Canada A1B 3X9.
- Nag, K., Munro J.G., Hearn, S.A., Rasmusson, J., Petersen, N.O., and Possmayer, F. (1997). Correlated atomic force and transmission electron microscopy of nanotubular structures in pulmonary surfactant. *J. Struct. Biol.* 126: 1-15.
- Nag, K., Pérez-Gil, J., Ruano, M.L.F., Worthman, L.A.D., Stewart, J., Casals, C., and Keough, K.M.W. (1998). Phase transitions in films of lung surfactant at the air-water interface. *Biophys. J.* 74: 2983-2995.
- Nag, K., Munro, G. J., Hearn, S. A., Rasmusson, J., Petersen, N. O., Possmayer, F. (1999a). Correlated atomic force and transmission electron microscopy of nanotubular structures in pulmonary surfactant. *J. Struct. Biol.* 126: 1-15.
- Nag, K., Munro, J.G., Inchley, K., Schurch, S., Petersen, N.O., and Possmayer, F. (1999b). SP-B refining of pulmonary surfactant phospholipids films. *Amer. J. Physiol.* 277 (6 Pt 1): L1179-1189.
- Nag, K., Panda, A.K., Au, B.H., Heyd, D.V., Harbottle, R.R., Schoel, M., Petersen, N.O., and Bagatolli, L.A. (2002a). Biophysical studies of nano-structured interfaces as models of lung surfactant membranes. *Rec. Res. Dev. Biophys.* 1: 53-70.
- Nag, K., Pao, J-S., Harbottle, R.R., Possmayer, F., Petersen, N.O., and Bagatolli, L.A. (2002b). Segregation of saturated chain lipids in pulmonary surfactant films and bilayers. *Biophys. J.* 82: 2041-2051.
- Nag, K., Harbottle, R.R., Panda, A.K., Hearn, S.A., and Petersen, N.O. (2004a). Physicochemical Mapping of Phase Heterogeneity in Biomembrane Films. *Microscopy and Analysis.* 18 (1): 13-15.

- Nag, K., Harbottle, R.R., Panda, A.K., and Petersen, N.O. (2004b). Chapter 17: Atomic force microscopy of interfacial monomolecular films of pulmonary surfactant. in *Atomic Force Microscopy: Biomedical Methods and Applications*. Eds. P.C. Brag and D. Ricci. Humana Press, Totowa, N.J. 242: 231-243.
- Nag, K., Rodriguez-Capote, K., Panda, A.K., Frederic, L., Hearn, S.A., Petersen, N.O., Schurch, S., and Possmayer, F. (2004c). Disparate effects of two phosphatidylcholine binding proteins, C-reactive protein (CRP) and surfactant protein A (SP-A) on pulmonary surfactant structure and function. *Amer. J. Physiol.* (Nov. 2004).
- Nag, K., Vidyasankar, V., Harbottle, R.R., Panda, A.K. (2005). Chapter 6: Chain Dancing, Super-Cool Surfactant, and Heavy Breathing: Membranes, Rafts, and Phase Transitions. In: *Lung Surfactant Function and Disorder*. Eds. Nag, K. Taylor and Francis group, Boca Raton, FL. 201: 145-172.
- Notter, R. H., and Wang, Z. (1997). Pulmonary surfactant: physical chemistry, physiology, and replacement. *Rev. Chem. Engineer.*, 13: 1-118.
- Notter, R. D., Shapiro, D. L., Ohning, B., and Whitsett, J. A. (1987). Biophysical activity of synthetic phospholipids combined with purified lung surfactant 6000 dalton apoprotein. *Chem. Phys. Lipids*. 44: 117.
- Notter, R.H. (2000). *Lung Surfactants: Basic Science and Clinical Applications*. Marcel Dekker Inc., New York, N.Y.
- Otsubo, E., and Takei, T. (2002). Characterization of the surface activity of a synthetic surfactant with albumin. *Biol. Pharm. Bull.* 25(12): 1519-1523.
- Panaiotov, I., Ivanova, Tz., Proust, J., Boury, F., Denizot, B., Keough, K.M.W., and Taneva, S. (1996). Effect of hydrophobic protein SP-C on structure and dilatational properties of the model monolayers of pulmonary surfactant. *Coll. Surf. B: Biointerfaces*. 6: 243-260.
- Panda, A. K., Nag, K., Harbottle, R. R., Rodriguez, R., Veldhuizen, R. A., Petersen, N. O., Possmayer, F. (2004). Effect of acute lung injury on structure and function of pulmonary surfactant films. *Am. J. Respir. Cell Mol. Biol.* 30: 1-10.
- Papahadjopoulos, D., Moscarello, M., Eylar, E. H., and Issac, T. (1975). Effects of proteins on thermotropic phase transitions of phospholipid membranes. *Biochim. Biophys. Acta*. 401: 317-335.
- Perez-Gil, J., and Keough, K. M. W. (1998). Interfacial properties of surfactant proteins. *Biochim. Biophys. Acta*. 1408: 203-217.

- Petri, W. A., Jr., Timothy, N. E., Ranajit Pal, Thompson, T. E., Biltonen, R. L and Wagner, R. R. (1980). Thermotropic behavior of dipalmitoylphosphatidylcholine vesicles reconstituted with the glycoprotein of vesicular stomatitis virus. *Biochemistry*, 19: 3088-3091.
- Petty, T.L., Silvers, G., Paul, G. W and Stanford, R. E. (1979). Abnormalities in lung elastic properties and surfactant function in adult respiratory distress syndrome. *Chest*, 75: 571-574.
- Phang, P. T., and Keough, K. M. W. (1986). Inhibition of pulmonary surfactant by serum from normal adults and from patients having cardiopulmonary by pass. *J. Thorac. Cardivasc. Surg*, 91: 248-251.
- Pison, U., Seeger, W., Buxhorn, R., Joka, T., Brand, M., Obertacke, U., Neuhof, H., and Schimdt-Neuerberg, K. P. (1989). Surfactant abnormalities in patients with respiratory failure following multiple trauma. *Am. Rev. Respir. Dis.* 140: 1033-1039.
- Pittet, J.F., Mackensie, R.C., Martin, T.R., and Matthay, M.A. (1997). Biological markers of acute lung injury: prognostic and pathogenic significance. *Amer. J. Respir. Crit. Care Med.* 155: 1187-1205.
- Possmayer, F. Physicochemical aspects of pulmonary surfactant. (1997). In: *Fetal and Neonatal Physiology*, edited by Polin RA, and Fox WW.. Philadelphia, PA: Saunders, 1997, p. 1259-1275.
- Pugin, J., Verghese, G., Widmer, M.C., and Matthay, M.A. (1999). The alveolar space is the site of intense inflammatory and profibrotic reactions in the early phase of ARDS. *Crit. Care Med.* 27: 304-312.
- Reilly, K. E., Mautone, A. J., and Mendelsohn, R. (1989). Fourier transform infrared studies of lipid/protein interaction in pulmonary surfactant. *Biochemistry*, 28: 7368-7373.
- Revak, S. D., Merritt, T. A., Degryse, E., Stefani, L., Courtney, M., Hallman, M., and Cochrane, C. J. (1988). Use of human surfactant low molecular apoproteins in the reconstitution of surfactant biologic activity. *J. Clin. Invest*, 81: 826-833.
- Rinaldo, J. E., and Rogers, R. M. (1982). Adult respiratory distress syndrome: changing concepts of lung injury and repair. *N. Engl. J. Med.* 300: 900-902.
- Robertson, B., and Lachmann, B. (1988). Experimental evaluation of surfactants for replacement therapy. *Exp. Lung. Res.* 14: 279-310.

- Rufer, R and Stolz, C (1969). Inactivation of alveolar surface films by lowering the surface tension of the hypophase. *Pflugers Arch.* 307 (2): 89-103.
- Schürch, S., Possmayer, F., Cheng, S., and Cockshutt, A. M. (1992). Pulmonary SP-A enhances adsorption and appears to induce surface sorting of lipid extract surfactant. *Am. J. Physiol. Lung. Cell. Mol. Physiol.*, 263: L210-L218.
- Seeger, W., Stöhr, G., Wolf, H. R., and Neuhof, H. (1985). Alteration of surfactant function due to protein leakage: special interaction with fibrin monomer. *J. Appl. Physiol*, 58:326-338.
- Seeger, W., Walmrath, D., Menger, M., and Neuhof, H. (1986). Increased lung vascular permeability after arachidonic acid and hydrostatic challenge. *J. Appl. Physiol.* 61:1781-1789.
- Seeger, W., Thede, C., Gunther, A., Grube, C. (1991). Surface properties and sensitivity to protein-inhibition of a recombinant apoprotein C-based phospholipids mixture in vitro – comparison to natural surfactant. *Biochim. Biophys. Acta.* 1081: 45-52.
- Seeger, W., Grube, C., Gunther, A., and Schmidt, R. (1993). Surfactant inhibition of serum proteins: differential sensitivity of various surfactant preparations. *Eur. Respir. J.* 6: 971-977.
- Shelley, S. A., Paciga, J. E. and Balis, J. U (1977). Purification of surfactant from lung washings and washings contaminated with blood constituents. *Lipids* 12, 505-510.
- Shiffer, K., Hawgood, S., Duzgunes, N., and Goerke, J. (1988). Interactions of the low molecular weight group of surfactant-associated proteins (SP 5-18) with pulmonary surfactant lipids. *Biochemistry*, 27: 2689-2695.
- Shiffer, K., Hawgood, S., Haagsman, H.P., Benson, B., Clements, J.A., and Goerke, J. (1993). Lung surfactant proteins SP-B and SP-C alter the thermodynamic properties of phospholipid membranes: a differential calorimetry study. *Biochemistry*, 32(2): 590-597.
- Spiker, R. C., and Levin, I. W. (1975). Raman spectra and vibrational assignments for dipalmitoyl phosphatidylcholine and structurally related molecules. *Biochim. Biophys. Acta*, 388: 361-373.
- Spragg, R.G., and Lewis, J.F. (2003). Surfactant therapy in acute respiratory distress syndrome. In: *Acute Respiratory Distress Syndrome*. Ed. M.A. Matthay, Ch. 19., M.Dekker, New York, NY

- Sznajder, S.I. (1999). Strategies to increase alveolar epithelial fluid removal in the injured lung. *Amer. J. Respir. Crit. Care Med.* 160: 1441-1442.
- Tabak, S. A., and Notter, R. H. (1977). Effect of serum proteins on the dynamic π -A characteristics of saturated phospholipids films. *J. Coll. Interf. Sci.*, 59: 293- 300.
- Taneva, S., Voelker, D.R., and Keough, K.M.W. (1997). Adsorption of pulmonary surfactant protein D to phospholipid monolayers at the air-water interface. *Biochemistry*. 36: 8173-8179.
- Taylor, F. B., and Abrams, M. E. (1966). Effect of surface active lipoprotein on clotting and fibrinolysis, and of Fbg on surface tension of surface active lipoprotein. *Am. Med.* 40: 346-350.
- Van Golde, L. M. G., Batenberg, J. J., and Robertson, B. (1988). The pulmonary surfactant system: biochemical aspects and functional significance. *Physiol. Rev.* 68: 374-455.
- Veldhuizen, R., Nag, K., Orgeig, S., and Possmayer, F. (1998). The role of lipids in pulmonary surfactant. *Biochim. Biophys. Acta.* 1408: 90-108.
- Veldhuizen, E. J., and Haagsman, H. P. (2000). Role of pulmonary surfactant components in surface film formation and dynamics. *Biochim. Biophys. Acta*, 1467: 255-270.
- Vidyasankar, S.(2004). Association and interaction of serum albumin with lung surfactant extract. *M. Sc. Thesis*, Department of Biochemistry, Memorial University of Newfoundland, St. John's, Newfoundland, Canada A1B 3X9.
- Vincent, J. S., Revak, S. D., Cochrane, C. D., Levin, I. W. (1993). Interactions of model human pulmonary surfactants with a mixed phospholipid bilayer assembly. Raman spectroscopic study. *Biochemistry*, 32: 8228-8238.
- Von Nahmen, A., Schenk, M., Sieber, M., and Amrein, M. (1997). The structure of a model pulmonary surfactant as revealed by scanning force microscopy. *Biophys. J.* 72(1): 463-469.
- Wang, Z., and Notter, R.H. (1998). Additivity of protein and nonprotein inhibitors of lung surfactant activity. *Amer. J. Respir. Crit. Care Med.* 158(1): 28-35.
- Ware, L.B., and Matthay, M.A. (1999). Maximal alveolar epithelial fluid clearance in clinical acute lung injury: an excellent predictor of survival and the duration of mechanical ventilation. *Amer. J. Respir. Crit. Care Med.* 159: Suppl: A694. Abstract.

- Ware, L.B., and Matthay, M.A. (2000). The acute respiratory distress syndrome. *New Engl. J. Med.* 342(18): 1334-1349.
- Weisel, J. W., Stauffacher, C. V., Bullitt, E., and Cohen, C. (1985). A model for Fbg: domains and sequence. *Science* 230:1388-1391.
- Whitsett, J. A., Ohning, B. L., Ross, G., Meuth, J., Weaver, T., Holm, B. A., Shapiro, D. L., and Notter, R. H. (1986). Hydrophobic surfactant-associated protein in whole lung surfactant extract and its importance for biophysical activity in lung surfactant extracts used for replacement therapy. *Pediatr. Res*, 20: 460-467.
- Yellin, N and Levin, I. W. Hydrocarbon chain disorder in lipid bilayers. Temperature dependence of Raman spectra of 1,2-diacylphosphatidylcholine-water gels. (1977). *Biochim. Biophys. Acta*, 489: 177-190.
- Yu, S.H., Harding, P.G., Smith, N., and Possmayer, F. (1983). Bovine pulmonary surfactant: chemical composition and physical properties. *Lipids*. 18(8): 522-529.
- Yu, S.-H., and Possmayer, F. (1986). Reconstitution of surfactant activity by using the 6kDa apoprotein associated with pulmonary surfactant. *Biochem. J*, 236: 85-89.
- Yu, S.-H., and Possmayer, F. (1988). Comparative studies on the biophysical activities of the low-molecular-weight hydrophobic proteins purified from bovine pulmonary surfactant. *Biochim. Biophys. Acta*. 961: 337-350.

